UNIVERSITY OF COPENHAGEN
FACULTY OF SCIENCE

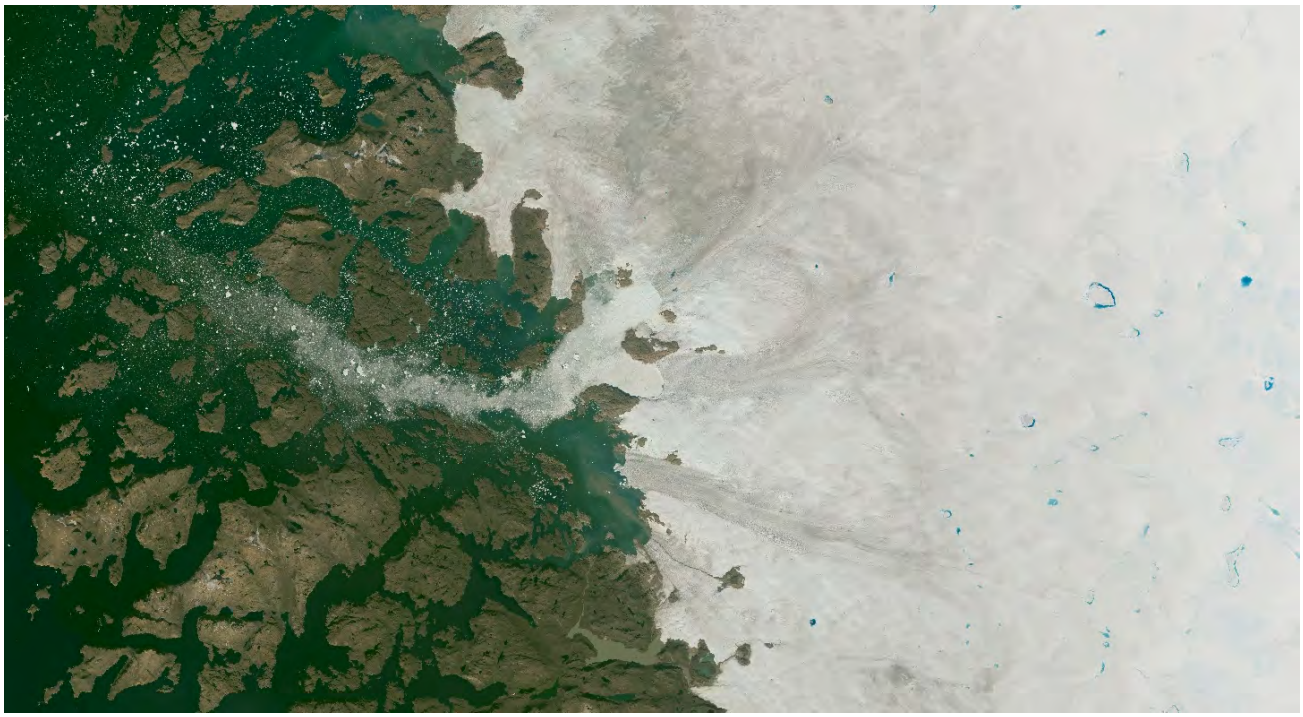

PhD thesis

Signe Hillerup Larsen

Dynamics of Upernavik Isstrøm

- Controlling mechanisms of ice stream flow

Advisors: Christine Schøtt Hvidberg and Andreas Peter Ahlstrøm

Handed in: November 3, 2017

GEUS

PREFACE

This thesis has been submitted to the PhD School of the Faculty of Science, University of Copenhagen. November 2017.

ADDITIONAL INFORMATION

Author
Signe Hillerup Larsen
Centre for Ice and Climate
Niels Bohr Institute
University of Copenhagen
and
The Geological Survey of Denmark and Greenland (GEUS)

Main academic advisor
Christine Schøtt Hvidberg
Centre for Ice and Climate
Niels Bohr Institute
University of Copenhagen

Second academic advisor
Andreas Peter Ahlstrøm
The Geological Survey of Denmark and Greenland (GEUS)

ABSTRACT

Fast flowing ice streams are responsible for draining the vast majority of the Greenland ice sheet. During the past few decades, the ice streams have undergone rapid acceleration and retreat Greenland wide. However, the controlling mechanism of the dynamic changes are still not well understood. Due to the ice streams' importance for the drainage of the entire ice sheet, the fifth assessment report (AR5) of the Intergovernmental Climate Panel (IPCC) deemed uncertainties in the flow of ice streams one of the major uncertainties in predicting future changes of the Greenland ice sheet. In this thesis, the dynamical changes at Upernavik Isstrøm (UI), Northwest Greenland, are analysed and an ice flow model is used to study specific controlling mechanisms of the ice stream flow. The analysis of observations of velocity, thickness and calving front position changes, reveals asynchronous behaviour of the neighboring ice streams at UI. However, overall dynamical changes at UI are in line with general trends in the region. Thus, establishing UI as an optimal study site for detailed process studies of controlling mechanisms of ice stream flow. A model study of velocity changes at the end of the melt season in 2014, reveals that the ice streams are increasingly sensitive to melt water changes towards the front. Part of the spatial trend in sensitivity is attributed to the softening effect of water entering the shear margins. A second model study focussing specifically on reproducing the observed flow, establish that including softer shear margins in ice flow models will improve the models ability to reproduce fast flow. Thus, a method for defining softer shear margins in ice flow models, without knowing details about the mechanisms behind the softening, is suggested to be included in future model studies of ice stream flow. The thesis establish the importance of understanding the inhomogeneity of the ice viscosity to be able to correctly model the dynamics of ice streams, and thus to be able to predict future changes of the Greenland ice sheet.

SAMMENFATNING

Hurtigtflydende isstrømme er ansvarlige for dræningen af is fra langt størstedelen af Grønlands indlandsis. I løbet af de seneste par årtier har isstrømmene vist acceleration og tilbagetrækning, men de styrende mekanismer bag disse ændringer er endnu ikke fuldt forstået. På grund af isstrømmenes rolle i dræningen af is fra hele indlandsisen, vurdere den seneste IPCC rapport (AR5, 2013) at manglen på forståelsen af de styrende mekanismer bag isstrømmenes ændringer, er

en af de største usikkerheder i forudsigelser af fremtidige ændringer for hele indlandsisen. Denne Ph.d. afhandling undersøger de seneste ændringer i Upernavik Isstrøm (UI) i Nordvestgrønland, og benytter en isflydemodel til at undersøge specifikke mekanismer der kan være afgørende for isens flydning. En analyse af observerede ændringer i hastigheder, tykkelse og frontpositioner, afslører asynkrone ændringer af isstrømme, der ligger lige ved siden af hinanden. De overordnede dynamiske ændringer i UI, er imidlertid repræsentative for de generelle tendenser i området. UI kan dermed anses for at være et optimalt sted til detaljerede undersøgelser omhandlende mekanismer der har indflydelse på isstrømmes flydning. Et modelstudie af hastighedsændringer i slutningen af smeltesæsonen i 2014, afdækker øget følsomhed over for ændringer smeltevandsproduktion i nærheden af fronten. En del af denne øgede følsomhed tilskrives effekten af vand der trænger ned langs isstrømmenes marginer. Et andet modelstudie, der fokusere på isstrømmenes marginer, fastslår samtidig, at det er nødvendigt at tage højde for blødere is langs med isstrømmens rand, for at kunne få en model til at reproducere de høje hastigheder der observeres i isstrømmene. Studierne konkludere at, indtil mekanismerne bag blødgørelsen af isen i isstrømmes marginer er bedre forstået, så bør blødere isstrømsmarginer tilføjes i modeller ved hjælp af en overordnet blødgøringsfaktor. Afhandlingen fastslår vigtigheden af at forstå inhomogeniteten af isens flydeevne, for at kunne reproducere isstrømmes hurtige flydning korrekt og dermed at kunne forudsige dynamiske ændringer af hele indlandsisen.

... all models are wrong,
but some are useful.
(Box and Draper, 1987, p. 424)

ACKNOWLEDGMENTS

This thesis is the result of a three years PhD degree, during which I have been employed at the Geological Survey of Denmark and Greenland (GEUS). The project was funded partly by the Nordic Centre of Excellence SVALI (Stability and Variation of Arctic Land Ice) and the Niels Bohr Institute. During February to May 2014 the work was performed at DTU Space, in collaboration with Shfaqat A. Khan. From August to December 2014 the work was performed at the Jet Propulsion Laboratory, in collaboration with Eric Y. Larour.

This work had not been possible without the support of all my colleagues, friends and family. First of all, I would like to express my sincerest gratitude to my supervisors who both have been my mentors for much longer than the PhD studies. Andreas for employing me in 2008, for good field trips and productive and positive guidance and Christine for being my mentor and for guiding me safely through all my university degrees. Thanks to my GEUS collegues for supporting working environment and fruitful discussions, friendships, guidance and open doors. Especially I would like to mention Konstanze for all the very good sparring at the 'Upernavik office' and friendship, Babis for making it fun, Signe for believing in me, Anne and Nanna for many good discussions, and Michele for being a mentor and many good field trips. Furthermore, I would like to acknowledge my CIC collegues and the ice flow modelling group, in particular Lisbeth. The people in the SVALI project - I wish all projects could be like this. Eric Larour and my collegues at JPL for welcoming and guiding me during my stay abroad. Abbas and my DTU collegues for making me feel at home at DTU. Love and gratitude to my family and friends and especially to Kalle for eternal love and support. And finally, Harald, for getting me up early... every morning... with a smile.

CONTENTS

1

INTRODUCTION

Fast flowing ice streams in Greenland have undergone acceleration (Moon et al., 2012; Rignot and Kanagaratnam, 2006), thinning (Csatho et al., 2014) and retreat (Murray et al., 2015) the past couple of decades. The dynamic changes have, in magnitude, contributed almost as much as the decrease in surface mass balance to the total mass loss of the Greenland ice sheet (Enderlin et al., 2014; Van Den Broeke et al., 2016). Yet, there is a lack of in depth understanding of the controlling mechanisms of dynamic behaviour of ice streams. Ice streams are responsible for draining the vast majority of the ice sheet (Rignot and Mouginot, 2012) and correct reproduction of these, in large scale models, is crucial. Uncertainties in the reproduction of the fast flow in ice streams was, for this reason, deemed one of the main areas of uncertainty in predicting the future of the Greenland ice sheet, by the fifth assessment report (AR5) of the Intergovernmental Climate Panel (IPCC).

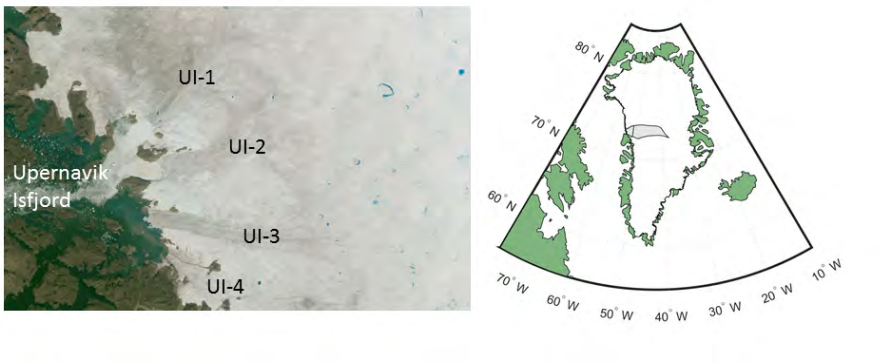

Figure 1.1: Left: Upernavik Isstrøm, Landsat image from 2017. The main four ice streams studied in this theses are UI-1, UI-2, UI-3 and UI-4. Right: Upernavik catchment location in Greenland.

By studying observations of ice stream behaviour in detail, considering the distinctive settings of the individual ice stream, processes important for changes in ice flow can be understood. In this thesis the fucus is on the single glacier catchment of Upernavik Isstrøm (UI) in Northwest Greenland. UI consists of several fast flowing ice streams draining a catchment area of around 3.7 % of the Greenland ice sheet (Figure 1.1). The UI ice streams terminate into the same fjord and, based on their proximity, they are expected to be influenced by similar climate. Thus, UI is a good study site for investigating controlling mechanisms of ice stream flow in similar climate settings. The sci-

entific questions posed in this thesis focusses on how mechanisms related to geometry, surface meltwater and lateral shear margins controls the flow of an ice stream. The specific scientific questions are:

(1) What changes did the UI glaciers undergo during the last three decades and how did the distinctive setting of each glacier influence the change?

These questions will be answered by collecting and interpreting available observations of changes in flow, thickness and calving front position of four UI ice streams. The dynamical changes will then be qualitatively related to the geometry of each ice stream. The results will provide the grounds for determining how representative UI glaciers are of the overall observed changes of the Greenland ice sheet, and a solid background knowledge of UI as a site for future detailed process studies.

(2) How does changes in glacier flow relate to surface meltwater through resistive forces and how sensitive are UI glaciers to changes in resistive forces?

This will be investigated by examining observed abrupt changes in ice flow in relation to the production of surface meltwater. Using an ice flow model, the changes will be simulated by perturbing resistive forces, in ways that can be related to surface meltwater production. The study will relate surface meltwater to changes in resistive forces and thus, in a simplified way, show the spatial pattern of ice flow sensitivity to surface meltwater.

(3) How does soft shear margins affect ice stream flow and how can soft shear margins be included in models?

An ice flow model is used to quantify the importance of inhomogeneous ice viscosity in reproducing the fast flow of an ice stream. The study will show the importance of uncertainty in ice viscosity for reproducing fast flow in models.

1.1 THESIS OUTLINE

The thesis is organised as follows.

SCIENTIFIC BACKGROUND Chapters 2 and 3 are covering the scientific background and method of the study. In chapter 2 a litterature review is used to describe and discuss the physical processes of ice flow, focussing mainly on ice streams. Chapter 3 then introduces the method for ice flow modelling as used in the last two studies of the thesis.

RESEARCH STUDIES The three main studies, described above, are written as scientific journal papers (Paper I, II and III). Going from the purely observational study in chapter 4, outlining the current state of UI, to the model studies of controlling mechanism of ice flow in chapters 5 and 6.

CONCLUDING REMARKS The final two chapters contains the concluding remarks. Chapter 7 comprise of an overall summary of the three studies with a focus on directions for future studies and chapter 8 outlines the main conclusions.

2 SCIENTIFIC BACKGROUND

In this chapter, current literature is reviewed with the purpose of presenting the observed changes, and present understanding, of the main controlling mechanism for ice stream flow.

2.1 TERMINOLOGY

Before going into detail about the scientific background, a definition of terminology is needed: An ice stream is defined by a fast flowing section of an ice sheet, bounded by slow flowing ice (or solid rock close to the front). Ice streams in Greenland usually forms in deep topographic troughs terminating into deep fjords and are thus defined as marine-terminating. The term marine-terminating glacier relates to any glacier, whether an ice stream or not, which terminates in water, either ocean, fjord or lakes. In Greenland most marine-terminating ice streams reach velocities of several km/yr near the terminus (Figure 2.1). The ice streams are responsible for the transport of ice from the interior of the ice sheet towards the margins. At the margins the ice is discharged into the water either as meltwater or as solid ice through calving. The margins of an ice stream are defined as shear margins, due to the high shear between the fast moving ice of the stream and the slower moving ice or solid bedrock at the sides. The shear margins can be visible on the surface as crevasses (see for example Figure 2.4 and 6.1).

2.2 OBSERVATIONS OF ICE FLOW

The main source of information about ice stream flow, in this thesis, comes from satellite derived observations of velocity. In order to understand the usefulness of these the basic methods for creating velocity maps is outlined. The short introduction of velocity mapping methods will be followed by a review of observations of Greenland wide velocity changes.

2.2.1 *Methods*

Velocity maps can be created by tracking specific features observable on two repeat satellite images. Feature tracking of optical images is, however, confined to areas with visible surface features, and depends on both daylight and cloud conditions. In the beginning of the 1990s a major advance was made in observations of glaciers as Synthetic

Name	Launched (year)	Repeat (days)
ERS-1	1991	35
ERS-2	1995	35
Radarsat-1	1995	24/Commercial
Radarsat-2	2007	24/Commercial
Envisat SAR	2002	35
ALOS	2005	46
TerraSAR-X	2007	11
COSMO-SkyMed (4 satellites)	2007	Commercial
Sentinel-1	2014	6

Table 2.1: SAR satellites

Aperture Radar (SAR) satellites provided the first data for observation of ice flow in Antarctica using SAR interferometry (inSAR) (Goldstein et al., 1993). In very simplified terms the method use the phase or intensity of the radar backscatter to track surface movements. The combination of tracking intensity and phase will make it possible to map velocities in areas with both fast and slow flow as well as areas of many or few surface structures (see Bamler and Hartl, 1998; Joughin, Smith, and Abdalati, 2010, for more detailed description of the inSAR method).

The main SAR satellites along with launch year and time between each repeat image are listed in table 2.1. The repeat cycle has several implications for velocity mapping since recognisability of features between the images depend on velocity. A longer repeat cycle, will make it harder to track fast flowing areas such as ice streams. The repeat cycle, furthermore, defines how often information about velocity can be obtained. In fast flowing ice streams, velocity changes can be expected on sub-seasonal timescales (e.g. Ahlstrøm et al., 2013; Sole et al., 2011) and in combination with the issues related to loss of recognisability between images, a high repeat cycle is desirable. Thus, the TerraSAR-X satellite launch in 2007 and the Sentinel-1 in 2014 opens possibilities for studying ice streams in much higher detail than previously.

To capture high frequency details in ice flow, continuous time series of velocity changes can be obtained using in situ Global Positioning System (GPS) trackers (as in Ahlstrøm et al., 2013). Using this method The GPS tracker is placed directly on the ice surface and the GPS transmits its position as it flows along with the glacier. Thus, this method is limited to single points.

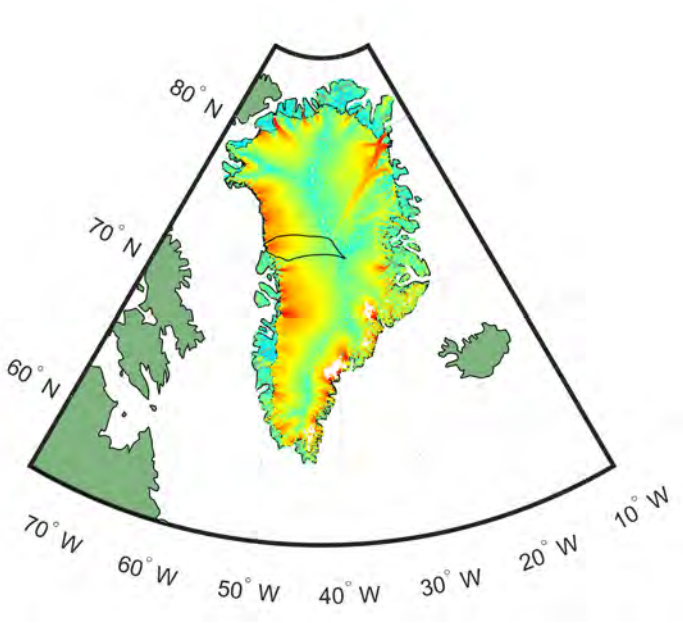

Figure 2.1: Surface velocity observed during winter 2016/2017 (note the color scale is logarithmic). Data from the European Space Agency (ESA), Climate Change Initiative (CCI) Greenland, using sentinel 1 Synthethic Aperature Radar. The black line outlines the ice flow catchment of Upernavik Isstrøm, defined by flow direction.

2.2.2 *Observations*

A Greenland wide velocity map (Figure 2.1) reveals fast flowing ice streams in particular in the Northwest and Southeast regions, where the ice sheet margin is dominated by marine-terminating ice streams.

The first Greenland wide velocity changes, mapped by Rignot and Kanagaratnam (2006), showed a widespread acceleration of glaciers in the southern part of Greenland (below 66°) between 1996 and 2002 which had rapidly expanded northward in 2005. A later study by Moon et al. (2012) mapped Greenland wide velocity in winters 2000/2001 and 2005/2005 to 2008/2009 showing that the acceleration in Southeast decreased after 2005 whereas in Northwest steady acceleration was maintained (reaching up to 76°) until the end of study period in 2010.

Howat et al. (2008) concluded that the speed-up in Southeast Greenland was a reaction to the thinning and subsequent retreat after an anomalously warm year in 2003. A study by McFadden et al. (2011) analysed the velocity changes on selected West Greenland glaciers, examining velocity, thickness, front position and surface slope. The study showed that the acceleration of the glaciers related to specific local settings, such as glacier slopes and the presence of a floating tongue. A complex reaction pattern was also observed in the study of 200+ Greenland wide ice streams by Moon et al. (2012). The results of

the above mentioned studies showed that the acceleration of glaciers, on long time scales, depend on climate, however, that they on shorter timescales show behaviour that depends on specific local settings.

With the introduction of satellites with shorter repeat cycles (e.g. TerraSAR-X in 2007) studies of seasonal changes in ice stream velocity has been made feasible. Moon et al. (2014) studied 55 marine-terminating ice streams and showed that the seasonal pattern of velocity changes can be roughly divided into three typical behaviour patterns depending on either the front position or surface meltwater production during the melt season. While some glaciers' velocity followed the melt curve throughout the melt season, others showed an increase in velocity in early melt season, followed by an abrupt slow-down in mid-melt season. The latter pattern was also observed by Ahlstrøm et al. (2013) using GPS trackers on eight of the major marine terminating glaciers in Greenland.

The above review of observations of ice flow velocity make it clear that the dynamic behaviour of the individual ice stream depends on mechanisms specific to this. Thus, following sections will look into the physics behind the feedback mechanisms of ice stream behaviour.

2.3 DYNAMICAL FEEDBACK MECHANISMS OF ICE STREAMS

Alley (1991) described how the build up of a sediment shoal in front of marine-terminating glaciers helps the glacier advance by stabilizing the front. Thus, advance can occur even in stable climate. The glaciers front position on a reverse slope will make it vulnerable to small fluctuations in the front, causing a rapid retreat. Thus, the marine-terminating glaciers can advance and retreat even in stable climates (described as the tidewater glacier cycle in Meier and Post, 1987). Brinkerhoff, Truffer, and Aschwanden (2017) furthermore suggested, that the increased amount of surface melt in warming periods can cause the glacier to advance due to the sediment feedback. This natural cycle makes it difficult to determine if the retreat of a single glacier is due to climate change. Observations of recent retreat and acceleration of marine-terminating glaciers in the entire Greenland (Moon et al., 2012; Murray et al., 2015) suggest that current overall changes is due to general trends in climate and range beyond the glaciers' advance and retreat cycles. However, the controlling mechanisms behind the individual glacier behaviour is still not well understood and thus inhibits predictions of future behaviour.

A glacier flows due to the driving stress, τ_d, that is the gravitational pull on the ice which can be approximated to be given by

$$\tau_d = \rho g H \alpha \tag{1}$$

where ρ is the density, g is the gravitational constant, H is the ice thickness and α is the surface slope (Cuffey and Paterson, 2010). This

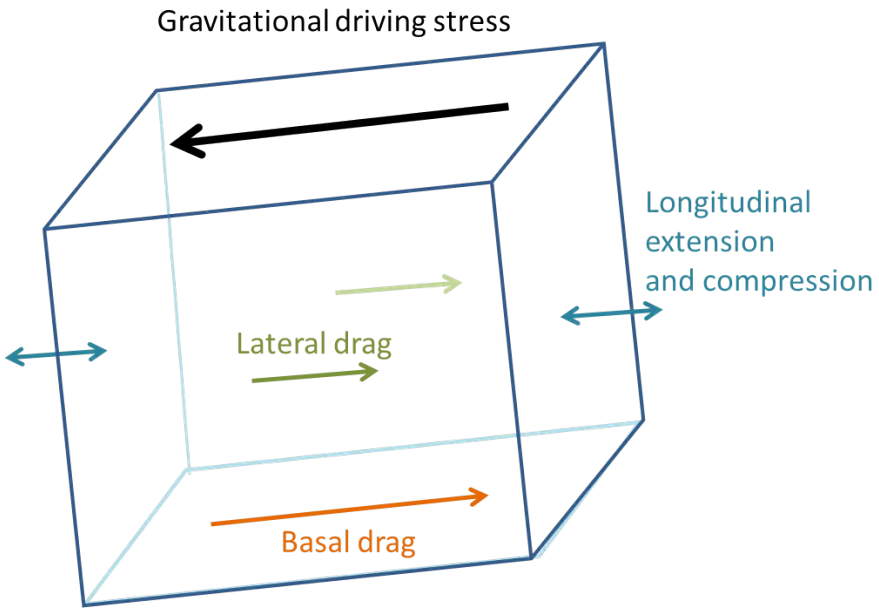

Figure 2.2: For balance of ice streams, adapted from www.AntarcticGlaciers.com

flow is balanced by the resistive stress of the base, τ_b, the lateral resistance, τ_{lat}, at the sides of the ice stream and the longitudinal stress, τ_{lon}, which is both tensile and compressional stresses. Thus,

$$\tau_d = \tau_b + \tau_{lat} + \tau_{lon} \tag{2}$$

(see Figure 2.2). Instability arises when any changes in the resistive stresses exceeds the driving stress (Pfeffer, 2007). An initial climate warming causing increased melt, and hence thinning of the ice stream, can cause major instabilities in a marine-terminating ice stream due to a number of different feedback mechanism. First of all, thinning has a self sustaining effect for all glaciers as the surface is lowered to altitudes of higher temperatures. Pfeffer (2007) furthermore, showed that thinning can cause irreversible retreat due to the loss in resistive forces at the bed as effective pressure reduces. Thinning will furthermore cause a reduction in lateral drag due to the area in contact with the sides becomes smaller. In addition to this the retreat of marine-terminating ice streams depends on bedrock geometry such as wider trunks and deeper basal topography. As the calving front retreats into a wider area the lateral drag will become relatively less important and the spreading of the ice will furthermore enhance calving. Similar effects of retreating into a deeper trunk will cause a reduction in effective pressure at the bed thus decreased basal resistance.

Studies by e.g. Bondzio et al. (2017) and Nick et al. (2009) show that an initial front retreat can cause major acceleration and retreat of marine-terminating glacier. Thus, the triggering mechanism is not necessarily thinning due increased melt caused by higher air temper-

atures, but rather an initial retreat caused by higher ocean temperatures. Increased ocean temperatures was suggested to be the main trigger of the retreat of Jakobshavn Isbræ during the 2000s (Holland et al., 2008) and Kangiata Nunaata Sermia (KNS) during the 19th century (Lea et al., 2014). Different triggering mechanisms for sudden glacier reactions can thus be at play and the strong feedback mechanism can make it hard to decipher from observations, what actually caused sudden dynamical changes in ice flow.

2.4 THE INFLUENCE OF SURFACE MELTWATER ON ICE FLOW

Understanding triggering mechanisms for dynamic changes is essential to be able to predict future changes. The above section showed that dynamic changes will be enhanced by the feedback mechanisms of thinning and front retreat. Surface meltwater is playing a large role in both thinning, ice flow and ice/ocean interaction. This role is reviewed in the following.

Studies have shown (e.g. Das et al., 2008; Zwally et al., 2002) that surface meltwater can affect glacier flow by the rapid ($<$ 2 hours) transport of surface meltwater to the bed through moulins. The water reaching the bed can, if the subglacial drainage system is overwhelmed by the inflow of water, cause a reduction in effective pressure thereby reducing basal resistance. Several studies comparing meltwater production and ice flow has been conducted in the coastal area of the West Greenlandic part of the ice sheet. Bartholomew et al. (2010) showed observations of mid-melt season slow-down to below winter velocities. They suggested, that it is likely that an efficient drainage system evolved at some point during mid-melt season, similar to what have been observed on alpine glaciers. The switch between inefficient and efficient drainage systems cause a sudden drop in ice flow velocity. This deceleration happens due to the efficient removal of basal water everywhere thereby reducing the weakening effect of the water. This theory is supported by a study conducted by Sundal et al. (2011). This study showed, that the mid-melt season slowdown only occurred in years with high meltwater production. In low melt years the velocity followed the meltwater production throughout the melt season. Thus concluding that the meltwater production was too low to to establish an efficient drainage system. A later study by Bartholomew et al. (2012) showed that, even in the case of the development of an efficient drainage system early in the season, subseasonal scale velocity changes show a reaction to changes in meltwater. The ice flow was seen to be sensitive to duration and rate of surface meltwater production, rather than volume. Thus, even though a well developed drainage system is established, peaks in meltwater production will still be able to overflow the capacity of the drainage system.

The above mentioned studies are all performed well inland of any marine-terminus. However, in the ice stream through, the fast flow is likely to destabilise the efficient channels. A study, by Slater et al. (2017), investigating the distribution of the meltwater plume at the calving front of KNS, showed that the drainage was distributed through main parts of the melt season. Thus concluding, that an efficient drainage system inland of an ice stream can break down close to the calving front. This means that the effective pressure at the base of the ice stream will be reduced close to the front, causing enhanced flow speeds in this area. This supports the findings of Andersen et al. (2011), where an analysis of ice flow changes, at Helheim Gletsher, in relation to surface melt water production, showed higher sensitivity to meltwater closer to the calving front.

The effect of meltwater on basal resistance and thus ice flow is important on sub-seasonal timescales. However, Sole et al. (2013) showed that the effect of increased surface melt water on flow beyond the course of a year is limited. The speedup is mediated by the slowdown to below average velocities when an efficient drainage system evolves. A recent study by Kulessa et al. (2017) showed that the different sensitivity to meltwater observed in velocities can also be explained by modifications of the sediment strength below the glacier. The effect of this resembles the effect of wakening due to changes effective pressure. However, while the pressure theory does not necessarily has an effect on annual timescales this sediment strength theory implies that an increasing amount of meltwater will lead to a weakening effect that can reach beyond sub-annual timescales.

Due to the permeability of the ice in crevasses and moulins most of the meltwater created at the surface of the ice sheet will be transported to the bed or internal channels. The meltwater that reaches the bed, will be transported towards the margin (see Figure 2.3). When reaching the grounding line it will form a turbulent plume rising upwards along the calving front of the glacier due to the density difference between the fresh meltwater and the saltier sea water. This meltwater plume can generate increased submarine melt affecting the position of the calving front and thus the resistive forces exerted at the front (Straneo et al., 2013). A study by Sciascia et al. (2013) showed that submarine melt rates were highly sensitive to the strength of the meltwater plume both due to the increased melting by the turbulence but also due to the increased mixing with the warm ocean water. Thus, the effect of increased meltwater and warmer ocean temperatures are likely to re-enforce one another.

Water reaching into the ice and firn will have a heating effect through refreezing which will be discussed in the the following section.

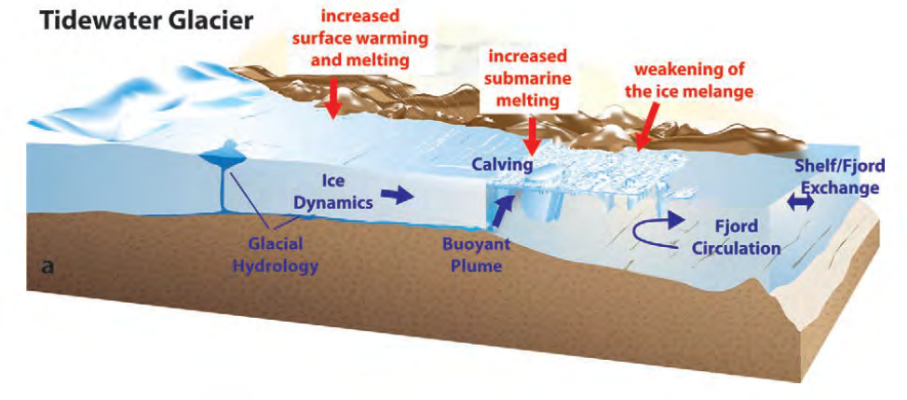

Figure 2.3: Figure from Straneo et al. (2013). Schematics of proposed mechanisms controlling marine-terminating ice stream flow.

2.5 ICE TEMPERATURES AND VISCOSITY

Ice flow is non-newtonian, thus the viscosity depends on strain rates (see equation 6 and Glen, 1955), which is a main reason for the flow law equations to be computationally demanding to solve (see further in chapter 3). However, ice viscosity is also highly dependent on temperature and an increase in ice temperature from $-15°C$ to $0°C$ will change the viscosity by approximately an order of magnitude (Cuffey and Paterson, 2010). Here surface, englacial and subglacial heat sources are reviewed along with the effects on ice viscosity.

A study by Dahl-Jensen et al. (1998) of the measured temperature in deep bore holes (dye-3 and GRIP) in the center of the ice sheet exemplified the speed at which surface air temperatures diffuse through the ice. The study showed that past surface air temperature can be measured directly in the borehole. Thus, the cold temperature of the little ice age (ca. 1550-1850 A.D.) was measured at a depth of around 140 m and the cold temperature from the last ice age (ca. 115 to 11 thousand years ago) was measured at depths of around $1.2 - 2$ km. Diffusion of temperatures in the ice is slow and thus, as ice is transported from the interior towards the margin of the ice sheet, the cold content of the ice will be transported along.

In the interior of the ice sheet the main heat source at the surface of the ice is the air temperature. This is balanced by the heat flux from the base of the ice due to geothermal heat. The geothermal heat flux is generally unknown and can only be measured at deep ice core cites (e.g. Buchardt and Dahl-Jensen, 2007). Several models for geothermal heat flux based on earth physics have been made (e.g. Pollack, Hurter, and Johnson, 1993; Shapiro and Ritzwoller, 2004), however, without constraints of actual measurements. Values for the UI area range between $50 - 70$ mW/m^2. As ice deforms and flows over the bed of the ice, frictional heating will also be a significant heat source at the

bed as well as within the ice. In particular basal ice, which is experiencing the highest deformation rates, will be influenced by heating due to deformation. Moreover, in the case of the ice sliding over the base, frictional heating will also occur. Measurements of temperature across Jakobhavn Isbræ (West Greenland), obtained and analysed by Funk, Echelmeyer, and Iken (1994) and Iken et al. (1993), showed that a basal temperate layer of 30 % of total ice thickness exists 50 km upstream of the terminus. Harrington, Humphrey, and Harper (2015) also found a basal layer of temperate ice upstream of a land terminating zone in West Greenland. In ice streams, the internal heat production due to high shear and strain in the shear margins will make these warmer than the surrounding ice. The fast advection of ice from the colder interior of the ice sheet will, furthermore, make the core of the ice streams cold.

When water is present an extra heat source is introduced due to refreezing. The latent heat released by freezing 1 g of water will release enough heat to warm up approximately 160 g of snow, firn or ice by 1°C. This can be a heat source at the surface, englacially or at the bed. For water refreezing near the surface or within the ice the effect was given the name cryo-hydrologic warming (described in detail by Phillips, Rajaram, and Steffen (2010)). As the ablation zone expands due to warming, this effect has the potential for changing ice viscosity and thereby ice flow. Lüthi et al. (2015) compared measured temperatures at four drill sites near Swiss Camp (West Greenland) with model temperatures obtained accounting for heat transfer by diffusion and advection as well as frictional heating, but neglecting cryo-hydrologic warming. The results showed that modelled temperatures were up to 15°C too cold. This discrepancy was attributed to both uncertainty in the effect of cryo-hydrologic warming and unknown ice viscosity.

Ice viscosity does not only depend on temperature but also the impurity content of the ice. Deep ice cores show, as seen for example at Dye 3 in Dahl-Jensen (1985), a sudden increase in deformation rates in the ice deposited during the last ice age, when atmospheric dust content was much higher than during the Holocene. The ice flow dependency on temperature and the fact that increased deformation will cause increased frictional heating results in a positive feedback mechanism (the temperature-viscosity feedback mechanism). Thus, ice age ice, for example, is not only softer due to higher dust content, but also due to warmer temperatures caused by enhanced deformation. This feedback mechanism has been proposed to be able to cause thermally induced oscillations such as surges, and streaming such as Antarctic ice streams that are not confined by basal geometry (see review by Schoof and Hewitt, 2013). A recent model study by Bondzio et al. (2017) concluded that the effect of the temperature-viscosity feedback mechanism played a significant role in the observed acceleration of Jakobshavn Isbræ.

2.6 SHEAR MARGINS AND THEIR ROLE IN CONTROLLING ICE STREAMS

Lateral drag becomes relatively more important than basal drag in fast flowing narrow ice streams. Thus, the ice flow becomes controlled by non-local resistive forces, and in the extreme case of a floating ice shelf where basal friction is zero, the ice flow can be said to be globally controlled (Cuffey and Paterson, 2010). Thus the lateral drag will balance the longitudinal stresses. In ice streams the shear margins are providing a lot of the lateral drag, and hence, constitutes an important area for the flow .

Softer shear margins will effectively let ice flow faster through the ice stream due to the reduced lateral drag they provide. However, the reasons for the increased softness are not well understood. From a force balance study of Whillans Ice Stream (formerly known as Ice Stream B) in Antarctica, Echelmeyer et al. (1994) concluded that the ice in the shear margins must be 10 times softer than the surrounding ice to be able to explain the observed fast flow. They suggested that a large part of this softening could come from deformational heating. However, other mechanisms are likely to contribute to the softening. As shear margins constitute an area with a high amount of damage, this could be a softening factor in it self as shown in Borstad et al. (2013) and references therein. Van Der Veen, Plummer, and Stearns (2011) proposed the possibility of water reaching in to the crevasses would effectively soften these areas. Increased amount of damage would increase this effect. Furthermore, the high amount of water in the shear margins could potentially make these areas extra vulnerable to cryo-hydrologic warming. Observations of meltwater lakes along the shear margins of ice streams (e.g. Joseph and Lampkin, 2017, and at UI in Figure 2.4) show that meltwater is abundant in these zones.

The force balance study by Van Der Veen, Plummer, and Stearns (2011) concluded that the most important factor for the accelerating behaviour of Jakobshavn Isbræ was due to progressive weakening of the shear margins. A similar conclusion was reached by the model study of Bondzio et al. (2017). Thus, understanding the mechanisms than influence shear margin softness is important for quantifying the lateral drag they provide. Moreover, understanding how changes in shear margin softness can enhance flow is crucial for reproducing acceleration of ice streams.

2.7 RECENT DEVELOPMENTS WITHIN MODELLING ICE STREAMS

As outlined in this chapter the dynamics of ice streams is complicated and relates to the three dimensional settings of the individual glacier i.e. thickness, width, slope etc. In order to reproduce this type of flow, three dimensional (3D) models are required. Recent develop-

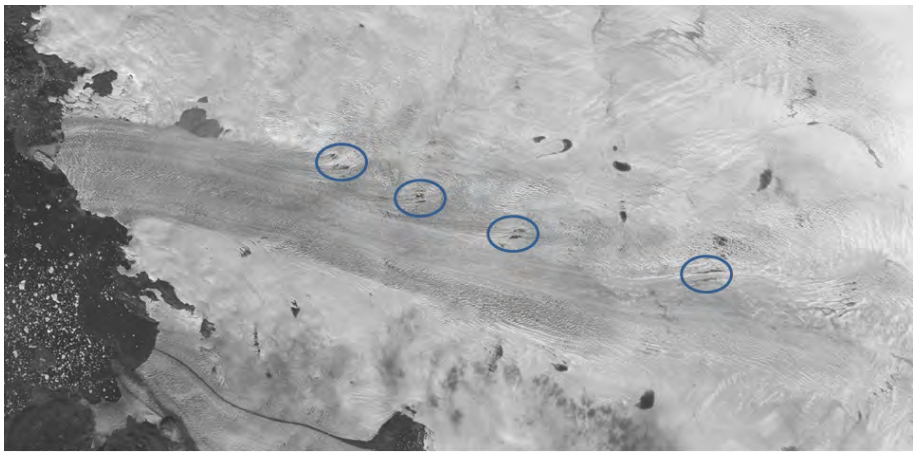

Figure 2.4: Upernavik Isstrøm (UI-3), Landsat image from June 18, 2014. Blue circles indicate supra-glacial shear margin lakes.

ment within this type of models, and not least the input data required, have made it possible to reproduce the complex flow of ice streams. Specific advancements important for this are outlined in the following.

2.7.1 *Basal topography*

Modelling studies by Enderlin, Howat, and Vieli (2013) and Larour et al. (2012b) highlighted that ice flow was highly dependent on thickness. Thus, basal topography constitutes an important model input that is not easily measured due to the inaccessibility of the bed.

Measurements of basal topography can be made by radar. These are usually performed from airplane and covers discrete lines (Gogineni et al., 2001). Thus, to make a basal topography map that is useful for ice flow modelling, a 3D map will have to be created from the lines. Interpolation approaches, as in Bamber et al. (2013), demands a relatively large smoothing of the observations and fails in areas with scarce data. A modelling approach to this problem was introduced by Morlighem et al. (2011). The method entails using the principle of mass conservation and observations of ice flow, to fill out gaps between measured lines of basal topography. Greenland wide basal topography maps, that are consistent with measured topography and velocity, are hence now available (from the BedMachine Morlighem et al., 2014, 2017). This has been a great improvement to model studies of, in particular, ice streams, where basal topography is highly important. The most recent update of the map by Morlighem et al. (2017) now includes the bathymetry of the fjords which will make ice/ocean interaction studies, as well as longer model simulations, with evolving terminus positions, possible. Despite the large improvement for bed topography as a model input, uncertainties remain and it is important to keep in mind that this is a model product and not actual

measurements. The implications of the uncertainties are discussed further, in the next chapter.

2.7.2 *Inhomogeneous viscosity*

Changes in the shear margins softness are, due to the global control of ice streams, of high importance to ice stream flow. However, little is known about the inhomogeneity of the ice viscosity in these zones as they are logistically hard to access in the field. Thus, this is an area subject to high uncertainty within ice flow modelling. However, the softer shear margins have been successfully applied in the model studies by Bondzio et al. (2017) and Joughin et al. (2012), by simply adding a softening factor to the ice viscosity in the shear margins. However, the two studies did not go into details about how the shear margins were defined or quantified the effect of adding the softer margins.

2.7.3 *Time efficient modelling*

As shown in the next chapter of this thesis, the governing equations of ice flow can be computationally demanding to solve. Thus, strategies for simplifying the flow equations, model resolution and model initialisation are of high importance for time efficient modelling.

SIMPLIFYING FLOW EQUATIONS First of all, different approximations to the flow equations can be done. Since the interior of the ice sheet is horizontally vast compared to the depth, simplifying assumptions about ice flow can be adopted. Models of different complexity and different approximations can be combined to cover the simple flow in the interior of the ice sheet and the more complex flow in the ice streams (e.g. Bueler and Brown, 2009; Seroussi et al., 2012).

MODEL RESOLUTION Secondly, adapting model resolution is an approach to make computations more efficient. Whereas the ice streams require high model resolution to resolve the complex flow in the narrow troughs (Aschwanden, Fahnestock, and Truffer, 2016), the more simple flow in the interior of the ice sheet can be solved at a much lower resolution. For three dimensional ice flow modelling there are two types of models available: the finite difference models (e.g. the Parallel Ice Sheet Model, PISM) and the finite element models (e.g. the Ice Sheet System Model, ISSM and Elmer/Ice). Finite difference methods are useful for long model simulations through several ice age periods, however, the method demands a uniform model grid. Finite element methods are computationally more demanding and are useful for process studies. In the latter case it is possible to adapt

model resolution to be high in areas of complex flow and low in areas of more simple flow.

MODEL INITIALISATION Finally, model initialisation is important for how complex flow equations and model resolution can be. Studies by e.g. Aðalgeirsdóttir et al. (2014) and Aschwanden, Aðalgeirsdóttir, and Khroulev (2013) highlighted that initialisation is crucial to model results in simulations of ice flow. There are two branches of methods for model initialization. (1) Since ice remembers both temperature and previous flow conditions, model initialisation can be done by running an ice flow model through several glacial periods, using proxy data for climate changes to force the model. The resulting initial model will be consistent with the physical laws that have been applied. However, due to the uncertainties in particularly the input data, the model will rarely be representing present day ice geometry very well, and are thus not useful for process studies. Furthermore, the long model initialisation will require simplified flow equations to be computationally manageable. (2) A second approach is to instantaneously initiate a model. This method applies present day measured geometry and surface velocity and then use an inverse method to adapt unknown model fields to match the present day conditions. This inverse approach is used by e.g. Gillet-Chaulet et al. (2016) and Morlighem et al. (2010) to infer a map of basal friction that will assimilate observed velocities. In this way, the model will be highly adapted to present day conditions, and is useful for process studies. However, due to the lack of any physical law, the inverted field (in this case basal friction) cannot evolve in time. As the focus in this thesis is on process studies, the second method of instantaneous initialization is used here.

3

MODELLING ICE FLOW

The above review of the flow of ice in ice streams highlights the importance of the three dimensional geometry as well as inhomogeneity of the ice rheology for understanding the flow of ice streams. A way to accumulate such knowledge is through the development of three dimensional ice flow models. The basis for the ice flow modelling in this thesis, will be presented in the following sections, where also practical issues related to input data will be discussed.

3.1 THE ICE SHEET SYSTEM MODEL

In this thesis, the Ice Sheet System Model (ISSM, Larour et al., 2012a), will be used as a tool to test different hypotheses about mechanism important for ice flow. ISSM is a thermomechanical finite element ice flow model with the capabilities for calculating the combined effects of stress, mass and energy balance to model velocities, thickness and temperature of the ice. The finite element method allows for adaptive mesh refinement where a high model resolution can be applied in areas of complex flow, such as ice streams, while keeping the resolution low in the interior of the ice sheet. ISSM was developed as a tool to infer knowledge about ice flow mechanisms, from velocity observations from satellites. This section will introduce the basic flow equations of ISSM (following Larour et al., 2012a).

3.1.1 *Mechanical model*

The stress balance relation is given by

$$\nabla \cdot \sigma_{ij} + \rho \mathbf{g} = 0 \tag{3}$$

Where σ is the stress tensor, ij denotes the direction of the stress (x, y, z), ρ is the density of ice and $\mathbf{g}$ is the gravitational constant. For incompressible viscous fluids the mathematical constitutive law for the deformation of ice under stress is given by

$$\tau_{ij} = 2\mu\dot{\epsilon}_{ij} \tag{4}$$

where the deviatoric stress tensor, τ, is the stress deviation from hydrostatic pressure. The strain rate tensor, $\dot{\epsilon}$, is the spatial gradient in velocity

$$\dot{\epsilon}_{ij} = \frac{1}{2}\left[\frac{\partial u_i}{\partial x_j} + \frac{\partial u_j}{\partial x_i}\right] \tag{5}$$

describing the internal deformation of ice. Where x is the spatial coordinate (x, y, z; cartesian with z in the vertical) so that $x_x = x$, $x_y = y$, $x_z = z$. u is the velocity field containing velocity components in all three directions (u,v,w) so that $u_x = u$, $u_y = v$, $u_z = w$. Finally, μ is the viscosity which, according to Glen (1955), is given by

$$\mu = \frac{B}{2\dot{\epsilon}_e^{\frac{1-n}{n}}} \tag{6}$$

where n is the flow law exponent found experimentally to be around the value of 3 (Cuffey and Paterson, 2010, and references therein). The effective strain rate $\dot{\epsilon}_e$ is given by the second invariant $\dot{\epsilon}_e^2 = \frac{1}{2}[\dot{\epsilon}_{xx}^2 + \dot{\epsilon}_{yy}^2 + \dot{\epsilon}_{zz}^2] + \dot{\epsilon}_{xz}^2 + \dot{\epsilon}_{xy}^2 + \dot{\epsilon}_{yz}^2$ and B is the temperature dependent viscosity prefactor. Glen's flow law is originally expressed by

$$\dot{\epsilon}_{ij} = A\tau_e^{n-1}\tau_{ij} \tag{7}$$

(Glen, 1955) where the effective stress is given by the second invariant $\tau_e^2 = 1/2(\tau_{xx}^2 + \tau_{yy}^2 + \tau_{zz}^2) + \tau_{xz}^2 + \tau_{xy}^2 + \tau_{yz}^2$. The creep parameter A relates to the viscosity parameter B through

$$B = A^{-1/n} \tag{8}$$

The viscosity parameter depends on temperature through an Arrenius law (Cuffey and Paterson, 2010)

$$B(T) = \left(A_0 \exp\left(\frac{-Q}{RT^*}\right)\right)^{-1/n} \tag{9}$$

where A_0 is the flow factor, Q the activation energy for ice creep, R the universal gas constant and $T^* = T - \beta p$ is the absolute temperature corrected for the dependence for melting point on pressure, and β is the rate of change of melting point with pressure.

Ice behaves as Stokes flow under the influence of gravity

$$\frac{\partial \tau_{ij}}{\partial x_j} - \frac{\partial p}{\partial x_i} = 0 \tag{10}$$

This can be written in terms of velocity components

$$\frac{\partial}{\partial x}\left(2\mu\frac{\partial u}{\partial x}\right) + \frac{\partial}{\partial y}\left(\mu\frac{\partial u}{\partial y} + \mu\frac{\partial v}{\partial x}\right) + \frac{\partial}{\partial z}\left(\mu\frac{\partial u}{\partial z} + \mu\frac{\partial w}{\partial x}\right) - \frac{\partial p}{\partial x} = 0 \tag{11}$$

$$\frac{\partial}{\partial x}\left(\mu\frac{\partial u}{\partial y} + \mu\frac{\partial v}{\partial x}\right) + \frac{\partial}{\partial y}\left(2\mu\frac{\partial v}{\partial y}\right) + \frac{\partial}{\partial z}\left(\mu\frac{\partial v}{\partial z} + \mu\frac{\partial w}{\partial y}\right) - \frac{\partial p}{\partial y} = 0 \tag{12}$$

$$\frac{\partial}{\partial x}\left(\mu\frac{\partial u}{\partial z} + \mu\frac{\partial w}{\partial x}\right) + \frac{\partial}{\partial y}\left(\mu\frac{\partial v}{\partial z} + \mu\frac{\partial w}{\partial y}\right) + \frac{\partial}{\partial z}\left(2\mu\frac{\partial w}{\partial z}\right) - \frac{\partial p}{\partial z} - \rho g = 0$$

(13)

Assuming incompressibility

$$\frac{\partial u}{\partial x} + \frac{\partial v}{\partial y} + \frac{\partial w}{\partial z} = 0 \tag{14}$$

The full stokes equations (equation 11 to 14) contains four unknowns (u, v, w, p), and in combination with the flow equation being highly nonlinear, the set of equations are computationally demanding. Thus, simplifying assumptions can be applied.

In this thesis the following approximation to the full stokes equations is used. To reduce the number of unknowns the above equations can be simplified by making two assumptions: (1) the horizontal gradients of vertical velocities are negligible compared to the vertical gradients of the horizontal velocities so that

$$\dot{\epsilon}_{xz} \approx \frac{1}{2}\frac{\partial u}{\partial z}; \qquad \dot{\epsilon}_{xz} \approx \frac{1}{2}\frac{\partial v}{\partial z} \tag{15}$$

and (2) the bridging effects are negligible (Schoof and Hindmarsh, 2010), thus vertical resistive forces are neglected. Which reduces equation 13 to

$$\frac{\partial}{\partial z}\left(2\mu\frac{\partial w}{\partial z}\right) - \frac{\partial p}{\partial z} - \rho g = 0 \tag{16}$$

Equations 11 and 12 then reduces to

$$\frac{\partial}{\partial x}\left(4\mu\frac{\partial u}{\partial x} + 2\mu\frac{\partial v}{\partial y}\right) + \frac{\partial}{\partial y}\left(\mu\frac{\partial u}{\partial y} + \mu\frac{\partial v}{\partial x}\right) + \frac{\partial}{\partial z}\left(\mu\frac{\partial u}{\partial z}\right) = \rho g\frac{\partial s}{\partial x} \tag{17}$$

$$\frac{\partial}{\partial x}\left(\mu\frac{\partial u}{\partial y} + \mu\frac{\partial v}{\partial x}\right) + \frac{\partial}{\partial y}\left(4\mu\frac{\partial v}{\partial y} + 2\mu\frac{\partial u}{\partial x}\right) + \frac{\partial}{\partial z}\left(\mu\frac{\partial v}{\partial z}\right) = \rho g\frac{\partial s}{\partial y} \tag{18}$$

Where s is the upper surface elevation (see Schoof and Hindmarsh, 2010, for a more detailed derivation). This is known as the Blatter-Pattyn or Higher-Order (HO) approximation and will leave two unknowns (u, v). Further shallow approximations are also included in ISSM, however, not used in this thesis.

Mechanical boundary conditions

The surface is assumed to be stress free and the basal drag is written as a viscous-type law and is an empirical relationship given by

$$\boldsymbol{\tau}_b = -k^2\mathbf{v_b} \tag{19}$$

Where $\mathbf{v_b}$ is the basal velocity vector tangential to the base plane and k is the friction coefficient. Where ice meets water the hydrostatic pressure is applied. In the case of the model domain not covering the entire ice sheet, as in this thesis, Dirichlet boundary conditions are applied at the lateral ice/ice boundaries thus here ice velocities are prescribed. k is usually inferred in a data assimilations process, as described in section 3.2, this method is also explained in detail by Morlighem et al. (2010).

3.1.2 *Mass transport model*

For forward model simulations mass transport needs to be applied. Considering the conservation of mass gives the ice thickness, H, through ice flux divergence in the following way

$$\frac{\partial H}{\partial t} = -\nabla H \cdot \bar{\mathbf{v}} + \dot{M}_s - \dot{M}_b \tag{20}$$

where $\bar{\mathbf{v}}$ is the depth averaged horizontal velocity, $\dot{M}_s$ is the surface mass balance (positive for accumulation, negative for ablation), $\dot{M}_b$ is the basal melting rate (positive when melting, negative when freezing).

Mass transport boundary conditions

In the case of the model not covering the entire ice sheet, the thickness at the lateral boundaries of the model domain is prescribed. The domain is kept fixed and for the purpose of this thesis, the ice front is defined by the model domain and all ice that passes through will be lost. ISSM does however, include capabilities of including a moving ice front as well as different calving laws (see for example Bondzio et al., 2017; Morlighem et al., 2016).

3.1.3 *Temperature model*

For thermomechanically-coupled forward model simulations, conservation of energy will give the temperature, T, of the ice,

$$\frac{\partial T}{\partial t} = -\mathbf{u} \cdot \nabla T + \frac{k_{th}}{\rho c}\nabla^2 T + \frac{\Phi}{\rho c} \tag{21}$$

Where $\mathbf{u}$ is the velocity vector, k_{th} is the thermal conductivity, c is the heat capacity and Φ is the internal heat production term given by

$$\Phi = 4\mu\dot{\epsilon}_e^2 \tag{22}$$

Because the ice sheet many places is near the pressure melting point it can be beneficial to formulate the energy conservation in terms of enthalpy as in Aschwanden et al. (2012). The enthalpy conservation equation can be written (from Seroussi et al., 2013):

$$\rho\left(\frac{\partial E}{\partial t} + \mathbf{v}\cdot\nabla E\right) = \Phi + \begin{cases} \nabla\cdot\left(\frac{K_i \nabla E}{C_i}\right) & \text{if } E < E_s \\ \nabla\cdot\left(k\nabla T_{pmp} + \frac{k_0}{L}\nabla E\right) & \text{if } E_s < E < E_l \end{cases} \tag{23}$$

where E is enthalpy, E_s is the enthalpy of pure ice, E_l is the enthalpy of pure liquid water at the pressure-melting point (T_{pmp}), K_i is the ice

diffusivity coefficient, C_i is the heat capacity of ice, $k = (1-\omega)k_i + \omega k_w$ is the mixture thermal conductivity (ω is water fraction, k_i and k_w is the thermal conductivity of pure ice and water) and k_0 is a small positive constant. The temperature, T will then be found for cold ice, where $\omega = 0$ and $E < E_s$, by

$$T = \frac{E - E_s}{C_i} + T_{pmp} \tag{24}$$

and for temperate ice where $\omega = (E - E_s)/L$ and $E_s < E < E_l$, by

$$T = T_{pmp} \tag{25}$$

This makes it possible to calculate the temperature of poly-thermal ice without having to track the phase transition.

Temperature boundary conditions

The ice surface temperature is assumed to be equal to the air temperature. At the base a geothermal heat flux Q_{geo} is applied. A relation between the frictional heat and the geothermal heat flux is given by:

$$k_{th}\nabla T \cdot \mathbf{n} = Q_{geo} - \boldsymbol{\tau_b} \cdot \mathbf{v_b} \tag{26}$$

Assuming no basal melt the heat flux from the base is thus given by a combination of the geothermal heat flux and the heat release from frictional heat as ice slides over the base.

3.2 USING ISSM

The specific setup of ISSM for the modelling studies in this this is explained in detail in chapters 5 and 6, where the model is applied in experiments. The purpose of this section is to present the work flow in ISSM, in general terms, in order to discuss the usefulness of the model approach. Thus, considerations concerning both method and input data will be presented here, without going into detail of the technical setup of the model.

The general work flow applied in this thesis is presented in Figure 3.1. The model is initially set up using present day geometry and an initial guess of basal friction. A mesh is created and resolution is adapted to observed velocities (see example of model mesh in Figure 3.2). Then the friction coefficient (k in equation 19) is inferred in a data assimilation process including several steps. First, the stress balance equations are solved according to the initial guess of basal friction. The model velocity misfit is then evaluated and the basal friction map is updated accordingly. The basal friction map will, finally, be used as a new initial guess and the process is run again until the velocity misfit is smaller than a given threshold. When a good match between model and observed velocity is obtained, the model can be

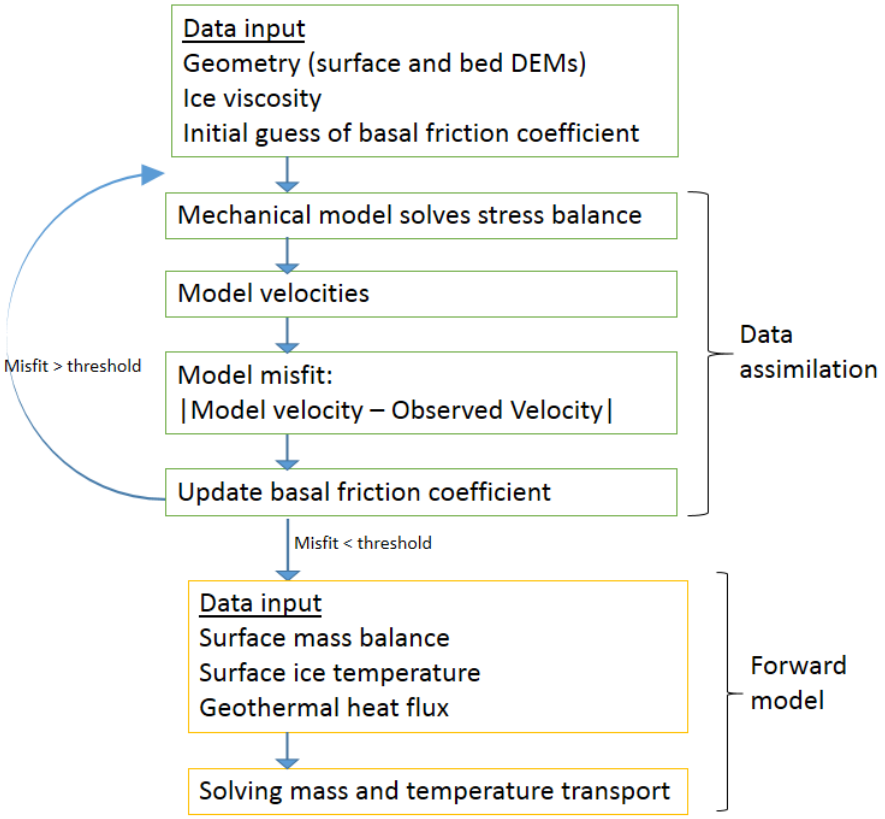

Figure 3.1: Idealised work flow of the use of ISSM in this thesis.

run forward. In the forward model simulation, additional input data is needed: Surface mass balance as well as ice surface temperature and geothermal heat flux if the thermal model is applied.

3.2.1 *Geometry*

Initial model geometry requires well known surface and basal topography. Digital elevation models (DEM) covering the surface of the Greenland ice sheet can be created by photogrammetry of optical stereo images e.g. Arctic DEM (Noh and Howat, 2015) and Greenland Ice Mapping Project (GIMP, Howat, Negrete, and Smith, 2014). The maps will consist of a combination of images from several years to cover larger areas. The different images are combined assuming only small change in elevation between the different years. In areas near the coast of Greenland the ice sheet can change by 10s of meters per year (Csatho et al., 2014), thus, the timing of the DEM creation can be very important for representing the surface correctly in the margin areas. The ice flow model will be sensitive to the initial geometry and become unrealistically stable or unstable in the case of the glacier surface slope being under or over estimated, respectively.

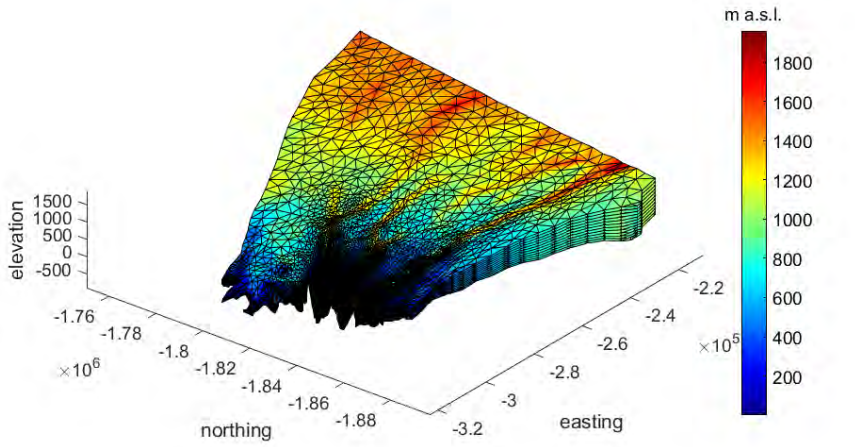

Figure 3.2: Model mesh of resolution 100 m to 5 km is plotted on top of thickness map in a three dimensional plot of the model domain of Upernavik Isstrøm.

The basal DEM is obtained from the BedMachine (Morlighem et al., 2014, 2017). The BedMachine DEM is generated using a model approach by Morlighem et al. (2013), to fill out gaps between discrete measured lines of observed basal topography. This approach implements the principle of mass conservation, where surface velocity measurements are used to infer the basal topography. In the process, the basal topography that will best match the ice flux and observed basal topography, is found. Thus, the map will be physically realistic and work well for ice flow modelling. However, several uncertainties are introduced. First of all, the bed map's dependence on velocity will introduce higher uncertainties in areas where velocity is uncertain. This is commonly the case in very slow moving areas, as well as close to the ice margin. Furthermore, the ice flow properties will have to be assumed to calculate the flux and this is done by assuming that the mean ice flow velocity equals the surface velocity. While this is physically realistic in areas with low basal friction and high basal sliding, such as ice streams, the assumption fails for areas with high friction and low sliding as the interior of the ice sheet. Thus, when using the BedMachine DEM it is important to keep in mind that this is a model product that contains high uncertainties.

3.2.2 *The inferred field*

In this thesis the basal friction is inferred by data assimilation (Figure 3.1). Basal conditions are a complicated matter as the bed can be everything between almost vertical cliffs, uneven bedrock and a thick sediment layer with a varying amount of water present. As the bed is generally not directly accessible, detailed information about the bed is unknown. Thus, the basal friction coefficient is an obvious

choice as a field to be obtained through data assimilation. However, this requires knowledge about the ice viscosity. As seen in equation 6, and discussed in the review in chapter 2, the viscosity is highly dependent on temperature through the prefactor B. However, B also depends on the impurity content of the ice as well as damage which becomes highly important in ice streams. Thus, ice viscosity is also highly unknown, and could be determined through data assimilation if the basal friction was known. In this thesis B will be assumed to only dependent on temperature (and micro water content for temperate ice).

3.2.3 *Running the model forward*

When the model is properly initialised it is possible to run it forward. Surface and basal mass balance will have to be applied, as well as ice surface temperatures and geothermal heat flux.

At the surface, the mass balance equation (equation 20) requires the time evolving surface mass balance (SMB), i.e., the balance between ablation and accumulation. This will most commonly come from a regional climate model (RCM). There are currently several well developed RCMs where simulated SMB is available including Modele Atmospherique Regional (MAR) (Fettweis et al., 2013), Regional Atmospheric Climate Model (Racmo, Noël et al., 2015) and HIRHAM5 (Christensen et al., 2007). The RCMs use different ways of calculating the SMB and are therefore also different and major uncertainties remain. Two studies by (Schlegel et al., 2013, 2014) show that model simulations of ice flux are sensitive to uncertainties in the spatial distribution as well as magnitude of SMB and this remain the area of highest estimated uncertainties within decadal scale simulations in ISSM. The temperature model will require an ice surface temperature which will be approximated to be equal to the surface air temperature. Implications of this will be described in the next section.

At the base, mass can be removed by melting, but also accumulated by refreezing ($\dot{M}_b$ in equation 20). The subglacial melt rate can be of several millimeters per year under slow moving temperate ice (Cuffey and Paterson, 2010), depending on the geothermal heat flux. Faster moving ice, such as ice streams will usually generate much higher melt due to the higher heat production at and near the bed. Generally it is hard to quantify the melt rate, but uneven melt rates can be detected in radar images as warping of the internal layers (Fahnestock, 2001). For the purpose of modelling the flow of ice streams on short time scales, the millimeter to centimeter scale changes at the bed can be neglected compared to the meter scale changes at the surface.

The basal friction coefficient, was inferred through the data assimilation process. The data assimilation process has the major drawback that it does not include any physical model and thus the basal friction

coefficient will have to be assumed constant in time. Furthermore, this coefficient will contain information about basal friction as well as all the other unknown processes which are not accounted for in the model. Keeping the basal friction coefficient constant on decadal timescales, will cause significant model uncertainties, as was shown by a study on a Svalbard glacier by Gong et al. (2016). In the effort to quantify the basal drag, several studies are working on developing more physical models of basal changes (e.g. Damsgaard et al., 2016; Fleurian et al., 2014; Werder et al., 2013), however, they remain complicated and not easily applied in ice flow models and thus not included here.

3.2.4 *Temperature*

Temperature is important to ice viscosity through the viscosity prefactor B in equation 6. As discussed in section 2.5, the heat diffusion through ice occurs relatively slowly and measurements are scarce. Thus, to obtain a realistic temperature field of the Greenland ice sheet, it is necessary to take past evolution of surface temperatures in to account. Hence, this requires a long forward model run. For this purpose the forward capabilities of the thermomechanically coupled ISSM is used. The forward model will be forced by changing ice surface temperatures, which are assumed to be equal to air temperatures. Thus, the effect of cryo-hydrologic warming is neglected and temperatures will likely be underestimated in the ablation area. Further approximations about a constant model domain, surface mass balance field and basal friction coefficient is also assumed. Thus, the temperature field includes high uncertainties and it is most likely too cold, due to the neglection of cryo-hydrologic warming. This will leave ice viscosity likely to be too high.

3.3 APPLICABILITY OF THE MODELLING METHOD

This chapter outlined how the ice flow model is set up and discussed some of the uncertainties in the model input data and setup. Any ice flow model will have some limitations in applicability due to the choice of model and setup. The evaluation and usefulness of cryospheric models was discussed in detail by Van Der Veen (1999), and key aspects of his discussion is still valid to present day models. A main conclusion was that models are a tool to evolve current knowledge, when they are used as virtual laboratories to test proposed hypotheses. The data assimilation capabilities makes ISSM exactly this: A virtual laboratory, where unknown mechanisms can be identified and hypotheses about flow can be tested. The model is used in this way in Paper III (chapter 6) of this thesis. The method of data assimilation to obtain a model field, like the basal friction, will result in the

fact that this field cannot evolve in time. Still, the model is applied in a forward way in Paper II (chapter 5). However, this is justified by the fact the forward simulation in used on very short timescales to test the time evolution of the basal friction field it self.

4

PAPER I: CURRENT STATE OF UPERNAVIK ISSTRØM

Figure 4.1: Upernavik Isstrøm (UI-3), seen from the sea, August 2014

This chapter is published in Journal of Geophysical Research - Earth Surface with the reference: *Larsen, S. H., S. A. Khan, A. P. Ahlstrøm, C. S. Hvidberg, M. J. Willis, and S. B. Andersen (2016), Increased mass loss and asynchronous behavior of marine-terminating outlet glaciers at Upernavik Isstrøm, NW Greenland, J. Geophys. Res. Earth Surf., 121, 241–256, doi:10.1002/2015JF003507*

4.1 ABSTRACT

In order to model and predict future behavior of marine terminating glaciers, it is essential to understand the different factors that control a glaciers response to climate change. Here we present a detailed study of the asynchronous changes in dynamic behavior of four adjacent marine-terminating glaciers at Upernavik Isstrøm (UI), Northwest Greenland, between 1992 and 2013. Velocities were stable for all outlets at UI between 1992 and 2005. The northernmost glacier started to accelerate and thin in 2006 and continued to do so into 2011 after which time the velocities stabilized. The second most northerly

glacier started to accelerate and thin in 2009 and continued to do so until the last observations in 2013, dramatically increasing the area affected by dynamically induced thinning. The southern glaciers show little change, with the most southerly glacier undergoing slight retreat and deceleration between 1992 and 2013. These observations point out the fact that the UI glaciers are reacting to climate change on different timescales. The asynchronous behavior of the four neighboring glaciers is explained in terms of the individual glaciers' geometry and terminus position. The northernmost glacier is believed to have had a floating tongue between 1985 and 2007 which disintegrated in 2007-2008. This release of back stress destabilized the glacier causing it to accelerate and thin rapidly. We suggest that the ice tongue broke up due to ocean-warming induced thinning in the late 1990s. Recent response on UI glaciers is found to be related to increased surface melt. Our investigations suggest that three out of the four main glaciers in the UI are likely to be in unstable positions and may have the potential to rapidly thin and accelerate and increase their contribution to sea level in the future.

4.2 INTRODUCTION

The mass loss rate of the Greenland ice sheet doubled from about 150 Gt yr^{-1} between 2000-2005 to more than 300 Gt yr^{-1} between 2009-2012 (Enderlin et al., 2014; Helm, Humbert, and Miller, 2014; Khan et al., 2014b). 30-50 % of the mass loss between 2000 and 2012 was through ice discharge in the form of calving at marine-terminating glaciers (Broeke et al., 2009; Enderlin et al., 2014; Khan et al., 2015). Marine-terminating glaciers show non-linear reactions to external forcings such as warming of ocean and air temperatures as well as differences in bed geometry as the grounding line advances and retreats (Meier and Post, 1987; Nick et al., 2009; Schoof, 2007). Neighboring glaciers can therefore react quite differently to similar climate forcings as observed by Khan et al. (2013) at Upernavik Isstrøm (UI) in NW Greenland. UI consists of several fast flowing ice streams that terminate into the same fjord (Upernavik Isfjord) (Figure 4.2) and is therefore an optimal study site for examining the interaction between climate, ice dynamics, bedrock topography and the influence of the ocean. UI was first observed in 1849 when it terminated in a single glacier trunk (Weidick, 1958) and has since retreated by 25-30 km and split into several glaciers.

In this paper we present a detailed study of the asynchonous changes of four marine-terminating outlet glaciers at UI. We focus on the four main east to west flowing glaciers which we number UI-1 to UI-4 from north to south, respectively (Figure 4.2). The study by Khan et al. (2013) provided evidence of two instances of increased dynamically induced thinning at UI outlet glaciers. The first event occurred

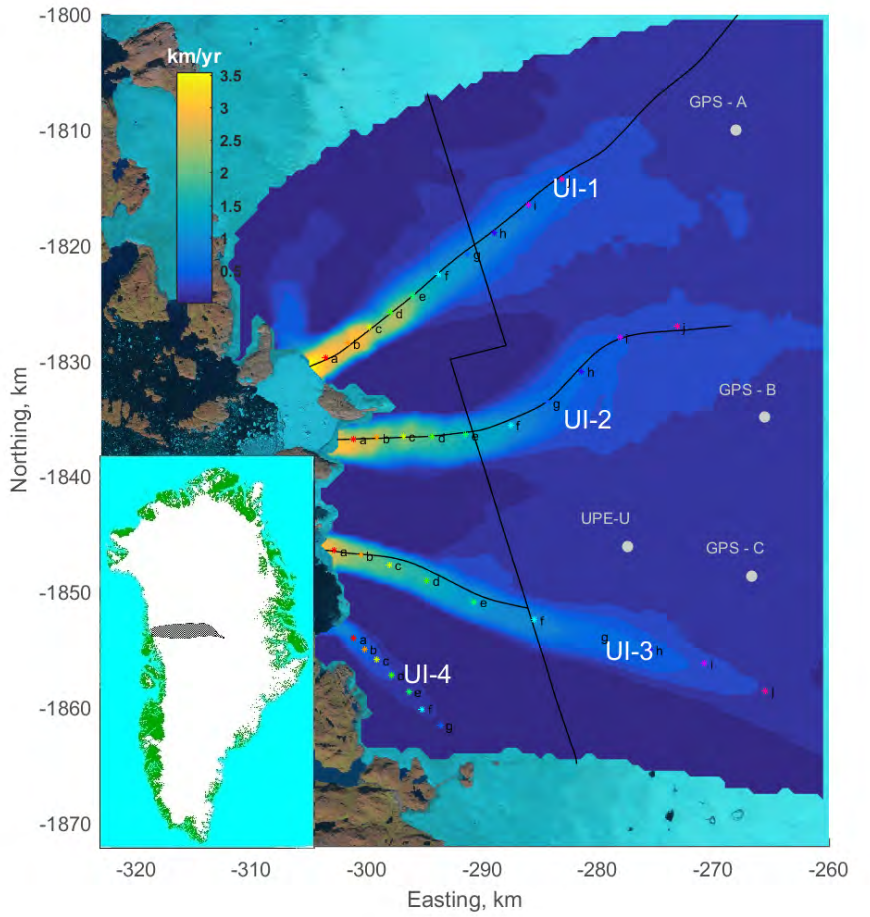

Figure 4.2: Velocity map of UI winter velocities 2000/2001 (Joughin et al., 2010) for the lower part of the UI catchment. Black north/south ward lines indicate CReSIS crossing lines, 2010 (Gogineni, 2012), used as flux gate. Black center lines of each glacier is the CReSIS lines from 2013 (Gogineni, 2012) used in Figure 4.3. Colored points marked a-j on each glacier mark the points along the center line where velocities are plotted in Figure 4.10 and 4.11. The dots indicate the position of the PROMICE automatic weather station UPE-U (966 m a.s.l.), and the position of the three permanent GPS stations used for elevation change studies. Landsat image (available from the U.S. Geological Survey) from 2000 is used as background. Inserted is Greenland ice/land mask (Citterio and Ahlstrøm, 2013), the shaded area indicate the catchment area of UI. Easting and northing are in polar stereographic projection using 45°W and 70°N as reference.

on the southernmost tributary (UI-4) between 1985 and 1991, while the second occurred on the northernmost tributary (UI-1) between 2005 and 2010. Both events occurred during periods when both air and ocean temperatures were observed to be anomalously high and the dynamic changes were suggested to be triggered by this according to Khan et al. (2013). However, the outlets of UI are, due to their proximity, considered to be subject to similar external forcing, from changes in the surface air temperature and precipitation as well as from changes in the ocean temperature. The different reactions to similar forcings must therefore be due to differences in the non-linear response to climate change of the individual UI outlet glaciers.

We aim to examine the asynchronous behavior of the four neighboring outlet glaciers and establish if it is likely that the glaciers will show continued increase in dynamic mass loss, providing a record for calibration and validation of future ice-dynamic modeling experiments. To do this we provide an extended analysis (compared to that of Khan et al. (2013)) of changes in velocity, terminus position and surface elevation, to show the detailed dynamic behavior of the UI outlets. We also examine the changes in regional climate model data of surface mass balance (SMB) and the different bedrock geometry of each of the UI glaciers. From this we are able to establish how differences in terminus position, bed and fjord geometry can cause different non-linear response of the glaciers.

We first present the geometry of the UI outlets from existing airborne radar data along the center lines of the glaciers (Gogineni, 2012) and then examine the sparse bathymetry of the fjord. We then present recent changes in SMB, calving front position and surface elevation and compare them to the changes in ice velocities. The velocity data are also used in a simple flux gate calculation to give an estimate of the increase in mass loss between 2000 and 2012 partitioned into surface melt and ice discharge. Finally the observations are discussed in terms of each individual glaciers' sensitivity to changes in climate forcing.

4.3 ENVIRONMENTAL SETTINGS

The stability of glaciers and ice streams have been shown to be related to the bedrock geometry beneath the glacier. The slope of the bed of a glacier and the width of the glacier trough both influence the dynamics of a glacier (e.g. Carr, Stokes, and Vieli, 2013; Enderlin, Howat, and Vieli, 2013; Khan et al., 2014a). If a glacier moves into deeper water or a wider fjord, the calving front area increases, which can increase the calving rate (Schoof, 2007). A fjord widening will, furthermore, cause divergence of the flow which will cause thinning of the glacier, reducing the relative lateral shear stress. In addition, a glacier with a floating tongue is likely to be more sensitive to ocean

temperatures due to the higher surface area in contact with ocean waters compared to a grounded calving front (Straneo et al., 2013). Measurements of bed geometry and fjord bathymetry are therefore crucial for understanding the glacier system as a whole.

The surface and bed of the center lines of the four glaciers were measured directly with radar in 2013 by the Center for Remote Sensing of Ice Sheets (CReSIS)(Gogineni, 2012) (Figure 4.3). From the radar data the calving front of UI-1 is observed to be 1 km in thickness, and grounded in 2013. The bedrock elevation gradually rises inland up to around sea level at a distance of about 45 km from the front. The inferred basal topography from Morlighem et al. (2014) suggests that the glacier trough is narrow but widens only a few km inland from the 2013 front position (Figure 4.3a and 4.4). The front of the second glacier, UI-2, is about 250 m thick according to radar data (Figure 4.3). The surface slope decreases towards the front, and the surface of the outermost 2-3 km of the glacier is horizontal. Although the quality of radar data decreases close to the calving front, the data indicates that UI-2 has a floating ice tongue of around 2.5 km in length. This is supported by the surface elevation being at buoyancy (Figure 4.3d). The elevation change observed between 2011 and 2014, using high resolution (3 m) digital elevation models (Figure 4.5) show low elevation change at the southern part of the frontal area of UI-2 compared to the northern part, indicating that this area of the glacier could be afloat. Landsat images from e.g. June 14, 2009 and June 17, 2010, show large tabular icebergs (~500 m in diameter) floating away from the front, supporting this interpretation. UI-2 has a downward sloping bed up to 25 km inland from the grounding line, and the inferred basal topography (Figures 4.3b and 4.4) shows the trough getting wider until about 7 km inland. The calving front of the third glacier, UI-3, is about 500 m thick according to radar data (Figure 4.3). The surface slope is steadily decreasing towards the margin and base is horizontal, suggesting that it is grounded. The bed is slightly downward sloping inland and the trough of UI-3 is by far the longest of the four glaciers and found to be below sea level for up to 142 km inland (Morlighem et al., 2014). The trough of UI-3 widens until about 5 km inland (Figure 4.3c) and the first 5 km have ice thicknesses that are within 100 m from being floating. For the fourth glacier, UI-4, the radar depth data has many data gaps and the profile is therefore not shown. The inferred basal topography (Figure 4.4) suggests that the base of UI-4 is less than 200 m below sea level at the front, and that the bedrock is above sea level about 5 km from the front ((Morlighem et al., 2014)). This suggests that UI-4 is shallow with ice thicknesses below 400 m between the front and 5 km inland.

The fjord bathymetry is important for fjord water circulation and for which water masses are able to reach the glacier margin (Straneo and Heimbach, 2013). Furthermore, it gives an indication of the

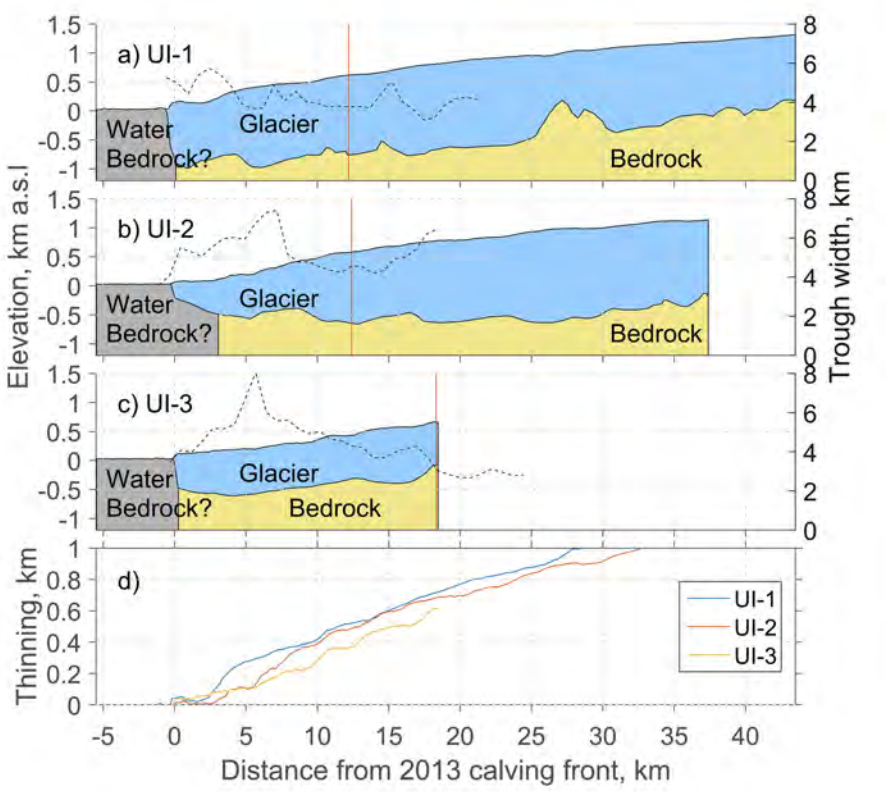

Figure 4.3: Surface and bed topography of glaciers UI-1 to UI-3 from CReSIS level 2 radar depth data (Gogineni, 2012) obtained April 18, 2013. Light blue indicates glacier ice, yellow indicate bedrock and gray indicate fjord water or bedrock. The bedrock in the fjord is unknown due to the impenetrability of radar through water. The vertical orange line indicates the position of the flux gate. UI-4 is not shown due to lack of good data.

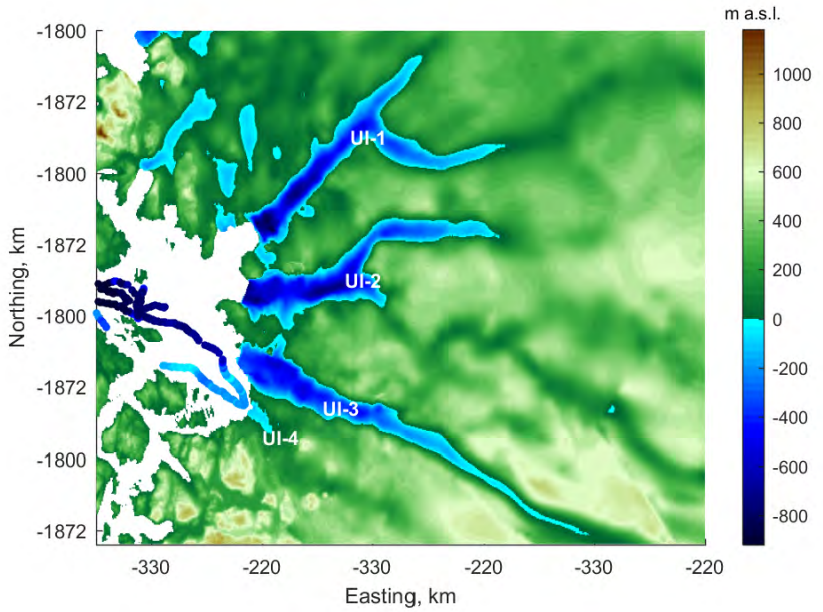

Figure 4.4: Inferred basal topography from Morlighem et al. (2014) and bathymetry data from Andresen et al. (2014). Easting and northing are in polar stereographic projection using 45°W and 70°N as reference.

glacier bed in the past at former, more advanced positions of the front. Bathymetry measurements from Andresen et al. (2014) (Figure 4.4) shows water depths of around 1 km in most of the fjord. Due to ice conditions it is not possible to measure water depths near the front of glacier UI-1 and UI-2. The glacier trough is inferred to be more than 900 m deep at the terminus of UI-1 (Figures 4.3 and 4.4) and so the inner parts of the fjord in front of UI-1 and UI-2 are also expected to be around this depth (Figure 4.4), but the presence of sills cannot be excluded. The water depth in front of UI-3 is below 900 m according to the bathymetry measurements by Andresen et al. (2014) (Figure 4.4). The southern part of the fjord, where UI-4 terminates, is shallower, and only about 200 m deep close to the front of UI-4 (Andresen et al., 2014). Warm subsurface ocean water, which is observed to occur at a depth below 200 m, can therefore reach UI-1 to UI-3 whereas UI-4 is more likely to be only affected by cold polar waters (Andresen et al., 2014).

4.4 RECENT CHANGES

As reported by Khan et al. (2013) and Nielsen et al. (2012), major acceleration, thinning and retreat have been observed, mainly at UI-1, between 2000 and 2010. Here we extend the observation record and show changes in surface climate and calving front position, and compare this with velocity and surface elevation changes until 2013. We

further analyze velocity changes by investigating seasonal changes in velocity from 2009 to 2013.

4.4.1 *Surface mass balance*

SMB data since 1958 (Figure 4.6) is provided as output from the regional climate model, MAR v3.5 (Modéle Atmosphérique Régional, Fettweis et al. (2013)). The most important finding is that SMB values are generally more negative during the last decade compared to the previous four decades. The SMB from MAR is averaged over the lower ablation area (downstream of the flux gate as indicated by black lines in Figure 4.2) and compared with the point measurement of SMB from an automatic weather station (UPE-U) operated by the Programme for Monitoring the Greenland Ice Sheet (PROMICE) (see location in Figure 4.2). The variations in SMB agree between the two data sets for the overlapping period between 2009 and 2012. The PROMICE data show higher values mainly due to the location of the weather station at a higher elevation than the area over which SMB from MAR is averaged.

4.4.2 *Calving front position*

Calving front positions are mapped from Landsat 7 and Landsat 8 images (Figure 4.7). To obtain a record from the time of annual minimum ice extent the latest cloud free image from August or September is used for each year. Years with no useful Landsat images in August and September are discarded. All glaciers exhibit an overall retreat during the period 1985-2013. The retreat of UI-1 leads the calving front into a wider fjord and the northern tributary of UI-1 detached from the main glacier around 2006. This is followed by a major (4 km) retreat of UI-1 between 2007 and 2008. Due to the very rapid retreat, and the observation of large tabular icebergs floating away (as seen on Landsat images from e.g. April 4, 2007 and May 8, 2008), this is interpreted as the disintegration of a floating ice tongue. The calving front retreat is investigated in more detail in Figure 4.8 and 4.9 where the retreat is defined using the rectilinear box method (e.g. Carr, Stokes, and Vieli, 2013; Lea, Mair, and Rea, 2014; Moon and Joughin, 2008). A rectilinear box is defined over the glacier front (Figure 4.7), and the retreat is then calculated as the area change of the box covering the glacier, divided by the width of the box. By using this method we are able to account for the asymmetric retreat of the calving fronts. However, mapping the calving front of UI-3 posed a problem as it appears that icebergs are grounded on a topographical high point just at the center of the calving front. In some years icebergs were not clearly detached from the glacier and are therefore mapped as part of the

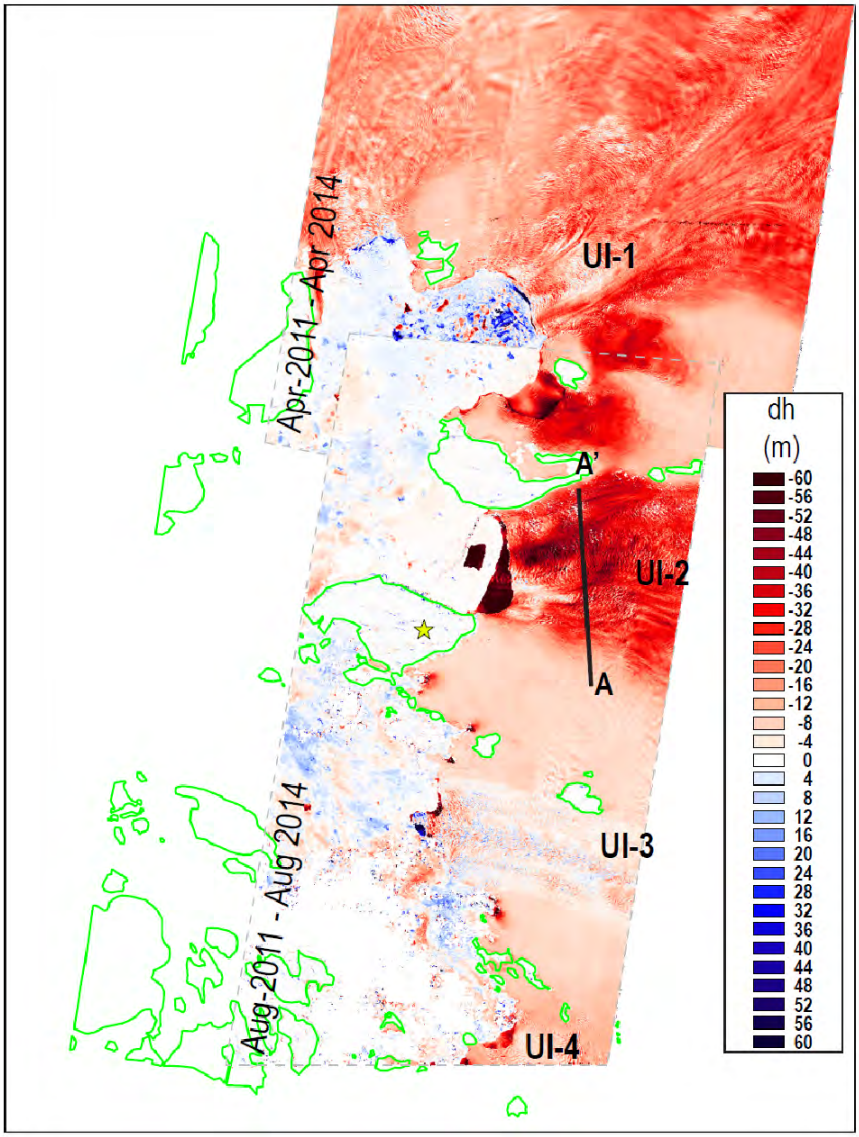

Figure 4.5: The elevation change between 2011 and 2014 from high resolution (3 m) digital elevation models.

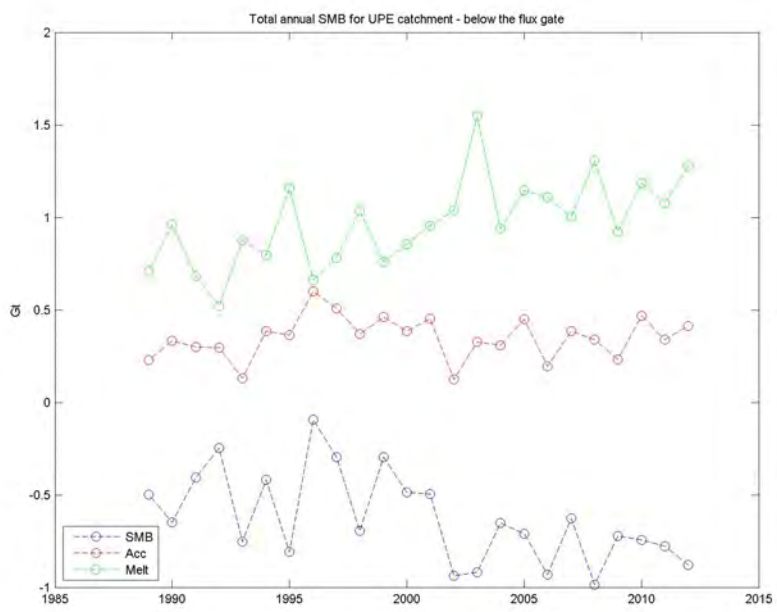

Figure 4.6: Blue, average SMB from the regional climate model MAR (Modéle Atmosphérique Régional, Fettweis et al. (2013)) for the years 1958-2013. MAR SMB is averaged over the area downstream of the flux gate (see Figure 4.2). Red, point measurements of net SMB from the PROMICE automatic weather station UPE-U for 2009 - 2012.

glacier (see Figure 4.7). Thus, the measured calving front fluctuations are not necessarily representative of the calving front behavior.

All of the glaciers exhibited an overall retreat during the 28-year period studied here. The retreat of UI-1 started around 1997 and rates peaked in 2007 and 2008 after which the retreat rate slowed to previous levels but the retreat continued through 2012. UI-2 showed fluctuations of $\pm$500m in the calving front position during 1997-1999 (Figure 4.9). The glacier retreated rapidly by 1.5km between 2008-2010 after which the calving front remained stable. UI-3 showed fluctuations in calving front position but only a slight retreat of 1.2 km since 1985, and the calving front of UI-4 showed a general retreat between 1985 and 2013 in which period the front retreated 3.3 km (Figure 4.8).

4.4.3 *Ice flow velocity*

Figure 6 shows winter velocities between the winter of 1992/1993 and the winter of 2013/2014. For the years 1992/1993 - 1996/1997 and again 2002/2003-2004/2005 velocity data are from ESA CCI (2015). For the period 2000/2001 and 2005/2006-2013/2014 velocity maps from Joughin and Alley (2011) and Joughin et al. (2010) are used. From 1992 to 2005 the glaciers were flowing with similar and constant

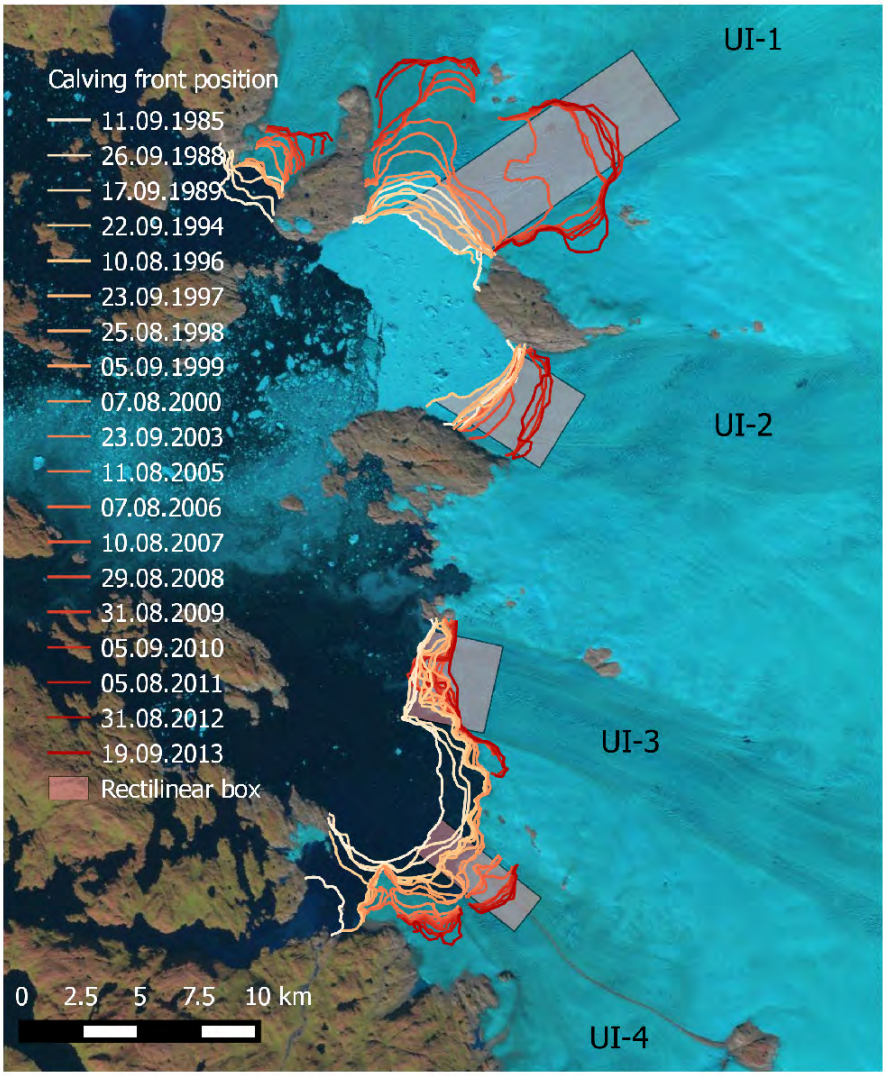

Figure 4.7: Calving front position from Landsat images. The calving fronts are digitized from the last available image from each year, usually around August - September. The colored boxes indicated the rectilinear boxes used for obtaining calving front retreat in Figure 4.8 and 4.9

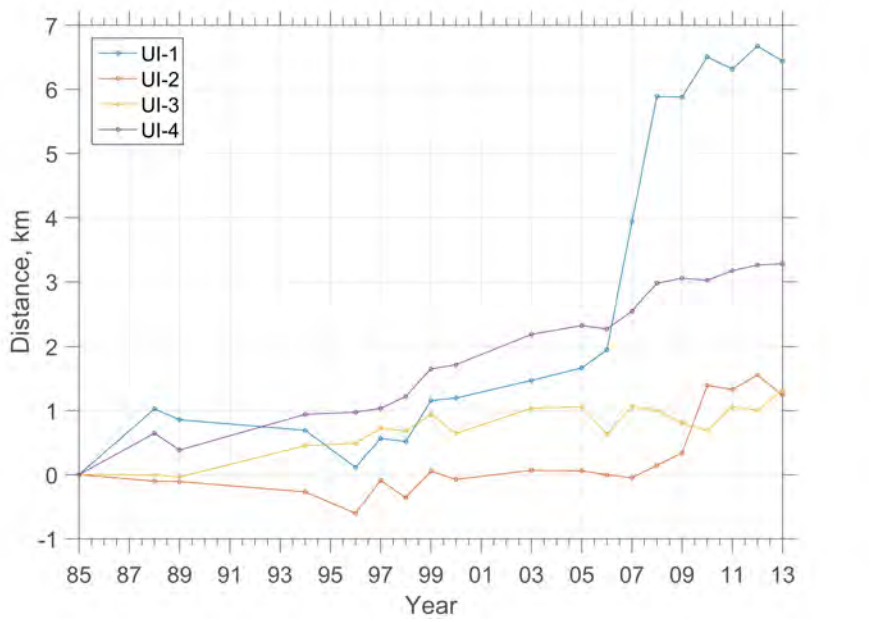

Figure 4.8: The distance from the 1985 calving front position using the rectilinear box method, boxes are shown in Figure 4.7.

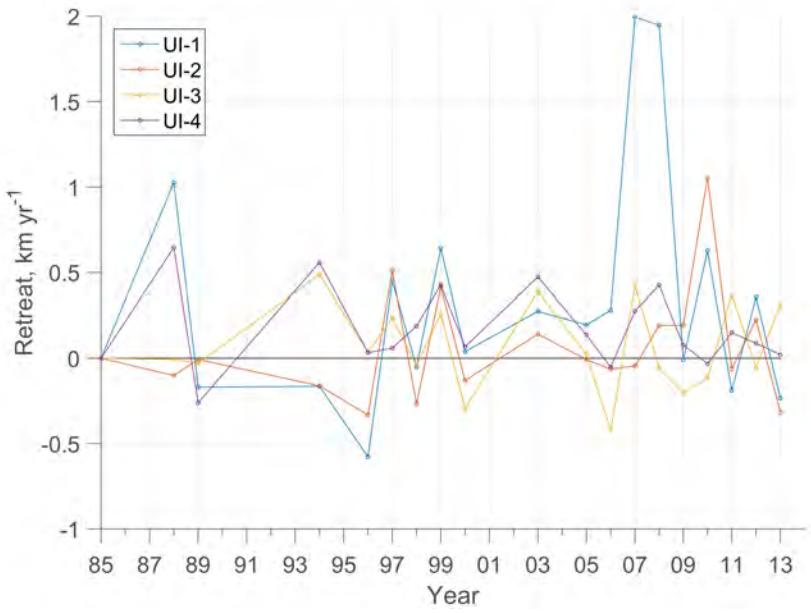

Figure 4.9: The retreat of the calving front since last measurement, using the rectilinear box method, boxes are shown in Figure 4.7. The retreat is divided by the number of years between measurements so the units are in km yr^{-1}. Positive values indicate that the calving front is further inland than the previous year and negative values indicate an advance of the calving front.

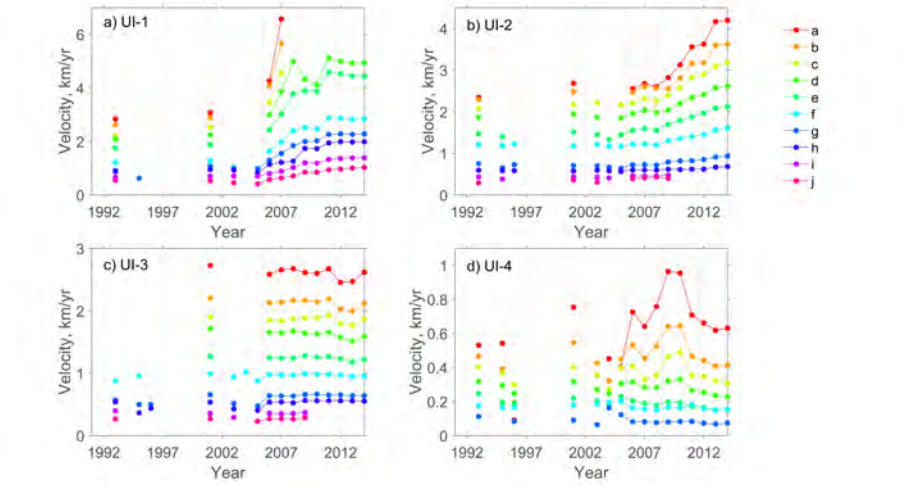

Figure 4.10: Winter velocities (data from Joughin et al. (2010) and ESA CCI (2015)) at points, denoted a-j and marked with colored points in Figure 1, along the flowlines of UI-1 to UI-4. Point "a" is closest to the calving front for each glacier. The dashed vertical lines show the three time intervals used in Table 1 and 2. Flow is fastest at the calving front of all glaciers, decreasing with distance upstream.

speeds. The asynchronous acceleration of the individual glaciers in the subsequent years is described below.

The speed near the terminus of UI-1 (Figure 4.10a, point a-d) increased by about 50-60% (2 km yr^{-1}) between 2006 and 2008 in response to the disintegration of the floating ice tongue (Figure 4.7). Acceleration reached at least 20 km inland, with a speed increase of around 25% (500 m yr^{-1}) at point h-j. Between 2009 and 2010 UI-1 decelerated by about 15% (1 km yr^{-1}) near the terminus (point c) and remained stable further inland (point d-e), before it resumed acceleration and reached its maximum observed speed in 2011 (5 km yr^{-1} at point c); in 2012-2013 the ice flow speeds remained at this high level. UI-2 started to accelerate after 2008 and at point a) the flow speed gradually increased by around 300 m yr^{-1} each year up until the last observation in 2013 (Figure 4.10b). In total, the gradual velocity increase is of around 50% (1.5 km yr^{-1}) since 2008 near the terminus and 15% (200-300 m yr^{-1}) about 20 km inland. UI-3 showed a slight decrease in ice flow speed (Figure 4.10c) (1-2% or 100-200 m yr^{-1} at point a and b) between 2000 and 2013. UI-4 showed a general decrease in flow speeds over the period with the exception of 2009-2010 when velocities increased by about 30-40% near the terminus (point a and b). After 2008 the glacier decelerated and returned to the background velocity.

Seasonal velocity patterns of marine terminating glaciers around the coast of Greenland were studied by Moon et al. (2014) and from velocity measurements between 2009-2013, glaciers were classified

within three types. Type 1 glaciers are glaciers where the seasonal speedup correlates well with the terminus position and are therefore primarily controlled by ice front position. Type 2 and 3 are glaciers where the seasonal velocity patterns are primarily correlated with meltwater runoff. Type 2 glaciers have a strong early summer speed increase, with a slowdown to winter speeds that occurs near midsummer indicating that the glacier bed is lubricated by meltwater reaching the bed. Type 3 glaciers have a late spring/early summer speedup and a late summer minimum where ice flow speeds are lower than winter velocities. This could indicate that there is enough meltwater available at the glacier bed for the sub-glacial hydrological system to become so efficient that all basal water is removed from the bed through large channels and the glacier bed is therefore less slippery. The glaciers UI-1, UI-2 and UI-3 were included in the study by Moon et al. (2014), and while UI-1 and UI-2 did not show any distinct patterns during 2009-2013, UI-3 showed type 2 behavior. Figure 4.11 shows the velocities 4-5 times per year, along the same profiles as in Figure 4.10, with the melt season highlighted in gray. All glaciers exhibited spring or summer speedup and while UI-1 and UI-2 showed variation in when and by how much the slowdown occurred, UI-3 showed type 2 behavior, confirming the description in Moon et al. (2014). UI-4 can be categorized as a type 3 glacier with early spring speedup and midsummer slowdown below winter speeds. This could indicate that an efficient drainage system can develop during the melt season at UI-4. For every melt season UI-4 decelerated to velocities lower than previous years resulting in a general deceleration between 2009 and 2013. From figure 4.10a we see that the acceleration event at UI-1 in 2010 was a short-duration event that occurred between July and August. In contrast, the acceleration of UI-2 was nearly constant throughout the 2008-2013 period (Figure 4.11b), highlighting the difference between the two glaciers' behavior.

4.4.4 *Ice surface elevation*

Surface elevation changes were highly variable between 2005 and 2011 for the lower parts of the UI ablation area (Nielsen et al., 2012). To get a better idea of the spatial and temporal changes between 2008 and 2012 we use Lidar elevations collected by the Airborne Topographic Mapper (ATM) (Krabill, 2013). Since the ATM lines do not repeat the same track every year, we use a SPOT 5 HRS DEM from 3 June 2008 (Korona et al., 2009) as a reference DEM and evaluate elevation changes relative to this. The SPOT DEM is the same as used in Nielsen et al. (2012), has a resolution of 40x40m and is corrected for a constant bias in elevation according to Nielsen et al. (2012) (Figure 4.12). In 2008 and 2009, major thinning of 15-20 m yr^{-1} was observed on UI-1, followed in 2010 or 2011 by thinning of around 20-

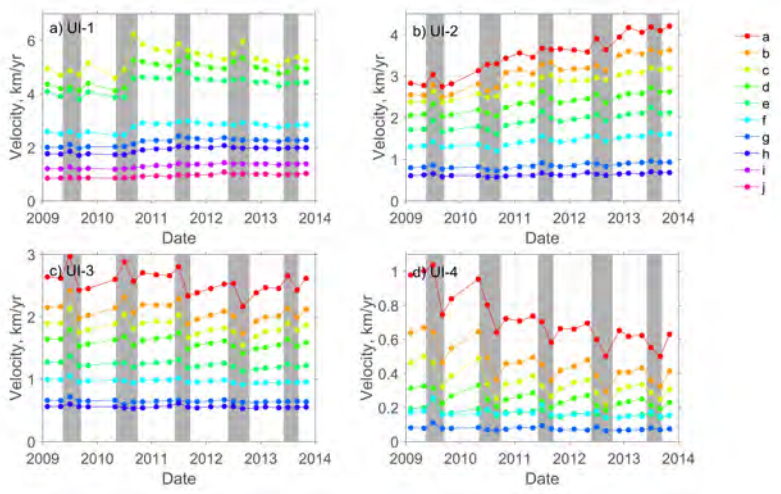

Figure 4.11: Monthly velocities for mainly February, April, July, August, November between 2009-2013, at points, denoted a-j and marked with colored points in Figure 1, along the center flow lines of UI-1 to UI-4. (2009-2011 data from Joughin and Alley (2011), 2012-2013 data from Joughin personal communication). The shaded areas indicate the periods with average daily temperatures above melting point at the PROMICE weather station UPE-L.

30 m yr^{-1} at UI-2, both continued to thin into 2012. While UI-1 and UI-2 thinned up to 80 m between 2008 and 2013, UI-3 showed a total surface lowering below 10 m and UI-4 a 10-20 m total elevation lowering (Figure 4.12). The measured elevation and the thinning rates at three permanent GPS stations located on ice 30-40 km upstream (see location in Figure 4.2) are shown in Figure 4.13. At GPS-A the thinning rates changed around 2005 from 0.2 m yr^{-1} to 1.3 m yr^{-1} and then again around 2010 to 2.3 m yr^{-1}. For GPS-B the thinning rate changed around 2010 from 0.5 m yr^{-1} to 1.7 m yr^{-1} and for GPS-C the thinning rate remained constant around 1.1 m yr^{-1}. SMB rates modeled by MAR indicate that surface melt rates were much smaller than the observed thinning rates at each of the GPS points. This suggest that the dynamically induced thinning of both UI-1 and UI-2 has propagated at least 40 km upstream. GPS-C is located approximately 25 km from the margin and 10 km north of UI-3 and therefore, it may be affected by dynamic thinning propagating from UI-2 or UI-3. From Figures 4.5 and 4.12 it is clear that UI-3 experienced only little thinning below 10 m between 2008 and 2013. The observed thinning at GPS-C exceeded the surface mass balance (Figure 4.13) and it is thus likely that dynamic thinning from UI-2 has propagated to the location of GPS-C (Figure 4.12).

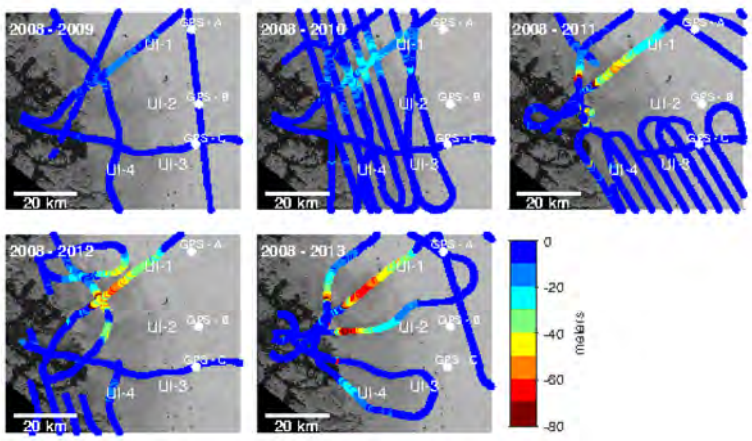

Figure 4.12: Total elevation change between the SPOT 5 HRS DEM from June 2008 (Korona et al., 2009) and ATM measurements 2009-2013. The ATM measurements were made in spring of each year and therefore represent the surface lowering from the previous year, ignoring changes in snow depth from year to year.

4.4.5 *Total and partitioned increase in mass loss since 2000*

To establish how closely changes in SMB and ice discharge are linked we calculate the individual components of the increase in mass loss since 2000.

The total increased mass loss since 2000 (ΔMB), is the sum of the contribution from surface melt (ΔSMB) and ice discharge (ΔD), expressed as

$$\Delta MB = \Delta D + \Delta SMB \tag{27}$$

To understand the relative magnitude of the increase in dynamic mass loss, ΔD, compared to the total mass balance anomaly (ΔMB), we need to close the mass balance budget.

The increase in ice discharge since 2000, ΔD, is calculated for the UI catchment (see insert in Figure 4.2) using a simple flux gate calculation. The flux gate is about 10 km upstream from the grounding line, following two CReSIS radar lines from 2010 that crossed the UI ice streams (Figure 4.2). ΔD is mainly given by the change in flux through the flux gate, ΔF. However, to account for the dynamic mass loss between the flux gate and the grounding line we add the change in ice volume, ΔV, down stream of the flux gate. The volume change due to SMB in the area downstream of the flux gate (Δsmb) is then subtracted to isolate the dynamic mass loss, thus

$$\Delta D = \Delta F + (\Delta V - \Delta smb) \tag{28}$$

The rate of ice volume change (ΔV) is estimated using altimeter surveys from NASA's ATM flights (Krabill, 2013) during 2003-2012

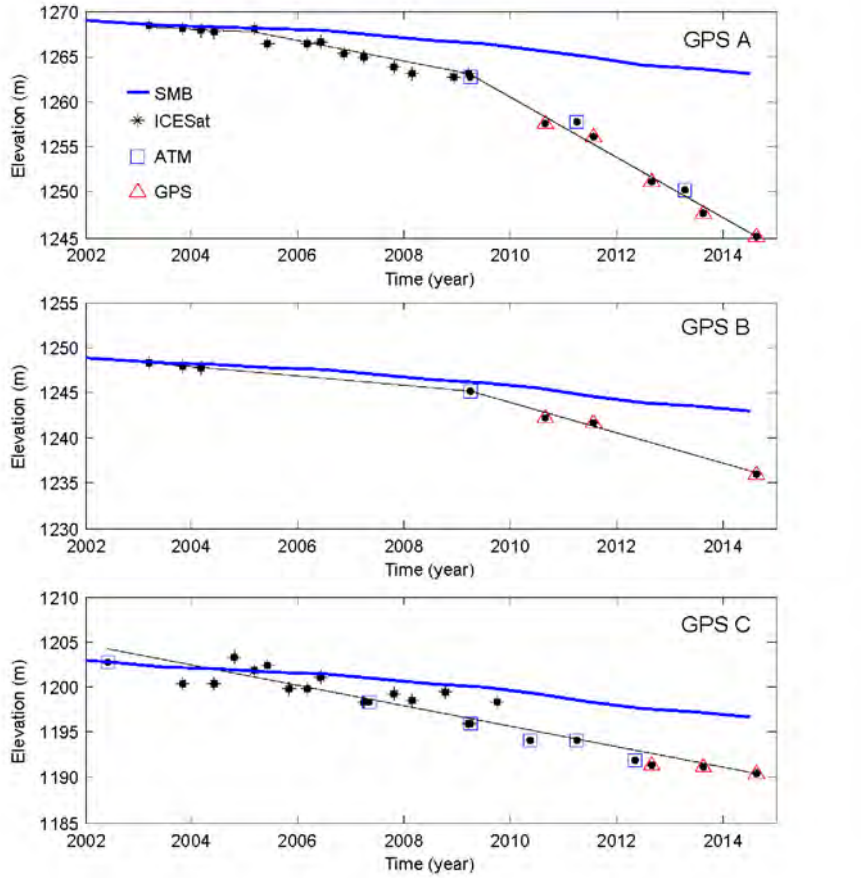

Figure 4.13: Elevation measured at the three GPS sites 30-40 km upstream, see positions in Figure 4.12. The elevations are extended back in time using Ice, Cloud and land Elevation Satellite (ICESat) data (Zwally et al., 2011) and ATM when available. Thinning rates in m yr^{-1} for GPS A: -0.2±0.3 (2003-2005), -1.3 ± 0.2 (2005-2009) and -3.3 ± 0.3 (2009-2014). For GPS B: -0.5 ± 0.3 (2003-2009) and -1.7 ± 0.3 (2009-2014). For GPS C: -1.1 ± 0.1 (2002-2014)

supplemented with Ice, Cloud and land Elevation Satellite (ICESat) data GLA12 Release 34 (Zwally et al., 2011) during 2003-2009. ICESat elevations have a single-shot uncertainty of σICESat = 0.2 m and ATM data have an elevation uncertainty of σATM = 0.1 m. Our procedure for deriving ice surface elevation changes is described in detail by Khan et al. (2013) and is similar to the method used by others (e.g. Ewert, Groh, and Dietrich, 2012; Kjeldsen et al., 2013; Smith et al., 2009). We use the observed ice elevation change rates to interpolate (using collocation) ice thinning values onto a regular 1 x 1 km grid. We correct for the elevation change due to firn compaction, and the density of ice $\rho_{ice} = 917$ kg m^{-3} is assumed to convert volume change to mass change. Figure 4b of Khan et al. (2013) suggest the lower part of UI-1 started to thin in 2004. Hence, we assume no significant thinning in 2000-2003 and estimate the volume change (ΔV) during April 2003 - April 2006, April 2006 - April 2009, April 2009 - April 2012. The volume change due to increased melt in the area below the flux gate, Δsmb, is obtained from the SMB product from MAR. Since we are only looking at the increase in mass loss since 2000 we use the SMB anomaly compared with the mean of 1970-1999. This reference period is used since it shows no general trends in SMB (Figure 4.6). The MAR SMB is converted from m w.e. to mass using a constant ρ_{ice} and summed over the area below the flux gate for the periods January 2000 - December 2005, January 2006 - December 2008, January 2009 - December 2011.

The increased flux through the gate for a given year (ΔF) is given by the difference in flux (F) between 2000 and the given year. F is calculated by dividing the flux gate into a number of columns, i, of width, w, and height, h, summing the contribution from each column, thus

$$F = \sum v_i \cdot h_i \cdot w_i \cdot \rho_{ice} \tag{29}$$

Where v_i is the ice speed for the given year and column, given by the ice velocity maps presented in Figure 4.10. We assume that the ice flow is independent of depth, i.e., that internal deformation is insignificant compared to the basal sliding velocity. This is a valid assumption in areas with high ice speed since they are dominated by sliding or basal till deformation (Cuffey and Paterson, 2010). The ice height, h, is given by the difference in bed elevation from the CReSIS depth radar data and surface elevation. The bed elevation is kept constant with an uncertainty of $\pm$7.09 m, obtained from a crossover analysis of all radar depth lines in 2009 and 2010 on the Northwest coast of Greenland (L3 radar depth sounder data, Gogineni (2012)). Between 2000 and 2012 there has been a significant change in surface elevation across the flux gate. We use the elevation change rates and uncertainties, as given in the calculations of ΔV, to obtain the surface elevation. In order to obtain an estimate of F for the period 2000-2005

Table 1. The Dynamic Mass Balance Anomaly for the Entire UI Catchment, Compared to 2000, Summed for Three Time Intervals[a]

Year	$\Sigma\Delta F$ (Gt)	$\Sigma\Delta$smb (Gt)	$\Sigma\Delta V$ (Gt)	$\Sigma\Delta D$ (Gt)	$\Sigma\Delta$SMB (Gt)	$\Sigma\Delta$MB (Gt)
2000–2005	-2.56 ± 7.61	-3.53 ± 2.16	-6.00 ± 0.12	-5.03 ± 9.89	-1.27 ± 10.06	-6.30 ± 19.95[b]
2006–2008	-9.38 ± 2.58	-2.71 ± 1.08	-8.91 ± 0.12	-15.58 ± 3.78	-9.69 ± 10.06	-25.27 ± 13.84[c]
2009–2011	-20.72 ± 2.70	-2.70 ± 1.08	-8.49 ± 0.12	-26.51 ± 3.90	-12.29 ± 13.41	-38.80 ± 17.31[d]

[a]The intervals are from the beginning of the first year to the end of the last year. The catchment is shown in Figure 1.
[b]-1.05 ± 3.33 Gt yr^{-1}.
[c]-8.42 ± 4.61 Gt yr^{-1}.
[d]-12.93 ± 5.77 Gt yr^{-1}.

Table 2. $\Sigma\Delta F$ (Gt) for the Individual Glaciers[a]

Year	UI-1	UI-2	UI-3 and UI-4
2000–2005	-2.84 ± 3.21	-0.24 ± 1.85	0.42 ± 2.34
2006–2008	-9.43 ± 1.20	-0.41 ± 0.55	0.44 ± 0.77
2009–2011	-18.40 ± 1.44	-3.25 ± 0.57	0.83 ± 0.64

[a]$\Sigma\Delta F$ is the change in ice flux through the fluxgate since 2000 summed over the three time intervals. The intervals are from the beginning of the first year to the end of the last year.

where only sparse velocity data is available, we assume that the acceleration between 2000-2005 occurred linearly. ΔF is estimated for the periods of winter 2000/2001 to winter 2005/2006, winter 2005/2006 to winter 2008/2009 and winter 2008/2009 to winter 2011/2012. We only use the change in winter velocities, so that any increased dynamic mass loss due to anomalies in acceleration during summertime is neglected.

As with Δsmb in equation 1, the anomaly compared to the period 1970-1999 is used and units are converted from m w.e. to mass using ρ_{ice}. The annual MAR SMB is summed over the entire catchment for the periods January 2000 - December 2005, January 2006 - December 2008, January 2009 - December 2011. The modeled SMB from MAR have uncertainties of around 40 cm w.e in the ablation zone and 5 cm w.e in the accumulation zone (Colgan et al., 2015).

The results, presented in Table 1, shows that the increase in dynamic mass loss is responsible for about 80 % of the changes in 2000-2005 (including both years), 62 % in 2006-2008 and 68 % in 2009-2011. While the dynamic mass loss is thus the dominant cause of mass loss, ΔSMB and ΔD increase at comparable rates over the three periods. Table 2 shows the change in flux through the flux gate of each individual glacier. The gates are divided at the point with the lowest velocity between the glaciers, UI-3 and UI-4 could not be separated due to the location of the gate. Table 1 shows that UI-1 was the main contributor to flux changes between 2000 and 2008. In 2009-2011 UI-2 flux increases and contributes with about 15 % of the total flux increase.

Although dynamic changes in ice streams may occur due to internal switching (Brinkerhoff and Johnson, 2015), we find that external forcing mechanisms are more likely for a topographically constrained setting like UI. This external forcing may be due to atmospheric changes or changes in the ocean water masses arriving at the marine-terminating front of UI. Atmospheric changes can be assumed to be equal to all the four glaciers included in this study due to their mutual proximity and similar orientation. According to the bathymetry measurements (Andresen et al., 2014) it is likely that the ocean water arrive through the same $>$ 1 km deep fjord to the fronts of UI-1, UI-2 and UI-3 (Figure 4.4), while UI-4 terminates in shallow waters and therefore it is not subject to the same oceanic forcing. Atmospheric changes causing an increase in surface melt may influence the ice dynamics in a variety of ways, apart from the direct dynamic consequences of ice sheet thinning. Indirect effects of surface melt may for example arise by increasing the basal water pressure under the ice stream (Iken et al., 1993), through meltwater releasing heat to the ice at depth (Meierbachtol et al., 2015; Phillips, Rajaram, and Steffen, 2010; Phillips et al., 2013), by enhancing calving through hydrofracturing (Benn, Warren, and Mottram, 2007) or by forcing convection at the ice-ocean boundary when the meltwater is released in the fjord at depth as buoyant plumes leading to enhanced melt and undercutting at the glacier front (Jenkins, 2011; Straneo et al., 2013). The melting at the ice-ocean interface due to forced convection depends on the ocean temperature as well as the run-off volume and the slope of the ice ocean interface (Jenkins, 2011). Changes in the water masses arriving at the marine-terminating glaciers will alter the submarine rate of melting directly and indirectly by its influence on forced convection at the ice-ocean boundary. We suggest that the asynchronous dynamic response to these essentially synchronous external forcing mechanisms is related primarily to differences in sensitivity between the glaciers due to their bedrock geometry and the proximal fjord bathymetry.

Three of the glaciers at UI (UI-1, UI-2 and UI-3) were flowing at similar and relatively constant speeds between 1992 and 2005. Over the period between 2006 and 2008 the total dynamic mass loss of UI increased by almost a factor of three compared to the dynamic mass loss between 2000 and 2005. The 2006-2008 increase was driven primarily by the acceleration, thinning and retreat of UI-1. UI-2 started to accelerate and thin in 2009. This, combined with continuing acceleration at UI-1 increased the dynamic mass loss contribution of UI by 65% from around 8.4 Gt yr^{-1} between 2006 and 2008 to around 12.9 Gt yr^{-1} between 2009 and 2011. The acceleration of the glaciers over the period 2005-2013 coincided with a period of increased mass

loss from surface melt. The ratio of mass lost by increased surface melt (20-40%) to increased ice discharge (60-80%) remained about the same for the whole UI catchment. Only UI-1 and UI-2 showed major changes in dynamic behavior during the period 2000 to 2013 and their responses occurred asynchronously.

The main acceleration of UI-1 happened between 2007 and 2008. The calving front retreated rapidly during these years (Figure 4.7) suggesting that the acceleration is due to the break-up of a floating ice tongue of about 4 km in length. To understand the mechanisms behind the retreat of UI-1 we need to establish whether the glacier already had a floating tongue in the years before the retreat or if it reached floatation just before the disintegration. The glacier tongue was determined to be floating between 2001 and 2007 by Enderlin, Howat, and Vieli (2013) due to the significant change in slope around the area where UI-1 is grounded today. Enderlin, Howat, and Vieli (2013) found submarine melt rates generally increasing from around 1.5 m day^{-1} during the melt season in 2001 to around 2 m day^{-1} in 2006. Evidence for the glacier tongue being floating since 1985 until the break up in 2007-2008, can be found in the crevasse pattern observed on the Landsat images from e.g. September 13, 1985 and September 19, 2001 showing a clear change in the crevasse pattern at the current grounding line as well as tabular icebergs floating away from the calving front. However, surface elevation profiles in McFadden et al. (2011) show a sloping surface of the tongue, around 70 m elevation rise in 3 km, indicating that the tongue was not freely floating. One possible interpretation of this is that the glacier is resting on a shallow shoal, in which case UI-1 would reach floatation as a result of surface-induced thinning just before the break-up in 2007-2008. A second interpretation that we find more convincing in light of the evidence provided by the Landsat imagery is that the high surface slope was instead due to lateral friction in the narrow trough.

Investigations show the calving front started to retreat around 1998, coinciding with observations of a sudden warming of the subsurface ocean waters along the entire west coast of Greenland (Holland et al., 2008). A floating ice tongue is more sensitive to changes in ocean temperatures compared to a grounded vertical calving front, due to the large surface area in contact with ocean water (Straneo et al., 2013). Since there were no trends towards unusually high surface melt rates in the late 1990s (Figure 4.6) we suggest that the initialization of the retreat of UI-1, which led to the disintegration in 2006 and 2007, was due to submarine thinning caused by increased ocean temperatures in the late 1990s. Thinning of a floating ice tongue will cause a reduction in lateral shear and an increase in crevassing and calving will happen more readily (Nick et al., 2010); these processes will cause retreat and acceleration. As the calving front of UI-1 retreated in the beginning of the 2000s, it moved into a wider fjord (Figure 6). This

caused divergence of the ice flow, effectively thinning the terminus, decreasing the lateral drag and increasing crevassing, that is likely to take larger sections of the terminus closer to buoyancy, thus promoting calving and terminus retreat. Furthermore, during the last decade surface melting has increased (Figure 4.6) leading to thinning of the ice sheet in general from around 2002/2003. Both these processes are likely to have enhanced the retreat rate leading to the disintegration of the floating ice tongue. The disintegration of the floating tongue caused a period of retreat, acceleration and dynamic thinning lasting at least until 2010. Between July and August 2010 UI-1 accelerated again, coinciding with increased thinning rates but no significant change in the calving front position. We speculate that in July 2010 the glacier had retreated due to the continued dynamically induced thinning and reached a topographical threshold which stabilized the front position. However, the bed topography data does not reveal enough detail to substantiate this. After 2011, UI-1 has been stable with no major changes in ice flow velocity and terminus position. In 2013 the calving front is believed to have been close to vertical and grounded (Figure 4.3), and therefore changes that occurred after 2010 where the front reached a stable position are likely to be less sensitive to ocean temperatures. The acceleration event in 2010 is therefore believed to be unrelated to changes in ocean temperatures. If thinning rates persist, the glacier may retreat further inland into a wider fjord (Figure 2) which could cause further thinning and retreat.

The gradual acceleration of UI-2, and the fact that it did not start to retreat before 2008, stands in contrast to the early retreat and stepwise acceleration of UI-1. The fluctuations of the calving front position observed in the late 1990s suggest that UI-2 was also affected by the change in ocean temperatures. However, the glacier remained stable compared to UI-1. This is believed to be due to the stable position of the calving front in a narrow fjord. The retreat of UI-2 started in 2008 or 2009 after a period of five years with unusually high surface melt rates (Figure 4.6). As UI-2 is relatively shallow, approximately 500 m near the calving front and likely to be close to or at floatation (see Figure 4.3), we expect that further thinning would lead to glacier acceleration due to loss of friction at the bed as well as the increase in driving stress from the steeper surface slope. The glacier is furthermore retreating inland on a reverse sloping bed and into a widening fjord, suggesting a significant potential for further retreat.

UI-3 showed a slight deceleration throughout the period 2000 to 2013 and the absence of any acceleration, thinning or retreat is noteworthy. At the glacier terminus we believe that a shallow point in the fjord is causing large icebergs to run aground. This is likely to prevent the glacier from calving freely and causes a back stress that stabilizes the glacier front, which in turn stabilizes the upstream flow. However, as Figure 4.3 and 4.4 show, UI-3 is located in a deep and

long trough and further thinning will at some point bring the glacier close to floatation and there is therefore a potential for UI-3 to retreat much further inland than the other glaciers.

Glacier UI-4 is quite different from the other glaciers as it is shallow (less than 200 m below sea level) and flowing with relatively slow velocities below 1 km yr^{-1}. From 1985-1991 the calving front rapidly retreated along with the entire ice margin between of UI-3 and UI-4 (Figure 4.7). From Andresen et al. (2014) we know that the glacier has been continuously retreating since 1849 and so the retreat event in the late 1980s is believed to be a response to the removal of back stress due to retreat from a pinning point on the south side of the glacier. UI-4 has continuously been retreating inland since then and showed clear and large seasonal variability in the period 2009-2013. The seasonal velocity pattern of speedup in spring and slowdown during mid-summer (type 3 according to Moon et al. (2014)) is indicating that an efficient drainage system develops at the glacier bed every year, causing it to slow-down. Increased meltwater could in this aspect have a slowing effect on UI-4 since the seasonal slow-down would occur earlier when more meltwater is available. UI-4 is located in a shallow trough, in contrast to the deep troughs at the other UI glaciers, and if the gradual retreat continues it will evenutally lose contact with the ocean and become land-terminating.

4.6 CONCLUSION

Dynamically induced mass loss tripled between the periods 2000-2005 and 2006-2008 followed by an increase of by more than 50% between the periods 2006-2008 and 2009-2011. The early increase in dynamic mass loss is attributed to the acceleration of UI-1 and the later increase is due to the acceleration of UI-2. Calculations of the partitioned increase in mass loss between 2000 and 2012 show that dynamic mass loss is the main cause of mass loss. However, the ratio between the mass lost by surface melt and that lost through ice discharge remained constant. While the increase in mass loss due to surface melt is expected to be equally spread over the four glaciers, the rapid increase in ice discharge is occurring only on two of the four outlets of UI, UI-1 and UI-2.

The different dynamic reactions of the four glaciers to similar climate forcings can be understood when looking into the detailed geometry of each individual glacier. UI-1 is the main contributor to the increased ice discharge due to the disintegration of the glaciers' floating ice tongue. The initial retreat of UI-1 is believed to be caused by warming of deeper ocean waters in the late 1990s. Furthermore, feedback mechanisms related to the width of the calving front played an important role in the retreat of the glacier. In 2009 UI-2 started to accelerate and retreat and showed dynamically induced thinning. The

acceleration of the glacier may have been amplified by the positive feedback mechanism as the calving front retreated into deeper water. There is a notable absence of any changes in UI-3 as the glacier is believed to have been stabilized by a grounding point near the calving front. Finally UI-4 showed thinning and slowing down which is mainly due to increased surface melt. At UI-1, UI-2 and UI-3 there are potential for further destabilization should the glaciers continue to thin due to upstream widening of the troughs and their fronts being close to floatation.

4.7 ACKNOWLEDGMENTS

This publication is contribution number 53 of the Nordic Centre of Excellence SVALI funded by the Nordic Top-level Research Initiative. We acknowledge the use of data products from CReSIS generated with support from NSF grant ANT-0424589 and NASA Operation IceBridge grant NNX13AD53A. Data from the Programme for Monitoring of the Greenland Ice Sheet (PROMICE) were provided by the Geological Survey of Denmark and Greenland (GEUS) at http://www.promice.dk. Work by Michael Willis was supported by US National Science Foundation grant number ARC-1111882 and we thank the University of North Carolina at Chapel Hill Research Computing group for providing computational resources that have contributed to these research results. Unfiltered 3-m resolution DEMs produced during this work are available through the University of Minnesota Polar Geospatial Center at
http://www.pgc.umn.edu/elevation/stereo/UpernavikIsstrom. The manuscript improved substantially from the review of James Lea and two anonymous reviewers and the authors would like to thank them for their constructive reviews.

5

PAPER II: ABRUPT VELOCITY CHANGES INFLUENCED BY SURFACE MELTWATER

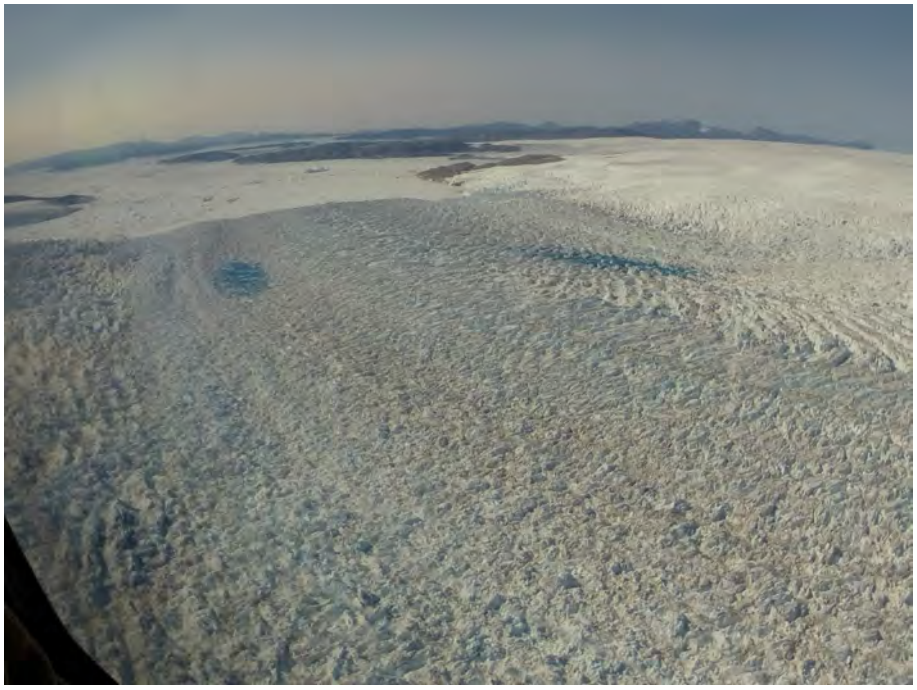

Figure 5.1: Upernavik Isstrøm (UI-2), seen from air, August 2013.

This chapter forms the foundation for the manuscript: *Larsen, S.H., Ahlstrøm, A.P., Kusk, A., Langen, P.L., Hvidberg, C.S. (in prep.), The importance of surface meltwater for abrupt velocity variations at Upernavik Isstrøm, Northwest Greenland*. The manuscript is planned to be submitted to the Journal of Glaciology.

5.1 ABSTRACT

Understanding the physical mechanisms behind rapid velocity variations of marine-terminating outlet glaciers is key to the correct representation of marine mass loss in large scale ice sheet models. While the penetration of surface meltwater to the bed of glaciers is known to affect ice velocity, ice streams represent an extreme case with a spatially complicated velocity and temperature structure. Here we use an observed abrupt synchronous slowdown event, at three neighboring ice streams in Northwest Greenland in late summer 2014, to evaluate different hypotheses regarding the spatial sensitivity of ice flow to changes in surface melt rates through changes in resistive forces.

Using the Ice Sheet System Model (ISSM; Larour et al. (2012a)) we investigate the sensitivity in the velocity of the three ice streams to changes in meltwater production through perturbations of basal friction and shear margin softness. We find that to best capture the spatial structure of the observed slowdown, basal friction has to change relatively more in the ice stream trough compared to the upstream area and increasingly so towards the front. Additionally, our results indicate that changes in the shear margin softness and the internal heat production are likely playing an important role for the ice flow sensitivity to changes in friction.

5.2 INTRODUCTION

The Greenland ice sheet is drained trough a large number of marine-terminating ice streams (Rignot and Mouginot, 2012). Thus, for ice sheet wide modelling, correct reproduction of flow in these narrow zones is crucial to avoid creating artificial plugs for the ice flow. Still, controlling mechanisms of ice stream flow are not well understood hence impeding robust predictions of future ice sheet wide changes (AR5, IPCC, 2013).

Surface meltwater can, due to transport of surface water to the bed of the glacier through crevasses and moulins, affect short term variations in ice flow by changing the basal resistance (Bartholomew et al., 2010; Das et al., 2008; Sole et al., 2011; Zwally et al., 2002). The effect of the meltwater will depend on rate and duration of single melt events as well as strength of the melt season (Bartholomew et al., 2012; Sundal et al., 2011). The above mentioned studies, on the effect of surface meltwater on ice flow, have mainly been conducted inland of ice streams and not directly within the narrow ice stream trough. Andersen et al. (2011) however, showed that the ice flow sensitivity to meltwater increased towards the front of the fast flow ice stream Helheim Gletcher in Southeast Greenland. A recent publication by Slater et al. (2017) studied the distribution of basal water discharged at the grounding line of Kangiata Nunaata Sermia (KNS) in West Greenland. They found that the subglacial drainage system was likely to be distributed in the ice stream trough, due to the destruction of efficient meltwater channels in the fast flowing streams. A distributed flow will induce a higher meltwater pressure thus, effectively increase the importance of water at the base close to the front.

The fast flowing marine-terminating ice streams in Greenland are usually located in topographical deep troughs terminating into fjords. As the ice streams are narrow, compared to their thickness, the latitudinal drag will have a high relative importance in providing resistance to flow compared to the basal drag. This is enforced by a low basal resistance in the fast flowing zone (Cuffey and Paterson, 2010). This means that a change in basal friction in these areas will be

relatively less important than changes in lateral drag. Lateral drag in ice streams is provided by both the ice/rock interface as well as the ice/ice interface where the fast moving ice stream meets the slow moving ice along the sides. Ice stream shear margins are expected to be softer due to effects of increased internal heat production (Echelmeyer et al., 1994), meltwater percolation (Van Der Veen, Plummer, and Stearns, 2011) and damage (Borstad et al., 2013).

In this study we present observations of a synchronous abrupt slow-down of surface velocities at three neighboring ice streams. These events are compared with the temporal evolution of surface melt from the regional climate model HIRHAM5 (Christensen et al., 2007) and shown to be correlated with the ceasing of surface meltwater production at the end of summer. To investigate the spatial sensitivity of ice flow to surface melt through changes in resistive forces we put forward a number of different hypotheses on how surface melt can affect resistive forces. The reactions to the changes in friction are tested in an ice flow model and compared to observed velocity changes. For this purpose we use the thermomechanical finite element ice flow model Ice Sheet System Model (ISSM Larour et al., 2012a). For each hypothesis we conduct a forward modelling experiment to asses its capability to reproduce observed abrupt slow-down events. We furthermore, test the importance of lateral drag provided by the shear margins by running the experiments with and without applying softer shear margins.

5.3 STUDY SITE

Upernavik Isstrøm is a glacier complex consisting of several fast flowing marine-terminating ice streams on the Northwest coast of Greenland (see Figure 5.2). The three main east/west flowing glaciers (UI-1, UI-2 and UI-3) are the focus of this study. The three glaciers terminate in the same fjord (Upernavik Isfjord) where UI-1 and UI-2 terminate in a relatively deep part of the fjord and UI-3 terminates in a shallower area (Andresen et al., 2014). Changes in the ice flow and terminus position since 1985 is investigated in Larsen et al. (2016) (Paper I) and shows that while UI-1 has had a major retreat and acceleration event around 2008 and UI-2 has slowly accelerated and retreated from 2009 an onwards (until the end of study period in 2013), UI-3 has remained remarkably stable. During 2014 (the study period in the present paper), the calving front position of UI-1 and UI-3 remains relatively stable while UI-2 shows a sudden increase in retreat in late summer (Figure 5.3).

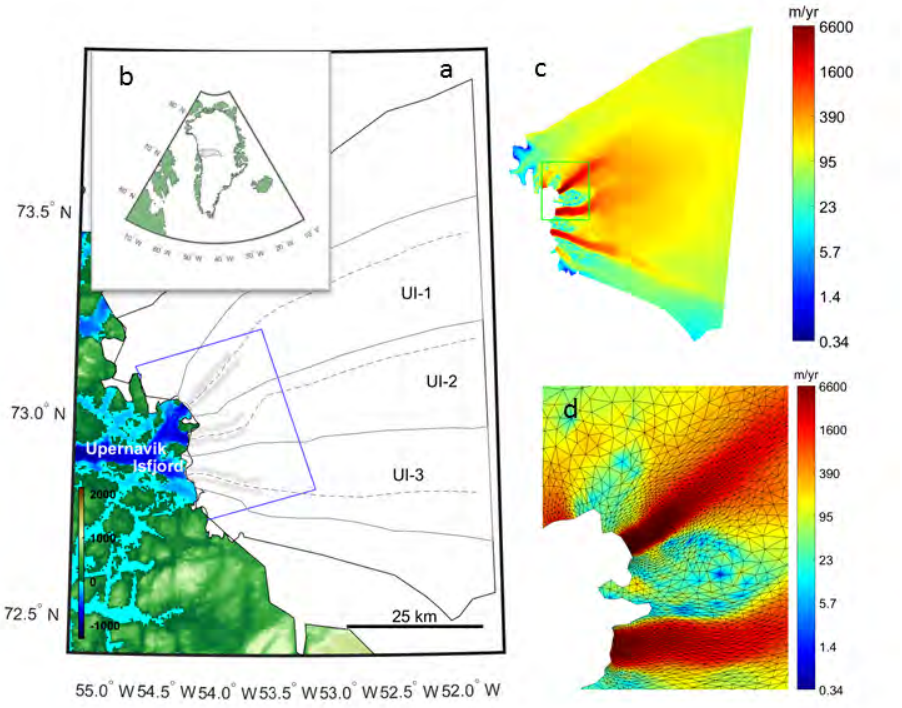

Figure 5.2: a) Overview map of Upernavik isstrøm, black line is the small model domain, gray lines is the glacier sub-catchments, dashed lines are center flow lines, blue line is the data coverage of COSMO-SkyMed velocity maps, the background is the bed map from BedMachine version 3 (Morlighem et al., 2017) overlain by the area covered by the Greenland ice sheet in white, gray zones indicate shear margins. b) Map of Greenland, black lines indicate the Upernavik catchment and model domain. c) Observed surface velocities winter 2014/2015 in the model domain. d) Example of mesh.

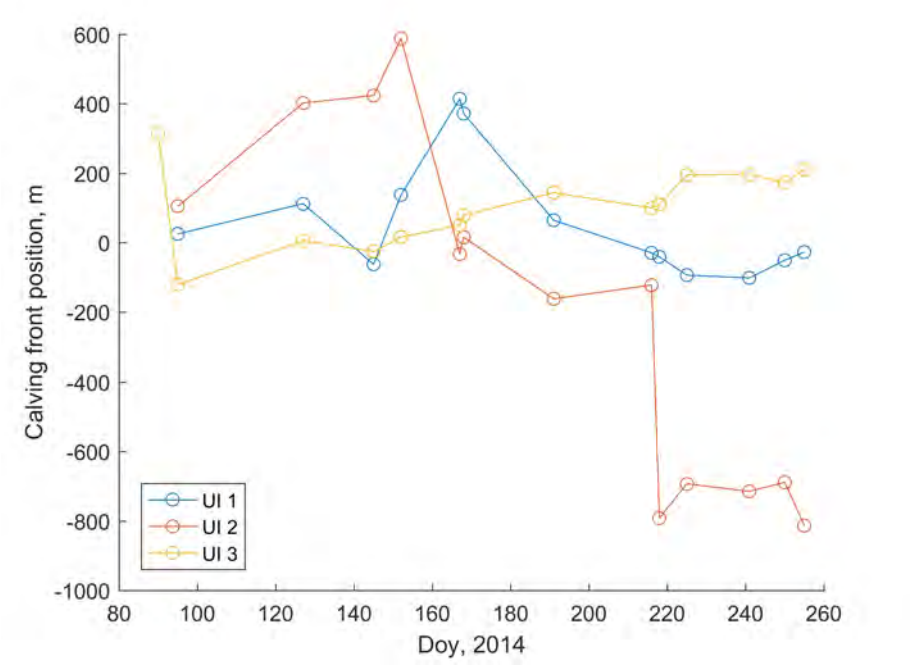

Figure 5.3: Relative calving front position based on the box method as used in (Larsen et al., 2016), where the retreat in meters is found based on the volume change of a box covering the main part of the glacier front.

5.4 OBSERVATIONS OF VELOCITY JULY-OCTOBER, 2014

In late summer of 2014, between 24 July and 2 October, 15 COSMO-SkyMed HIMAGE (3x3 m resolution) stripmap images of the area were acquired, utilizing all 4 satellites in the constellation to achieve temporal baselines from 1-12 days. This resulted in 26 pairs covering the period. Ice velocities were retrieved using intensity cross correlation with a window size of 128x128 pixels (corresponding to approximately 300x300 m on the ground). Processing was carried out with the IPP (Interferometric Post Processing) ice velocity processor, developed by DTU Space (Dall et al., 2015). The velocities were calibrated using ground control points on stable rock and geocoded using the GIMP DEM (Howat, Negrete, and Smith, 2014). The COSMO-SkyMed dataseries gives us an opportunity to study the spatial variability of seasonal velocity behaviour of several neighboring outlet glaciers at the same time over the course of days. The interpretation of the observations will form the foundation of the modelling study.

There is in total 14 consecutive velocity maps giving mean velocity for periods from down to 2 days up to 9 days (data coverage shown by horizontal bars in Figure 5.4). The velocity maps reach up to around 40 km inland from the calving front of the glaciers (see extend in Figure 5.2). Over the observation period we see rapid variation in flow speed within a timescale of days (Figure 5.4). We observe a peak in velocity around 19th August followed by a slow-down of 7-

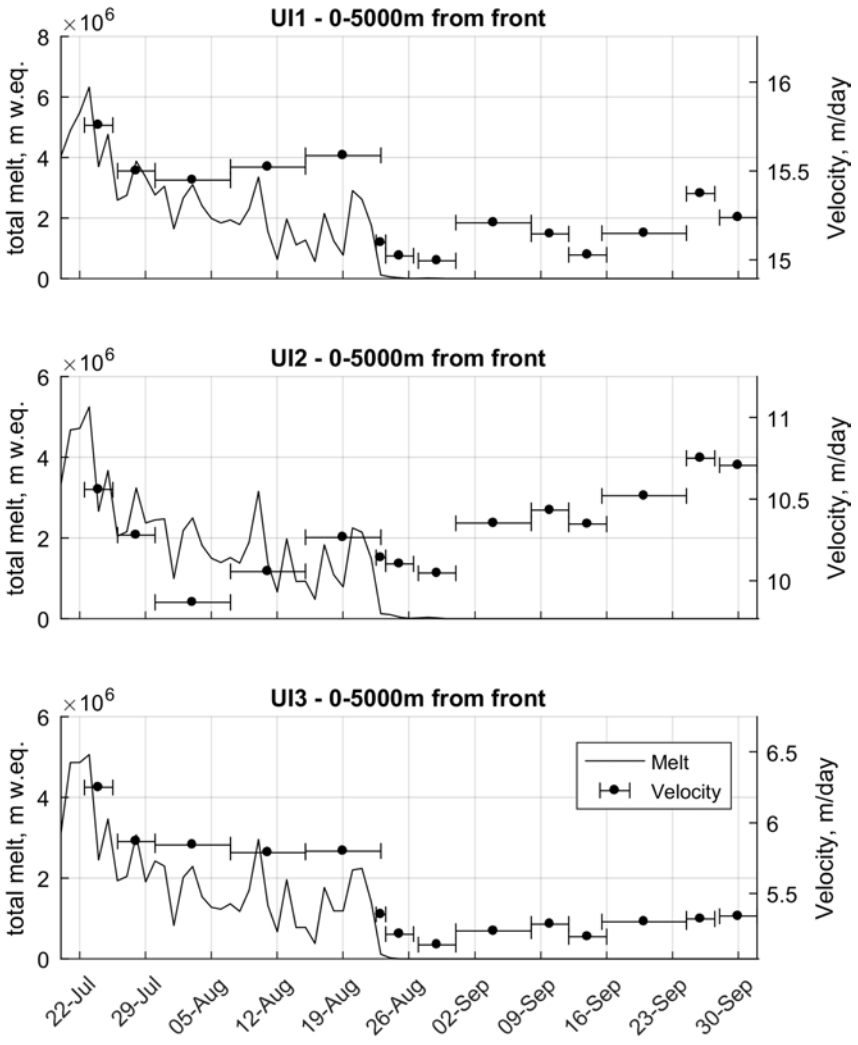

Figure 5.4: Left hand axis shows the total meltwater (HIRHAM5 Langen et al., 2017) produced daily in the sub-catchments (Figure 1). Right hand axis shows velocity at the 10 first 500 m spaced points between 0 and 5000 km from the front. The horizontal bars show the timing of the two images used to obtain velocities.

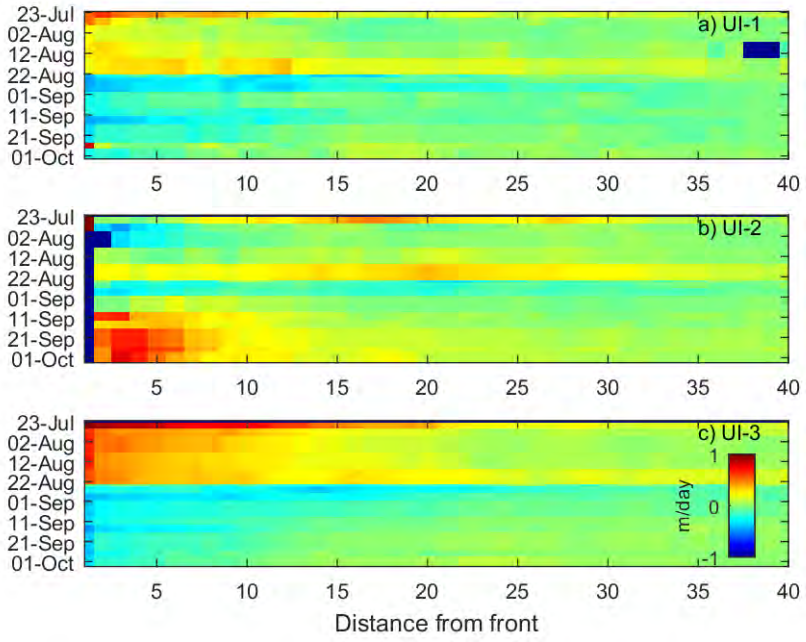

Figure 5.5: The velocity deviation along centerline points at 500 m distance. The mean is calculated for each point along the flow line.

10 % at UI-1 and UI-2 and 10-15 % change in velocity at UI-3 within the course of 4-10 days. The event occurs in the period when meltwater production ceases at the end of the melt season. The spatial pattern of the velocity change compared to the mean (Figures 5.5) show that for both the speed-up and the following slow-down high changes occur up to 20 km inland. We interpret this as an indicator for the changes originating from the upstream side and not the front. Moreover, the observed abrupt changes occur at the same time for all three glaciers, and the overlapping with the ceasing of meltwater production, points towards surface meltwater production as the main forcing. This interpretation is supported by the studies of Andersen et al. (2010) and Sole et al. (2011) both showing a correlation between surface meltwater and short term velocity changes at Helheim Gletscher (SE Greenland) and up stream of Kangiata Nunata Sermia (Southwest Greenland), respectively. In the effort to find a simple way to understand surface velocity sensitivity to meltwater production we investigate how we can relate changes in surface meltwater to changes in resistive forces in an ice flow model with the goal of reproducing the observed abrupt slow-down at the end of the melt season 2014.

If we assume that the surface meltwater drains to the bed in the vicinity of where it is produced, the spatial pattern of surface meltwater can give us a rough estimate of how the spatial pattern of basal resistance could change. Accordingly, we investigate the spatial pattern of surface melt and hypothesise on how glacier resistance could be affected by this.

We use data from the regional climate model HIRHAM5 to obtain a daily record of simulated spatially distributed melt rates and runoff. Melt rates and runoff are calculated as in Langen et al. (2017, with the parameter setting "MOD-ref" therein). The HIRHAM5 regional climate model (Christensen et al., 2007) is run over a Greenland-wide domain at 5.5 km resolution (0.05°x0.05° on a rotated pole grid; Lucas-Picher et al. (2012)). Six hourly inputs of wind, temperature, and specific humidity are supplied from the ERA-Interim reanalysis dataset (Dee et al., 2011) at the lateral domain boundaries and the model then computes the atmospheric circulation within the domain at 90 s time steps. The resulting ice sheet surface fluxes of energy (turbulent and downwelling radiative) and mass (snow, rain, evaporation, and sublimation) are used to drive a snow/ice subsurface scheme which provides melt, runoff and refreezing rates (as in Langen et al., 2017).

According to HIRHAM5 surface melt reaches up to an elevation of around 1900 m a.s.l. (Figure 5.6b and c) and increase with decreasing elevations to a total sum of $2-3$ m water equivalent near sea level, close to the ice margin. Some of this meltwater refreezes in the surface snow and firn. In HIRHAM5 the refreezing is quantified by considering cold content, impermeable layers and other parameters (Langen et al., 2017) and an estimate of the actual runoff is given. According to this, runoff occurs up to an elevation of $1600-1800$ m a.s.l., reducing the area where surface meltwater will be able to reach the bed (Figure 5.6b and d). Assuming a permeable ice sheet the water reaching at the bed will be transported towards the margin according to the hydraulic potential gradient, which depends mainly on surface and bedrock slope. Hence, all the water reaching the bed will accumulate towards the front in the narrow ice stream troughs as seen in the stream lines in Figure 5.6a. Without accounting for the topographical focusing, the accumulation of water alone, will make the water availability increase drastically towards the front (Figure 5.7)

As meltwater reaches the bed it can influence basal resistance in a number of different ways depending on the origin of the bed and the efficiency of the drainage system. Without including a detailed model accounting for basal hydrology the spatial sensitivity of the basal resistance to abrupt changes in water availability is not trivial and in

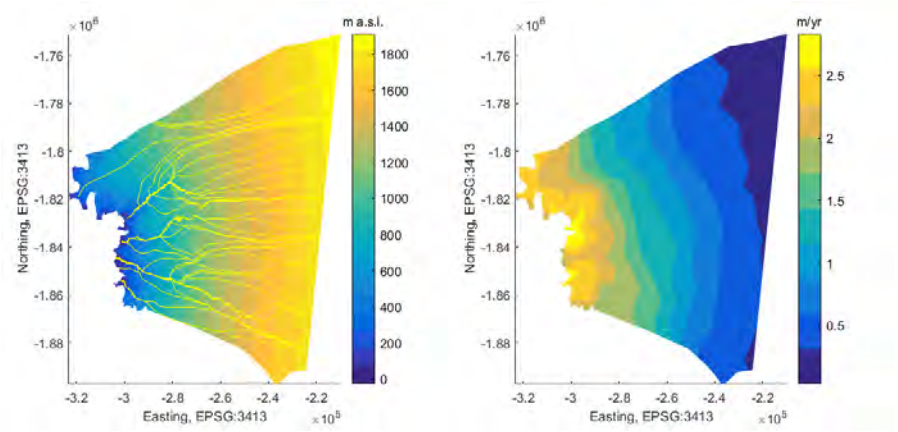

(a) Elevation and basal water stream lines

(b) Annual melt rates

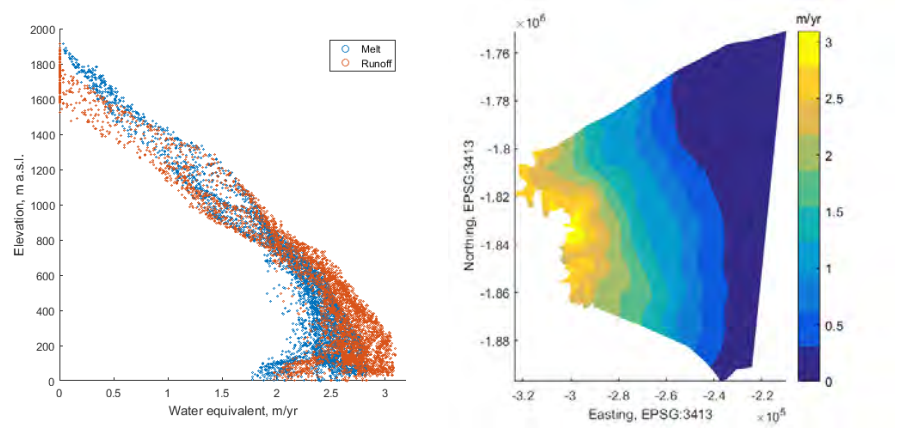

(c) Annual melt and runoff with elevation

(d) Annual runoff

Figure 5.6: (a) surface elevation from Arctic DEM version 2.0 and preferential drainage paths along the bed, according to the hydraulic potential gradient. (b) and (d) annual sum of melt rates and runoff respectively from HIRHAM5 (Langen et al., 2017). (c) as in (b) and (d) but plotted against elevation

the following we put forward four hypotheses on how a simplified spatial pattern of friction/resistance sensitivity could look.

(H1) In this study, we look at the end of melt season where water supply has been plenty throughout the summer and then abruptly comes to an end. As meltwater production cease, the water availability at the bed will drop everywhere thus, it can be hypothesised that this drop everywhere will result in an even relative change in basal resistance.

(H2) As meltwater production increase towards the margin, the basal friction sensitivity to an abrupt reduction in meltwater production could depend on how much meltwater is present. In the most simple case, this could be approximated by how much

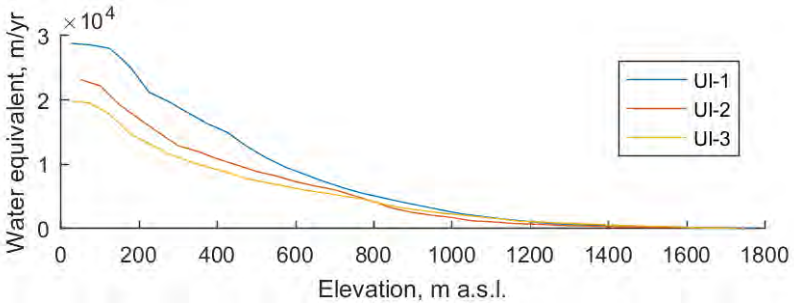

Figure 5.7: The downstream accumulated annual melt rates of each glacier sub-catchment.

surface meltwater is being produced locally, resulting in an increase in relative changes towards the front (Figure 5.6b).

(H3) As shown in the stream lines of Figure 5.6a and the accumulation plot of Figure 5.7 the meltwater available at the base increases drastically as water is accumulated towards the margin and thus the relative changes in basal resistance could depend on the actual water available thus, increasing according to the increase in accumulated water.

(H4) The final hypothesis is based on the fact that the lateral resistance is more important for ice stream flow than basal resistance. In the case of meltwater softening the shear margins as it penetrates through the crevassed zones, an abrupt end of meltwater production could also affect the softening effect the water has. Thus as meltwater production ceases the basal resistance does not only change but so does the shear margins softness thus changing lateral resistance of ice flow.

5.6 MODEL SETUP

We use the Higher-Order approximation in the thermomechanically coupled ice flow model Ice Sheet System Model (ISSM). For a detailed description of the model see Larour et al. (2012a). The model domain is based on the Upernavik glacier catchment, defined by the surface flow direction (Rignot and Mouginot, 2012) and the calving front position is mapped from a Landsat image from 11 July, 2014. For most of the model runs we are only concerned with the near terminus area so in these, the model domain is cut to be the lower part of the catchment (Figure 5.2a) to save computing time. The domain is divided in a triangular mesh which is adapted to observed surface velocities from winter 2014/2015 (From the European Space Agency, ESA, Climate Change Initiative, CCI, Greenland). Mesh resolution is between 50 m and 5 km (Figure 5.2d). The horizontal mesh is extruded to 12 vertical layers, increasingly thinner towards the bed.

In the model, the ice flows according to Glen's flow law (Cuffey and Paterson, 2010), modified with a damage factor, D, where the ice viscosity is given by

$$\mu = (1 - D)\frac{B(T, w)}{2\dot{\epsilon}_e^{(n-1)/n}} \tag{30}$$

where B is the ice viscosity parameter, D is ice damage (Borstad et al., 2012) set to zero when no damage is applied, $\dot{\epsilon}_e$ is the effective strain rate and the flow law exponent, n, is set to 3. Temperature, T and water fraction w is given by the enthalpy conserving temperature model (Seroussi et al., 2013). The temperature dependence of B is given by Cuffey and Paterson (2010) (table 3.4 p. 75) by relating the creep parameter, A to be through $B = A^{-1/n}$.

At the boundaries we assume a stress free surface, except at the lateral domain boundaries (excluding the ice front) where Dirichlet boundary conditions are applied, keeping surface velocities and ice thickness constant at present day levels. At the ice front hydrostatic pressure is applied where ice is below water level. The glacier front remains at the same position fixed by the domain. At the base drag is given by

$$\tau_b = -k^2 N u_b \tag{31}$$

Where, k is the basal friction coefficient explained below, N is the effective pressure at the base of the glacier, in this case only accounting for the hydrostatic pressure, and u_b is the basal sliding velocity. For the thermal model the basal boundary condition is given by a constant geothermal heat flux of 50 mW/m^2 everywhere.

5.6.1 *Model initialisation*

The model surface is initialized using the Arctic DEM (Digital Elevation Model) version 2.0, where surface elevation observations in this area are compiled from images taken during the period 2011-2013. The basal topography is provided by the BedMachine version 3 (Morlighem et al., 2017), using a mass conservation approach to make a basal topography map from observed discrete lines from radar surveys of the bed.

Basal friction is generally unknown and so we use a control method as described in (Morlighem et al., 2010) to assimilate the friction coefficient k based on observed velocities from winter 2014/2015. This method will give us a spatially distributed value of k, which we will refer to as the friction coefficient map. Since we are working with ice streams located in steep troughs it is worth mentioning that there is no distinction between basal and lateral drag in the model.

The initial temperature and water fraction is given by the temperature model described in the next section.

To reduce instability in the experiments introduced by interpolation and uncertainties in surface and basal topography, the model is initially run for 10 years. During this period we use the surface mass balance forcing from the regional climate model Modéle Atmosphérique Régional (MAR) (Fettweis et al., 2013).

5.6.2 *Temperature model*

To obtain a spatially varying temperature field of the ice we run a model, using the whole catchment as domain (Figure 5.2 inserted panel), through the Holocene varying only surface temperature. We run the model in two steps, with different resolution to save computational time. For the period from 9700BC to year 0 we use a model domain with a resolution between 500 m and 5 km. From year 0 to 2015 we use a model mesh with a higher resolution between 100 m and 5 km. The model is initiated with present day values as described in section 5.6.1 and the initial temperature is given by the steady state temperature solution of 9700BC surface air temperatures. The model is run forward keeping all forcings constant except surface air temperature. The surface temperature field is generated from the MAR surface temperature field of present day (an average of 1960 to 1999) scaled by the temperature anomalies from Vinther et al. (2009). The constant SMB forcing is given by the mean SMB value from MAR during 1960 to 1990. We run the model with monthly time steps, first from 9700BC to 1958 with the above mentioned forcing. From 1958 and onwards we continue running the model up to 2015 forced with MAR surface air temperatures.

The results from the temperature run shows that a large part of the catchment has basal temperatures at pressure melting point, indicating that basal meltwater is present all year round (Figure 5.8). The temperature model run also illustrates the importance of deformation heating at the shear margins that are several degrees warmer than the surrounding ice (Figure 5.8 inserted panel).

5.7 MODEL EXPERIMENTS

The purpose of the experiments is to reproduce the abrupt slow-down event we observe at the end of the melt season (between 19 and 26 August) to investigate the sensitivity ice flow resistance to changes in surface meltwater, thus indirectly investigating glacier flow sensitivity to changes in surface meltwater. The four hypotheses, put forward in section 5.5, are tested by perturbing the basal friction map and the shear margin softness, according to each of the hypotheses, in a forward simulation of the ice flow model of UI. The simulated change in ice flow velocity is then used to evaluate each hypothesis by comparing with observed slow-down at all three glaciers.

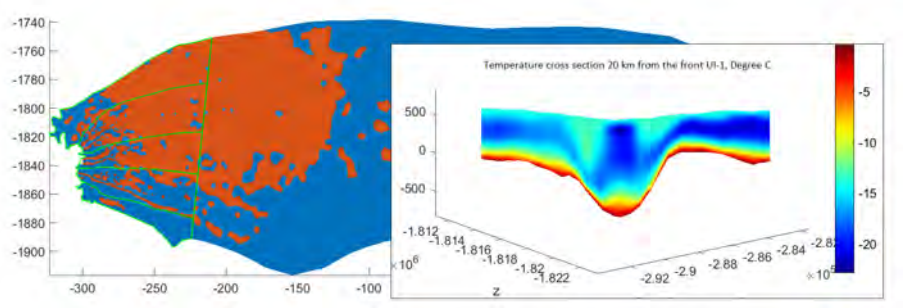

Figure 5.8: Areas at pressure melting point in the lower model layer of the temperature model. Green lines indicate the small model domain used for the experiments and the sub-catchments of each glacier. The inserted panel shows a temperatures along a cross-section of UI-1 at approximately 20 km from the front.

For all experiments we run the ice flow model, on daily time steps, through 2014 continuing the monthly mean SMB forcing from the initialisation run. The perturbation is applied within one time step at August 19th and the perturbed friction map is given by

$$k_{pertubed} = F \cdot k \tag{32}$$

Where F is the perturbation map.

To test the importance of potentially softer shear margins, the experiments are all done with two different viscosity settings: (1) where $D = 0$ everywhere and (2) shear margins are softened by $D > 0$. The shear margins are defined by the zones with effective stress higher than 250 kPa (Figure 5.2a). This limit in stress is given based on the review of Colgan et al. (2016) showing that crevasses form at stresses between 100 and 400 kPa and at increasingly lower stresses as ice temperature decrease. At temperatures around $-25°C$, which is the temperature of the coldest part of the ice streams, the critical stress is around 250 kPa. In these zones we add a damage D (as in Bondzio et al., 2017) using a maximum of 0.4 at the front decreasing linearly to zero at an approximate distance of 20 km inland. Since the viscosity will be changed by D, the best matched friction map will change and so for each value of D the model is initialized again. The value of D is then kept constant throughout the spin-up and experiment except for Experiment 4 where we perturb D.

(Exp1) The most simple hypothesis (H1) is assuming that the relative change in availability of meltwater matters but the actual amount of meltwater is unimportant. Thus, in the first experiment we will perturb the friction map by an equal percentage everywhere. This means that there will be a higher actual change in friction in areas with high friction and lower actual change in in areas with low friction. The perturbation F is varied between

Experiment	F increase with	F_{max}
Exp1	Equal percentage everywhere	$2-17$ %
Exp2	Decreasing elevation	$5-25$ %
Exp3	Increasing cummulated melt	$5-25$ %
Exp4	As in Exp1 + shear margin hardening	$7-15$ %

Table 5.1: Experiments

1.02 and 1.17 which means an increase in friction between 2 % and 17 % of the local value.

(Exp2) The second hypothesis (H2) is that the amount of meltwater produced locally is important for the friction change. To keep the experiment as general as possible, we will relate the friction perturbation to elevation which can be approximated to be linearly related to surface meltwater production (Figure 5.6c). Thus, in the second experiment we decrease the friction linearly with increasing ice surface elevations. The maximum value of F will be between 1.1 and 1.25 (10 to 25 %) decreasing linearly to 1 at 1600 m a.s.l.

(Exp3) The third hypothesis (H3) is stating that the actual amount of meltwater available at the base is important for the friction change. Thus, in the third experiment we let the friction change according to a cubic function that is based on the cumulated sum of meltwater from HIRHAM5 towards the front. The maximum value of F is varied between 1.1 and 1.3 (10 - 30 %) and then it decreases according to the cubic function to 1 at 1600 m a.s.l.

(Exp4) The fourth hypothesis (H4) is based on the theory that meltwater draining into the shear margins have a softening effect. Thus, in the fourth experiment, we abruptly harden (by lowering D) the shear margins in the same setting as in the Exp1 models where damage D is applied. The perturbation on D is varied by a percentage ranging between 5 and 15 %.

(Exp4_a) Exp1-4 are all solved using the thermomechanical coupling. To test the importance of this coupling we also run Exp4 without constant temperatures and thus neglecting the temperature changes in strain.

5.8 EXPERIMENT RESULTS

The experiments are evaluated by comparing observed velocity change, along the center flow lines (Figure 5.2) of each of the three glaciers,

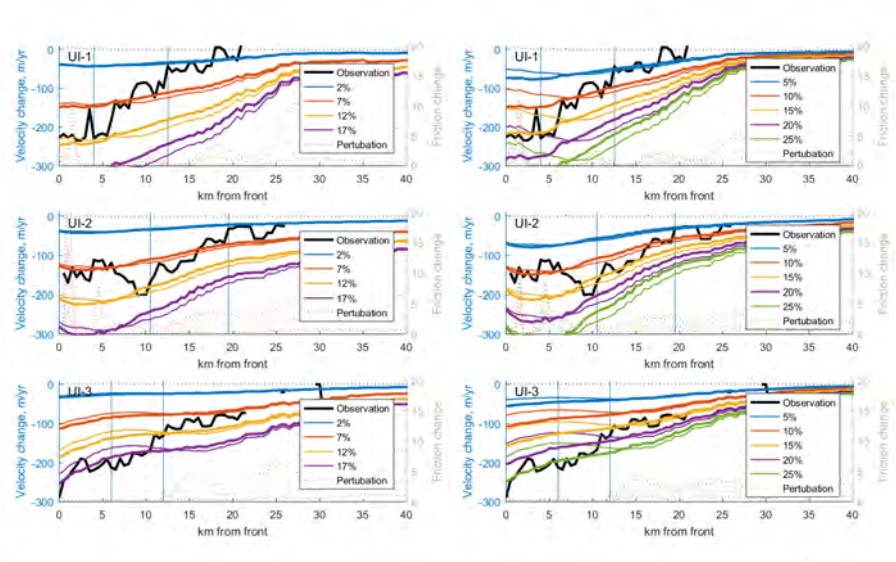

(a) Exp1 (b) Exp2

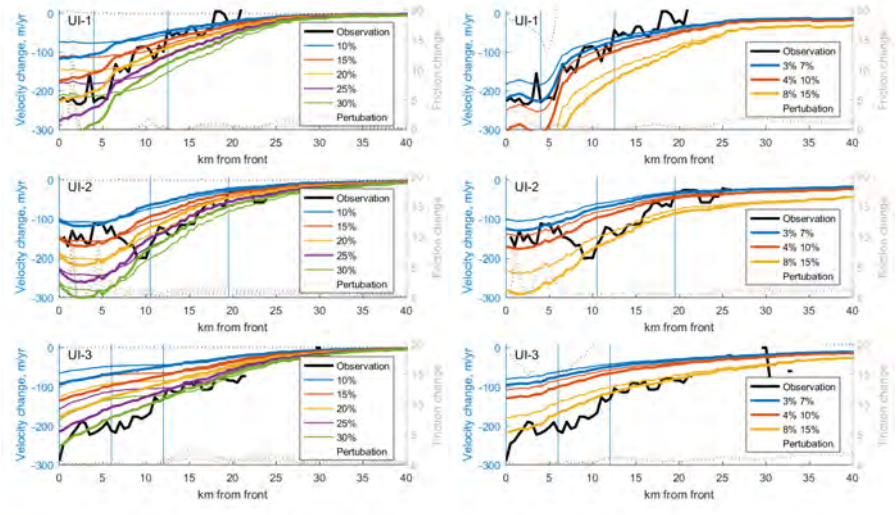

(c) Exp3 (d) Exp4

Figure 5.9: Experiment results. (a)-(c) Thick lines indicate model runs with $D > 0$, thin lines indicate model runs with $D = 0$. (d) Thick lines indicate model runs including thermomechanical coupling, thin lines indicate model runs with constant temperature

during the abrupt slow-down event (19-26 August, 2014). The velocity observations of the event only covers an area up to 40 km from the front and thus we only evaluate the model in this area. This area the main trunk of the ice stream where ice is being pushed into the bottle neck of the ice stream trough.

When we change the friction with an equal percentage everywhere in Exp1 (Figure 5.9a), the gradient in modelled velocity changes is not high enough to match the increasing observed changes towards the front. Thus, the experiment shows that the change in mass flux from the upstream area, where friction change has a relatively large effect compared to the low friction zone in the trough, is not transported fast enough to the ice stream trough to reproduce the observed high changes as we get closer to the front. Dispite th efact that softer shear margins facilitates faster transport through adding softer shear margins does not change the model results by very much.

In Exp2 (Figure 5.9b) the friction perturbation is relatively higher near the ice margin than inland (compared to Exp1) and the results also show an increase in velocity changes near the front. However, for UI-1 and UI-3 the gradient in magnitude of change from the front inland is again not high enough to match observations. At UI-2 on the other hand, the observed velocity change can be reproduced near the front and at the back, however, not catching the correct magnitude of change around 10 km inland. This could imply that less change needs to occur locally at UI-2, compared to its neighboring glaciers, to reproduce observed changes. Adding the softer shear margins are improving results in particular at UI-1 and UI-3.

In Exp3 (Figure 5.9c) the increased friction change near the front reproduce observed velocity changes well at UI-1 and UI-3 if we include soft shear margins. The soft shear margins are hence, very important for the model results here. Also at UI-2 we see improved results upstream of 10 km, however, with too large changes near the front.

Results from Exp4 (Figure 5.9d) resembles experiment 2 and 3 in the way that we introduce a larger relative perturbation near the front, in this case very specifically at the sides of the ice stream. The results from this experiment are comparable with Exp3, however, in particular at UI-1 the shear margin hardening appear to be reproducing the spatial pattern of the observed slow-down almost perfectly. By keeping the temperature constant throughout the experiments in Exp4_a (Figure 5.9d) the effect of the perturbation in Exp4 decrease with about 20%. This shows that the fact that accounting for the effect of reduced internal heating is playing a significant role in the reproduction of the abrupt slow-down event.

The short time series of COSMO-SkyMed velocity maps revealed abrupt synchronous slow-down of magnitudes between 5 and 15 % at the main three ice streams of UI. These occurred at the same time as meltwater production ceased at the end of the melt season in 2014. Observations suggest that surface meltwater has an effect on the basal resistance of flow as the water is transported to the bed of the glacier through crevasses and moulins (Das et al., 2008; Zwally et al., 2002). However, the sensitivity of the basal friction to meltwater is not easy to reproduce as it depends on both the origin of the bed and the state of the subsurface drainage system. The effect of changing basal friction due to meltwater is therefore not included in most ice flow models. Thus, the purpose of the experiments was to find a simplified way of understanding the spatial sensitivity of ice flow to changes in surface melt rates, through changes in resistive forces in the ice streams.

The results from the experiments showed that a flux change from the interior of the ice stream is not enough to reproduce observed abrupt velocity changes. Thus, local changes in the ice stream trough is necessary to reproduce the observations of velocity change. The change in resistive forces, furthermore, needed to increase towards the front. In Exp1-3 the friction is only changed at the ice/rock interface. However, Exp4 showed that abrupt changes in flow are also reproduced by changing the ice hardness in the shear margins, hence the friction in the ice/ice interface, while only changing slightly at the ice/rock interface. Thus pointing towards the fact that changes in lateral drag in the shear margins is important for the flow of ice streams. A higher relative friction change needed to reproduce changes will indicate a higher sensitivity of the glacier flow to the actual forcing which is surface melt. Thus, supporting the hypothesis (H3) of Exp3, of the friction changing increasingly due to the cumulation of melt towards the front explains this result. However, also the results of Exp4, where abrupt changes in shear margin hardness, explains the increase in sensitivity towards the front. These result supports the results from Helheim Gletcher (Andersen et al., 2011) who showed that velocity changes were increasingly sensitive to changes in meltwater production towards the front. The results from Slater et al. (2017), showing how basal water pressure could be higher towards the front of the glacier, suggest the same effect.

Results from several studies (e.g. Bondzio et al., 2017; Joughin et al., 2012; Van Der Veen, Plummer, and Stearns, 2011) show that softer shear margins are necessary to reproduce the observed fast flow at Jakonbshavn Isbræ. Comparing our model results including and excluding the softening effect at the shear margins clearly shows better

results when shear margins are softer. Thus, supporting the theory of soft shear margins are important for the flow in ice streams.

By comparing the model results between the neighboring glaciers of UI, it is clear that the glaciers show different sensitivity to changes. A much higher friction change was needed at UI-3 than at UI-1 and UI-2 in all experiments. Since there are no local differences in the amount of meltwater being produced at each of the sub-catchments this implies that UI-3 is much more sensitive to changes in meltwater transport to the bed than UI-1 and UI-2. The three glaciers exhibit a slow-down of approximately the same absolute size (Figure 5.9), however, UI-3 is flowing at much slower speeds (Figure 5.4) and so a higher friction change is necessary to reproduce the observed slow-down. The slower flow of UI-3 is related to the smaller sub-catchment and more shallow trough. Perhaps more importantly, the temperature model also showed that whereas the sub-catchments of UI-1 and UI-2 have a bed at melting point, the bed at UI-3 is cold based (Figure 5.8). This means that water will be present all year round at the bed of UI-1 and UI-2, but at UI-3 water will mainly be present when it is transported to the bed from the surface during the melt season. Thus, the ceasing of meltwater transport to the bed will leave a cold-based bed relatively dry.

The need for an increasingly higher relative change in basal friction towards the front indicates that changing longitudinal stresses at the calving front can cause a similar effect. This could be a change in submarine melt rates at the front due to changes in the meltwater plume as meltwater production ceases. Furthermore, none of the experiments showed a good match to the observed slow-down at UI-2. As UI-2 is the only glacier showing retreat during the study period (Figure 5.3), we expect the retreat is affecting the glacier flow speed by stress perturbations related to the calving front position. Hence, it is likely that the observed abrupt slow-down is an effect of both changes in inland resistive forces combined with changes in longitudinal forces at the front. Ideally, the relative importance of the changes at the calving front compared to upstream changes should be identified by including submarine melt rates and changing calving front position in the model. However, this was beyond the scope of this study.

By excluding the thermomechanical coupling in Exp4 we saw that this mechanism matters significantly for the model results. This supports the conclusions of Bondzio et al. (2017) that rheological changes due to stress perturbations is playing an important role for the observed acceleration during the last decade.

5.10 CONCLUSIONS

The retreat of Upernavik Isstrøm has caused the formation of a complex of outlet glaciers all terminating into the same major fjord (Larsen et al., 2016). The glacier complex offers a live-size laboratory for testing assumptions about glacier behavior on a set of marine-terminating glaciers with different geometries but similar external forcing from the atmosphere and ocean. We observed a synchronous abrupt slowdown event within a few days at the three neighboring ice streams of Upernavik Isstrøm, at the end of melt season 2014. We attribute this slowdown to the change in resistive forces of ice flow as melt water production ceases. The observations were used as the basis for a model study where the sensitivity of ice flow to changes in resistive forces at the base and in the shear margins was tested. The resistivity changes were hypothesized to be related to the spatial pattern of surface meltwater production and thus the glacier flow sensitivity to changes in surface meltwater is indirectly tested.

The results from the model experiments show that the observed abrupt slow downs events in the ice streams are controlled by changes within the ice stream trough, most likely along the margins of the ice stream. An increasing relative change in resistive forces towards the margin was required in order to reproduce the observed abrupt slowdown in the model. The ability of the model to reproduce the observed ice velocities was found to increase by assuming that the change in resistive forces took place through the entire ice column at the shear margins and not only at the bed and sides along the bedrock. From this we suggest that ice stream behavior is not only defined by the ice/rock interface, but that the interface between the fast and slow flowing ice in the ice stream is likewise important.

The fact that we needed to change the resistive forces increasingly towards the front in the model to capture the slowdown events could also indicate that changes in longitudinal stresses at the calving front plays a role. Moreover, the model failed to reproduce observed changes correctly at UI-2 and a recent abrupt calving front retreat is expected to have an influence on this. These shortcomings in reproducing the observed glacier behavior probably indicate the lack of information about changes at the calving front in the model which is kept steady in the experiments. Future similar studies should include frontal changes to separate the effect of upstream changes and front position changes.

We found a clear distinction between the sensitivity to changes in resistive forces between the two northern ice streams (UI-1 and UI-2) and the southern glacier (UI-3), respectively. We speculate that this is due to the difference in basal temperatures that were mainly at melting point at the two northern glaciers while being well below the melting point at the southern glacier. A cold-based ice catchment would presumably have a less well developed drainage system and

react more strongly to the ceasing of surface melt water transportation to the base.

In conclusion, we find that in order to reproduce the spatial structure of the observed slowdown in the model, basal friction is required to change relatively more in the ice stream trough compared to the upstream area and increasingly so towards the front. Furthermore, we find that changes in the shear margin softness and internal heat production are most likely important for the sensitivity of the ice flow to changes in friction.

5.11 ACKNOWLEDGEMENTS

This publication is contribution number 90 of the Nordic Centre of Excellence SVALI funded by the Nordic Top-level Research Initiative. The ArcticDEM are provided by the Polar Geospatial Center, https://www.pgc.umn.edu/ under NSF OPP awards 1043681, 1559691 and 1542736. Velocity maps from ESA are obtained from the Sentinel 1 satellite generated by Enveo for the ESA CCI Greenland project. The BedMAchine bedmap version 3 is aquired from the National Snow and Ice Data Center (NSIDC):
http://nsidc.org/data/docs/daac/icebridge/idbmg4/. The Ice Sheet System Model is downloaded from https://issm.jpl.nasa.gov/ and we thank the ISSM team for model support.

6

PAPER III: INHOMOGENEOUS VISCOSITY IN ICE STREAMS

Figure 6.1: Upernavik Isstrøm (UI-3), seen from air, August 2013. Note the a sudden change in surface structures due to crevassing of an area with high strain

This paper forms the foundation of the manuscript: *Larsen, S.H., Ahlstrøm, A.P., Hvidberg, C.S. (in prep.), Importance of inhomogeneous viscosity in reproducing fast the flow of ice streams*

6.1 ABSTRACT

Model reproduction of fast flow of ice streams is crucial for ice sheet wide modelling of the Greenland ice sheet. The lateral drag is a particular important resistive force for the ice streams and thus the material strength of the shear margins providing lateral drag is of high importance. Shear margins are suggested to be softer due to increased internal heat production due to deformation, damage and the presence of liquid water. Yet, shear margin softness and the mechanism behind this softening are still not understood in detail. Here we present a simple way to introduce softer shear margins in ice flow models and test model performance for different grades of softness in the Ice Sheet System Model (ISSM). We find that model reproduction of fast

flow can be greatly improved by including softer shear margins. Our model results cannot quantify the mechanisms contributed to the extra softness of the margins, however, we suggest that including softer margins is necessary to reproduce the fast flow of ice streams.

6.2 INTRODUCTION

Fast flowing ice streams are responsible for the ice transport towards the ocean for a large part of the Greenland ice sheet (Rignot and Mouginot, 2012). The narrow ice streams thereby constitute a bottle neck that the ice has to pass trough. Ice flow models, thus, depend on reproducing the ice streams correctly to avoid creating non existing plugs for the flow. However, ice flow models are still underestimating flow speeds in these ice streams due to unresolved issues relating to model resolution, exact grounding line position and unknown ice viscosity (e.g. Aschwanden, Fahnestock, and Truffer, 2016; Bondzio et al., 2017; Joughin et al., 2012).

Greenlandic ice streams are most commonly located in deep narrow troughs (Morlighem et al., 2014) terminating in deep fjords. In these ice streams the basal drag is low and ice slides over the bed resulting in low vertical gradients in flow speed (Cuffey and Paterson, 2010). The lateral drag thus becomes relatively more important. The lateral drag is provided by both the bedrock in the trough but also the ice/ice interface between fast and slow moving ice. As an example, several studies have shown that to be able to reproduce the fast flow of Jakobshavn Isbræ the shear margins have to be softer than the surrounding ice (e.g. Bondzio et al., 2017; Joughin et al., 2012; Van Der Veen, Plummer, and Stearns, 2011). The shear margins are expected to be softer due to increased deformation heat in high shear areas and increased damage (Borstad et al., 2013). The heat released from refreezing of meltwater (cryo-hydrologic warming Phillips, Rajaram, and Steffen, 2010) is also likely to play an important role in the highly crevassed margins. A study by Lüthi et al. (2015) showed that the effect of refreezing water in deep crevasses could cause the ice to be 10-15°C warmer than a model only accounting for air temperature diffusion, advection and strain heating thus this extra heat source can be significant. None have so far been able to measure the temperature (or ice viscosity) in shear margins directly and so the effect of temperature, refreezing and damage on the ice softness remains unresolved.

In this study we investigate the importance of the soft shear margins on the center line velocity of a fast flowing glacier in Upernavik Isstrøm (Northwest Greenland). We hypothesize that the shear margins are softer than what would be given by the temperature difference due to strain heating alone. This is tested by looking into how well glacier flow is reproduced in an inverse ice flow model under different viscosity settings for the shear margins. More specifically, we

use the Higher-Order approximation in the Ice Sheet System Model (ISSM, Larour et al., 2012a), to set up a temperature model accounting for diffusion of surface air temperature, advection and strain heating throughout the Holocene. The temperature model is used to obtain a reference ice viscosity, which is then decreased in the shear margins in a number of model experiments. The model reaction to changing ice viscosity is evaluated by comparing model misfit of each experiments to observed ice flow along the center flow line.

6.3 STUDY SITE AND OBSERVATIONAL DATA

Upernavik Isstrøm (UI) is located on the Northwest coast of Greenland. We focus on the the northernmost of the main ice streams at UI (named UI-1, Figure 6.2), as this was the glacier that showed highest sensitivity to softer shear margins in earlier work (Paper II). Observations of winter velocities 2016-2017 are obtained from the European Space Agency (ESA), Climate Change Initiative (CCI) Greenland, where sentinel 1 Synthethic Aperature Radar (SAR) data are used to obtain Greenland wide velocities (Nagler et al., 2015). Winter velocities at UI-1 are between 5 and 6 km/yr near the front reducing to below 100 m/yr around 25 km inland (Figure 6.2).

6.4 MODEL SETUP

The basic model setup in the Higher-Order model of the Ice Sheet System Model (ISSM, Larour et al., 2012a) is described in the following.

The horizontal model domain is defined by the ice margin position in summer 2016 (Landsat 8 date?) and the flow catchment of UI outlined by flow directions from observed velocities (Rignot and Mouginot, 2012). This domain is divided into a triangular mesh with a resolution adapted to strain rates and velocity so that mesh resolution varies between 100 m and 15 km (Figure). The horizonal domain is extruded to 15 vertical layers that decrease in thickness towards the bed. The ice thickness is given by the surface geometry from Arctic DEM version 2.0 (created by the Polar Geospatial Center from DigitalGlobe, Inc. imagery) and the basal topography map by the BedMachine version 3 (Morlighem et al., 2017).

For incompressible viscous fluids the creep relation is given by

$$\tau_{jk} = 2\mu\dot{\epsilon}_{jk} \tag{33}$$

where τ_{jk} is the deviatoric stress tensor, $\dot{\epsilon}_{jk}$ is the strain rate tensor. The viscosity, μ, is derived from Glen's flow law (Glen, 1955) and adapted to include a damage factor D, which is between 0 and 1:

$$\mu = (1 - D)\frac{B(T, w)}{2\dot{\epsilon}_e^{(n-1)/n}} \tag{34}$$

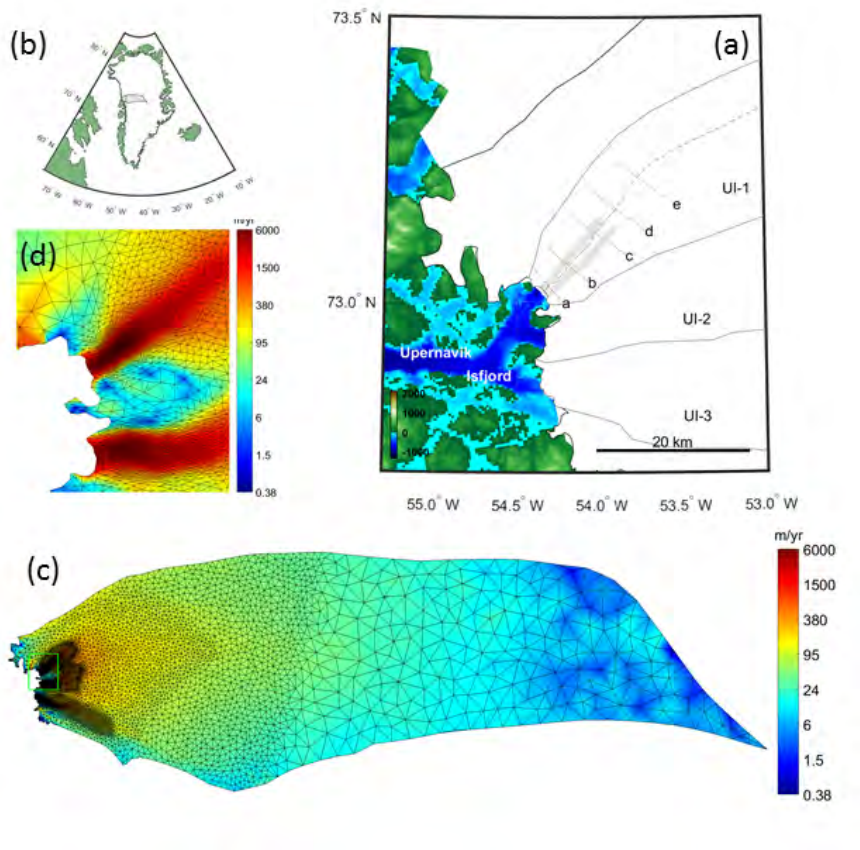

Figure 6.2: (a) Overview map of Upernavik Isstrøm, black line is the model domain, gray lines is the glacier sub-catchments, dashed line is the center flow line, the background is the bed map from BedMachine version 3 (Morlighem et al., 2017) overlain by the area covered by the Greenland ice sheet in white, gray zones indicate shear margins. (b) Map of Greenland, black lines indicate the Upernavik catchment and model domain. (c) Observed surface velocities winter 2014/2015 with model mesh outlined. (d) Zoom of area outlines by a green line in figure (c).

where $\dot{\epsilon}_e$ is the effective strain rate and the flow law exponent, n, is set to 3. The ice viscosity parameter B relates to Glen's flow law creep parameter through $A = B^{-1/n}$ and is dependent on temperature, T, and water fraction, w. The temperature dependence is given by Cuffey and Paterson (2010) (table 3.4 p. 75). D is a damage factor, introduced in the model to account for the softening effects of damage (Borstad et al., 2012), however, the origin of the softening can be anything and $(1 - D)$ can be compared to the enhancement factor E used on the creep parameter A.

6.4.1 *Boundary conditions*

We assume a stress free boundary at the surface of the ice however, at lateral domain boundaries (excluding the ice front) velocities and thickness are kept fixed at present day values. At the ice front water pressure is applied whenever ice is below sealevel. At the base we assume a basal drag given by

$$\tau_b = -k^2 \mathbf{u}_b N \tag{35}$$

where $\mathbf{u}_b$ is the basal sliding velocity and N the effective pressure in this case given by the hydrostatic pressure. The friction coefficient k is found using a control method (described by Morlighem et al., 2010) where k is spatially changed to make the model best match present day observed velocities. The temperature model is bounded by surface air temperature and a geothermal heat flux of 50 mW/m^2. Finally, the mass balance model is bounded by the surface mass balance (SMB) at the surface and a melt and accumulation rate of zero at the base. The lateral model domain is kept fixed which in practice means that all ice that passes through the domain boundary is lost.

6.5 TEMPERATURE MODEL

To obtain a spatially varying temperature field, we run a model through the Holocene (9700BC to 2016) varying only surface temperature. The thermal model is using the enthalpy formulation (Seroussi et al., 2013) allowing for both cold and temperate ice, in the latter case a water fraction, w, will also be calculated. The surface temperature through the Holocene is given by the mean present day surface temperature (an average of 1960 to 1999, from MAR) scaled by the temperature anomalies from Vinther et al. (2009). During the temperature run the SMB is kept constant at present day values (an average of 1960 to 1999, MAR). To save computational time the first part (9700BC to year 0) of the model run is done on a coarse mesh with a resolution between 500 m and 15 km. During the entire temperature run there is no softening applied, i.e. $D = 0$.

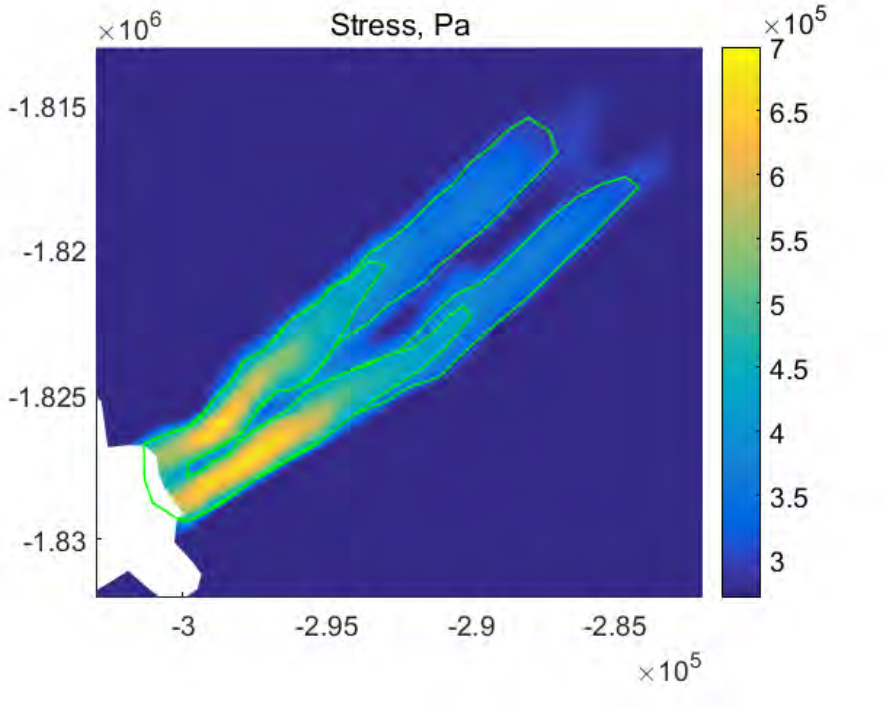

Figure 6.3: Stress calculated from observed velocities

6.6 DEFINING SHEAR MARGINS

Shear margins are defined as zones with higher shear than the surroundings resulting is crevassed ice. In this study we will define them in a strict sense as areas that are likely to be cresvassed based of stress fields of observed temperatures.

In a review study of crevasses Colgan et al. (2016) found that crevasses form within stress limits between 100 and 400 kPa and that crevasses form at lower stresses in colder ice. Based on the values given there, we define shear margins based on two different thresholds. The smallest shear margin zones are defined by the area with stress above 400 kPa and an extended zone is defined by stresses above 250 kPa (Figure 6.3).

6.7 EXPERIMENTS

With the purpose of testing the importance of including soft shear margins in ice flow models to reproducing the observed fast velocities, we set up a number of different experiments.

We start by setting up a reference model using the obtained temperature field from the temperature model (section 6.5) with $D = 0$. The control drag method is then applied to obtain a basal friction map, k, to best fit observed velocities. This inversion procedure will

Experiment	Margin type	D_{max}	note
reference	-	0	
exp1.10	250 kPa	10	
exp1.20	250 kPa	20	
exp1.30	250 kPa	30	
exp1.40	250 kPa	40	unstable
exp2.10	400 kPa	10	
exp2.20	400 kPa	20	
exp2.30	400 kPa	30	
exp2.40	400 kPa	40	unstable

Table 6.1: Table

result in a model velocity misfit to observed velocities, based on whatever mechanism the model was not able to account for by changing k alone. The same thing is done in eight different experiments applying $D > 0$ decreasing linearly from a given value, D_{max}, at the front towards 0 at the end of the shear margins (approximately 10 km and 20 km from the front for the two types of shear margins respectively). D_{max} is varied between 0.1 and 0.4 and the experiments are divided in two, exp1 and exp2 (see list of experiments in Table 6.1), depending on which shear margin definition is used (small and large shear margin zones respectively, Figure 6.3).

6.8 RESULTS

The temperature model show shear margins that are up to 10°C warmer than surrounding ice (Figure 6.4). Close to the margin (profile a) it is only the center of the ice stream that remains cold (down to −20°C) and the shear margins and ice along the sides are up to 10°C warmer than the center. Moving inland the shear margins remain warmer than the surrounding ice, however, at a distance of 20 km (profile e) the difference is only by a few degrees.

The reference run shows that the velocity misfit is relatively large as the velocity starts to increase drastically towards the margins from 10 km inland (Figure 6.5). When we include softer shear margins the velocity misfit becomes smaller, the higher the value of D_{max}. At around $D_{max} = 0.4$ (exp1.40) and above the model starts to become numerically unstable. At a distance of 5 km from the front the velocity increases by 10 % when D_{max} increases from 0 to 10 % and by 6 % when D_{max} increases from 30 to 40 %. The experiment results are similar for both types of shear margin definition (i.e. exp1 show similar results as exp2).

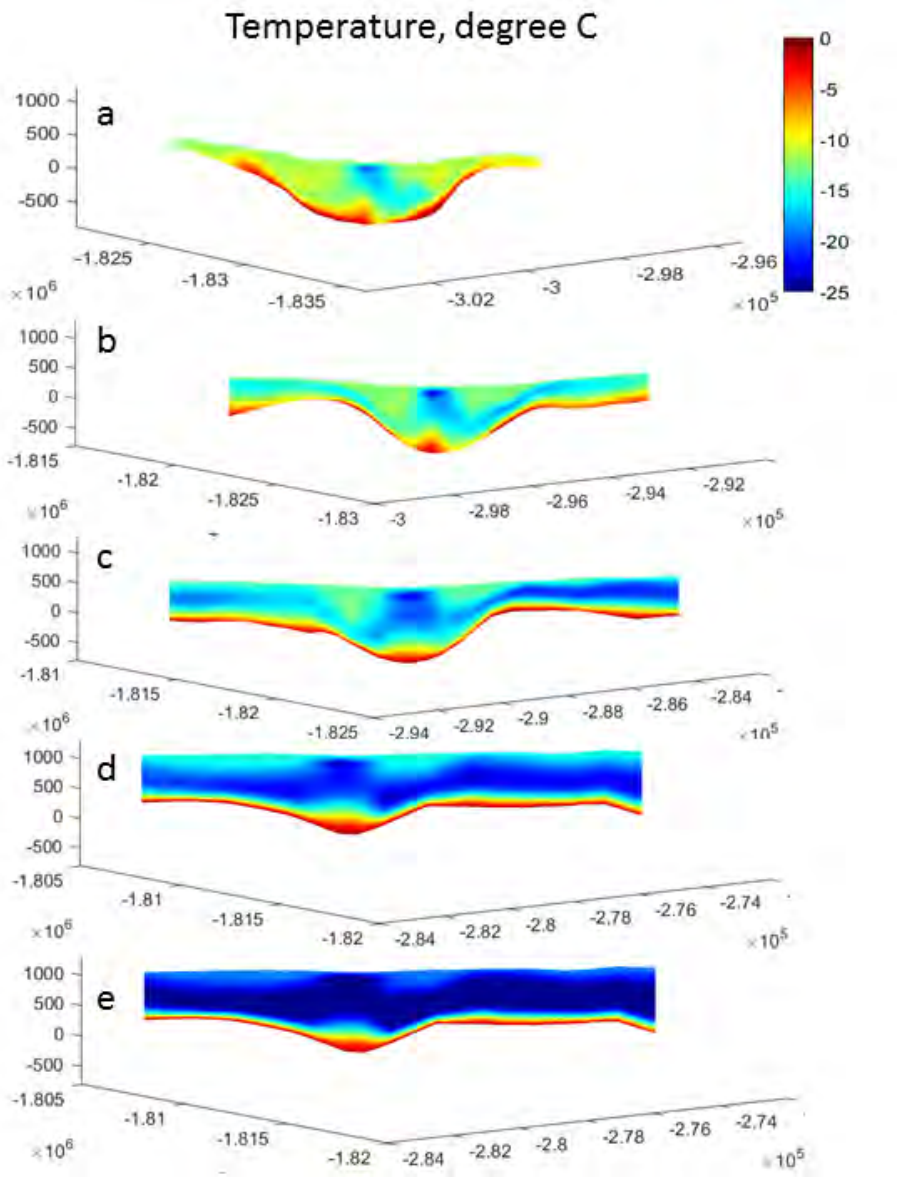

Figure 6.4: Temperature transect of each profile in figure 6.2, a is close to the margin e is furthest inland.

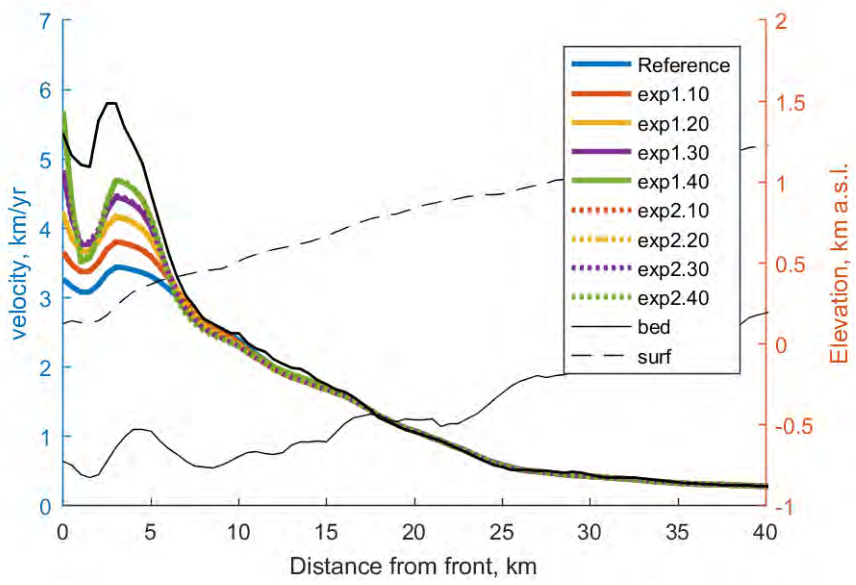

Figure 6.5: The model misfit from the control drag run for all experiments.

6.9 DISCUSSION

The shear margins of fast flowing ice streams are expected to be softer than the surrounding ice due to strain heating, crevassing and cryo-hydrologic warming. The shear margins' softness is important because they are forming the ice/ice boundary that provides lateral drag in ice streams where this is relatively more important than basal drag. In the experiments, we tested whether softening the shear margins would improve model performance in these areas. We used an ice flow model to test how increasing softness of the shear margins would affect the model misfit in the initialisation of an ice flow model by inverting for basal friction. To get more information on the origin of the extra softness we first calculated the ice temperature in the case that this was only affected by the diffusion of surface air temperature, advection and strain heating. This temperature field was used to make a reference model where the obtained temperature is the only reason for inhomogeneity in ice viscosity. We then applied increasingly softer shear margins in well defined shear margin zones to see how the model misfit changed.

The temperature model showed a temperature difference between the shear margins and the surrounding ice of up to 10°C with values around −15°C in the shear margins where they are warmest and around −20°C in the main part of the ice stream surrounding ice. The study of Lüthi et al. (2015) showed that in areas where deep crevasses occur this type of model could be too cold by up to 15°C due to the neglection of cryo-hydrologic warming. The investigations by Lüthi et al. (2015) where made in an area with few, however deep, crevasses

due to the logistical issues in drilling in areas with a large number of crevasses. The crevassed state of the shear margins could mean that these areas are highly affected by this heating process (Phillips, Rajaram, and Steffen, 2010, show that heating is more efficient in areas with short distances between crevasses) hence, it is not unrealistic that the temperature model could be too cold by $10-15^{\circ}$ in the most crevassed areas. This could mean that the shear margins in fact could be temperate in the areas with the highest strain. The difference in B from ice at -15° to ice at melting point is around 50 % (according to table 3.4 p. 75, Cuffey and Paterson, 2010). This means that it is not unrealistic to suggest that B could be 50% smaller in areas close to the front as we do in exp1.50 and exp2.50.

In the reference run the model was not able to change friction enough to reproduce the observed fast flow near the front (Figure 6.5). This suggests that the model is lacking information about specific mechanism in this area. In the case of model shear margins being too hard, the ice would be too rigid to deal with the abrupt change in friction between the fast and slow moving areas, thus resulting in the ice experiencing too high resistance to flow along the margins. Hence, the model velocities will be too slow and increasing the shear margin softening should improve this misfit. This is exactly what the experiments show (Figure 6.5). As we increase the shear margin the ice flow velocities increase until the model becomes numerically unstable (exp1.40 and exp2.40).

It is clear that increasing shear margin softness improves model performance as also seen in Bondzio et al. (2017) and Joughin et al. (2012). Thus, we believe that it is likely that they are softer than just given by the reference viscosity. Based on the findings of Lüthi et al. (2015) this softening could be due to warmer shear margins than what is given by the temperature model. However, the fact that crevasses form at stresses much lower than we observed in the main part of the glacier trunk, could also indicate that ice is softer due to damage (Borstad et al., 2013). The effect of this softening is significantly improving model performance near the front of the glacier through an increase in the modelled velocity of more than 30 %. The cryo-hydrologic warming that is unaccounted for in the temperature model could play a role, not only in the shear margins, but in the larger ablation zone of the catchment. Hence, it is likely that the viscosity in a much larger part of the model domain is too high due to the ice being assumed too cold.

As D_{max} increase beyond 40 % the model becomes numerically unstable, this could be a reaction to the crude way of applying D only changing with distance from the front and not laterally. It could also indicate that it is simply not physically possible to consider the shear margin zones as a continuum and they should rather be treated as rifts as in Larour et al. (2014b). In the case of ice viscosity being too

high everywhere due to too low model temperatures, it is unlikely that the difference in viscosity between shear margins and surrounding ice would reach up to 50 %.

The little difference that is seen between the results of the two types of shear margins (exp1 versus exp2) could point to the fact that it is, in this case, only necessary to deal with the shear margin zones that are defined by the maximum amount of stress (400 kPa). However, this should not be directly interpreted as the softer shear margin zones should only be of the latter type. The shear margins could easily be softer all the way up to 20 km distance from the front, but the model is able to accommodate this by changing basal friction alone. This highlights the limitations of this method to reveal actual quantitative knowledge about the actual softness, as part of the effect will be masked by the inverted basal friction adapting to accommodate uncertainties related to other mechanisms than friction.

Other limitations to interpretations are related to the fact that the ice front and grounding line is considered to be at the same position. We do not know whether this is the case. Thus, basal friction could be zero in an area near the front. Furthermore, in the Higher-Order approximation bridging effects are neglected which they cannot be close to the glacier front. Thus, basal friction is likely to be too high close to the front using this approximation (Morlighem et al., 2010).

This study does not claim to give the answer to what the cause of the softening is, but we show that model underestimation of shear margin softness is a plausible cause for model velocity misfit. Thus, applying softer shear margins is important for reproducing ice flow near the margins of ice streams. The method of defining the shear margins according to stress of observed velocities is an approach to include soft shear margins without knowing the specific physics behind the softening mechanisms, in order to better reproduce the observed fast flow of ice streams. Further investigations could include a temperature model that accounts for cryo-hydrologic warming (Phillips, Rajaram, and Steffen, 2010) as well as applying a better method for defining the areas that could be more strongly affected by this and softening due to damage (the shear margin zones in this study).

6.10 CONCLUSIONS

A realistic model reproduction of ice flow near the margin of ice streams is necessary to reproduce the correct ice flow of the entire ice sheet. In conclusion, our model results show that misrepresenting shear margins as too hard in ice flow models, is a likely cause for model velocity misfit near the margin of ice streams. The study highlights that the representation of ice viscosity is crucial for how well ice flow models reproduce fast flow, thus eliminating the knowledge gap of the inhomogeneity of ice viscosity should be the focus of con-

tinued studies. Until this is accomplished, the results from this study suggest that simple representation of softer shear margins according to stress can improve model performance.

6.11 ACKNOWLEDGMENTS

This publication is contribution number 91 of the Nordic Centre of Excellence SVALI funded by the Nordic Top-level Research Initiative. Velocity maps are obtained from the Sentinel 1 satellite generated by Enveo for the ESA CCI Greenland project. The Arctic DEMs provided by the Polar Geospatial Center under NSF OPP awards 1043681, 1559691 and 1542736. The Ice Sheet System Model is downloaded from https://issm.jpl.nasa.gov/ and we thank the ISSM team for model support.

7

SUMMARY AND OUTLOOK

Ice streams in Greenland have have generally undergone acceleration, retreat and thinning during the last couple of decades. Many ice streams show abrupt changes, likely initially triggered by climate changes but enhanced by feedback mechanisms related to the geometry of the individual glacier. Controlling mechanisms of the ice stream behaviour and how they interact are yet not fully understood, thus, inhibiting robust prediction of future changes. Evolution within observational methods, in particular velocity, and model development now makes it possible to study the mechanisms behind the changes in detail. This chapter summarise the work done in this thesis on improving current understanding of controlling mechanisms for ice stream flow. The purpose of the chapter is to give directions for future work.

7.1 CONTROLLING MECHANISM OF VELOCITY CHANGES AT UI

During the period 2000-2012 the three main glaciers of UI experienced asynchronous dynamic changes (Paper I). UI-1 showed a sudden retreat followed by acceleration and thinning around 2007. The sudden retreat was due to the loss of a floating ice shelf, after the front had gradually been retreating into a wider and possibly deeper trough for 5-6 years. The calving front of UI-2, which is located in a stable position between two high mountains, showed a more gradual retreat, thinning and acceleration from around 2008 and onwards. While both UI-1 and UI-2 showed changes, UI-3 remained remarkably stable. The stability of UI-3 is most likely due to the glacier being stabilised by basal topography at the calving front. These different reactions exemplifies the complexity of ice stream dynamics and shows the importance of geometry for glacier response as a consequence of climate chage. The acceleration and retreat of the glaciers increased the dynamic mass loss considerably, in the same period as the SMB decreased. Consequently, the ratio between mass lost by increased melt (not balanced by increased accumulation) and solid ice discharge remained the same (20-40% surface melt and 60-80% dynamic mass loss). During the same period the dynamic mass loss in the entire Greenland contributed between 30-50% to the total mass loss (Enderlin et al., 2014), hence, UI is losing more mass than average for the ice sheet, during the period. Many other studies are often focusing on the extreme case of Jakobshavn Isbræ (e.g. Bondzio et al., 2017; Joughin et al., 2012; Van Der Veen, Plummer, and Stearns, 2011),

that lost a floating ice tongue and retreated around 20 km since 1990s. UI glaciers appear to be more representative of the general trends in the region, as shown by the slightly higher dynamic mass loss than average for the ice sheet. This is mainly due to the more moderate size of UI ice streams compared to Jakobshavns Issbræ. In addition to this, the UI ice streams show different types of response in close vicinity of each other which makes UI an optimal study site for detailed process studies.

7.1.1 *Importance of inhomogeneous viscosity for ice flow*

The overall reaction to climate change of the three main ice streams at UI, are controlled by bedrock geometry (Paper I). However, on smaller scales the shear margins are playing an important role in controlling the ice streams through inhomogeneity of ice viscosity (Paper II and Paper III).

The shear margins are providing lateral resistance in the ice streams, and thus, the viscosity of the shear margins is important for ice flow. Increased softness of shear margins is due to strain heating, damage, the weakening effect of water within the crevasses and cryo-hydrologic warming. Both studies in Paper II and Paper III, showed improved results when softer margins were applied to the ice flow models. Thus, indicating that inhomogeneity in ice viscosity is an important factor to include when modelling ice stream flow. Until better physical models are developed, softer shear margins can be applied as zones of softer ice using a general softening factor (as shown in Paper III) in order to improve model performance.

At UI-1, the ice shelf disintegration in 2007 implied a significant perturbation of the glacier flow causing acceleration. The continued high velocities following the perturbation points to feedback mechanisms related to accelerated flow that caused continued high velocities at UI-1 for years after the perturbation. In Paper II the temperature-viscosity feedback mechanism was shown to be important by providing viscosity changes that were able to account for up to 20 % of the abrupt slow-down. Thus, this could also have an important effect on the acceleration of UI-1 that cause ice flow velocities to double within a few years. In future model studies, the importance and duration of the effect of the temperature viscosity feedback mechanisms could be tested by modelling ice flow response to calving front changes, similarly to the study of Jakobshavn Isbræ by Bondzio et al. (2017).

7.1.2 *Importance of surface melt for ice stream flow*

The direct effect of increased melt is thinning, which will be followed by retreat and acceleration, enhanced by ice stream feedback mechanisms. However, due to the permeability of the ice (through crevasses

and moulins), the surface meltwater also has an impact on basal and lateral resistance. On sub-seasonal timescales the meltwater has a large control on flow. In Paper II this control on flow was seen in observations of abrupt slow-down of ice flow, at the ceasing of surface meltwater production. The model study in Paper II revealed that the sensitivity to the changes in surface meltwater increased towards the front of the ice streams. This was interpreted to be due to the increase of meltwater as it accumulates towards the front and the effect of meltwater percolating trough shear margins. The study in Paper II concluded that an effective hardening of the shear margins, as surface meltwater production ceased, could be a likely contributor to the observed slow-down. Sensitivity to changes in resistive forces is, furthermore, likely to depend on basal temperatures. The results of Paper II showed that basal resistance had to change much more at the cold based UI-3, than at UI-1 and UI-2 where basal temperatures are at melting point. The reason for this different sensitivity is believed to be due to the ceasing of surface melt water will leave cold based ice relatively dry, compared to areas where basal melt occurs.

7.1.2.1 *Limitations of the model studies*

In addition to the changes in resistive forces at the base and lateral boundaries of the ice the influence of meltwater on the turbulent plume is likely to be important. As surface meltwater production increase, the increased plume strength could potentially enhance the frontal melt rates and ice/ocean interaction. Thus, an increase in surface meltwater could also increase the effect of warming ocean waters. Ice/ocean interaction was neglected in the modelling studies. Thus, this remains one of the major shortcomings of the model studies in the thesis. Present development within ISSM includes a calving criterion and subglacial melt rates (Bondzio et al., 2016; Morlighem et al., 2016). Thus future studies should include ice/ocean interaction to be able to separate the effect of changes happening directly at the front and further inland.

The model studies performed in Paper II and III both assume ice temperatures that are based on a long forward model run, including only surface air temperature as a source of temperature variations. Thus, by neglecting the effect of cryo-hydrological warming in the ablation zone, the model will most likely have a cold bias. The temperature and water fraction, as calculated from the enthalpy solution in the temperature model, are the only dependencies of the viscosity prefactor B (in equation 6). Hereby, neglecting the influence of dust, damage and possible other effects. The overall effect of this is that the model ice viscosity will be higher than in reality. This is likely to influence the conclusions on the importance of softer shear margins, resulting in the difference in ice viscosity, between the shear margins and the surroundings, is not as large as the model studies suggests.

7.2 THE MERIT OF ICE FLOW MODELS

Ice flow models can act as virtual laboratories in which different processes can be investigated in relation to observations. The ultimate goal of doing this is to improve ice flow models to increase the robustness of future projections.

In the virtual laboratory however, care should be taken when the process being tested is something that cannot be directly tested by observations. This is the case for the experiments done in Paper II and III. Both the basal boundary condition and the ice viscosity in the shear margins cannot be observed in high spatial resolution with current technology. This means that very little is known about the magnitudes of the processes and results are therefore likely to be biased towards the process being studied. While some neglected processes are known and neglected due to constraints of the models, such as ice/ocean interaction in Paper II and III, there could also be other unknown processes that remain unaccounted for. Despite this, the model results of such studies can be used to investigate whether hypotheses are worth pursuing in observational studies or if the effect of the hypothesised process is negligible. In the case of Paper II and III it was found that it is very likely that models are underestimating the softness of the shear margins and that this could be due to both the temperature being underestimated or the weakening effect of damage and water penetrating through the crevassed areas. To prove the model findings future observational studies should therefore focus on investigating the viscosity of shear margins in more detail.

7.3 OUTLOOK

With the launch of the Sentinel 1 satellite in 2014, velocity maps can now be created ever 6th or 12th day. Thus, opening up for detailed studies of seasonal dynamics of ice streams. The continuous data series of velocity maps to be obtained from this will provide an unprecedented opportunity for studies of, for example, effects of surface meltwater on ice flow similar to the study on Paper II. This study was limited to the short time period where the COSMO-SkyMed satellite images were acquired in the late melt season of 2014. The high repeat velocity maps, furthermore, opens up for data assimilation studies evolving in time, as in Larour et al. (2014a). In this study Larour et al. (2014a) assimilate observed changes in ice thickness by changing surface mass balance and basal friction in a forward running model. Thus, adding the time dimension in the assimilation process, it is possible to estimate changes in the inferred fields.

8

CONCLUSIONS

In this thesis observations about the dynamic behaviour of Upernavik Isstrøm (UI) have been collected and used in an ice flow model to investigate controlling mechanisms for ice stream flow. The thesis was based on three studies with the purpose of: (1) establishing the current state of UI using observations and determining how UI ice streams have reacted to current climate change; (2) Using an ice flow model to investigate ice flow velocity sensitivity to changes in surface melt; (3) Investigating the importance of soft shear margins for ice flow models to reproduce fast flow. The main conclusions of the three studies can be summarised to be:

1. The UI glaciers showed a higher than average dynamic changes during the 2000s, mainly due to the disintegration of an ice shelf at UI-1. However, the changes here are in line with the general trends in the region (Northwest Greenland). The main ice streams of UI behaves distinctively different and constitute a good study site for determining controlling mechanisms for fast flow of ice streams.

2. Ice flow sensitivity is increasingly sensitive to changes in meltwater near the front, possibly due to the softening effect of meltwater percolating into the crevassed shear margins.

3. Soft shear margins are important for the flow of ice streams. By including them as zones of softer ice, model performance in reproducing the fast flow of ice streams can be improved significantly.

Reproducing the fast flow of ice streams is crucial for modelling ice flow of the entire ice sheet. Thus this thesis outlines the importance for understanding the inhomogeneity of the ice viscosity for more robust future projections of the Greenland ice sheet.

BIBLIOGRAPHY

Aðalgeirsdóttir, G., A. Aschwanden, C. Khroulev, F. Boberg, R. Mottram, P. Lucas-Picher, and J. H. Christensen (2014). "Role of model initialization for projections of 21st-century Greenland ice sheet mass loss". In: *Journal of Glaciology* 60.222, pp. 782–794. DOI: 10.3189/2014JoG13J202.

Ahlstrøm, A. P. et al. (2013). "Seasonal velocities of eight major marine-terminating outlet glaciers of the Greenland ice sheet from continuous in situ GPS instruments". In: *Earth System Science Data* 5.2, pp. 277–287. DOI: 10.5194/essd-5-277-2013.

Alley, R. B. (1991). "Sedimentary processes may cause fluctuations of tidewater glaciers". In: *Annals of Glaciology* 15, pp. 119–124.

Andersen, M. L. et al. (2010). "Spatial and temporal melt variability at Helheim Glacier, East Greenland, and its effect on ice dynamics". In: *Journal of Geophysical Research: Earth Surface* 115.4, pp. 1–18. DOI: 10.1029/2010JF001760.

Andersen, M. L., M. Nettles, P. Elosegui, T. Larsen, G. Hamilton, and L. Stearns (2011). "Quantitative estimates of velocity sensitivity to surface melt variations at a large Greenland outlet glacier". In: *Journal of Glaciology* 57.204, pp. 609–620. DOI: 10.3189/002214311797409785.

Andresen, C. S., K. K. Kjeldsen, B. Harden, N. Nørgaard-pedersen, and K. H. Kjær (2014). "Outlet glacier dynamics and bathymetry at Upernavik". In: *GEUS Bullitin* 31.August 2014, pp. 81–84.

Aschwanden, A, G Aðalgeirsdóttir, and C Khroulev (2013). "Hindcasting to measure ice sheet model sensitivity to initial states". In: *The Cryosphere*, pp. 1083–1093. DOI: 10.5194/tc-7-1083-2013.

Aschwanden, A., M. A. Fahnestock, and M. Truffer (2016). "Complex Greenland outlet glacier flow captured". In: *Nature Communications* 7.May 2015, p. 10524. DOI: 10.1038/ncomms10524.

Aschwanden, A., E. Bueler, C. Khroulev, and H. Blatter (2012). "An enthalpy formulation for glaciers and ice sheets". In: *Journal of Glaciology* 58.209, pp. 441–457. DOI: 10.3189/2012JoG11J088.

Bamber, J. L. et al. (2013). "A new bed elevation dataset for Greenland". In: *The Cryosphere* 7.2, pp. 499–510. DOI: 10.5194/tc-7-499-2013.

Bamler, R. and P. Hartl (1998). "Synthetic aperture radar interferometry Synthetic aperture radar interferometry". In: *Inverse Problems* 14.4, p. 55. DOI: 10.1088/0266-5611/14/4/001.

Bartholomew, I., P. Nienow, D. Mair, A. Hubbard, M. a. King, and A. Sole (2010). "Seasonal evolution of subglacial drainage and

acceleration in a Greenland outlet glacier". In: *Nature Geoscience* 3.6, pp. 408–411. DOI: 10.1038/ngeo863.

Bartholomew, I., P. Nienow, A. Sole, D. Mair, T. Cowton, and M. a. King (2012). "Short-term variability in Greenland Ice Sheet motion forced by time-varying meltwater drainage: Implications for the relationship between subglacial drainage system behavior and ice velocity". In: *Journal of Geophysical Research* 117.F3, F03002. DOI: 10.1029/2011JF002220.

Benn, D. I., C. R. Warren, and R. H. Mottram (2007). "Calving processes and the dynamics of calving glaciers". In: *Earth-Science Reviews* 82.3-4, pp. 143–179. DOI: 10.1016/j.earscirev.2007.02.002.

Bondzio, J. H., M. Morlighem, H. Seroussi, T. Kleiner, M. Rückamp, J. Mouginot, T. Moon, E. Y. Larour, and A. Humbert (2017). "The mechanisms behind Jakobshavn Isbrae's acceleration and mass loss: a 3D thermomechanical model study". In: *Geophysical Research Letters* May, pp. 1–9. DOI: 10.1002/2017GL073309.

Bondzio, J. H., H. Seroussi, M. Morlighem, T. Kleiner, M. Rückamp, A. Humbert, and E. Y. Larour (2016). "Modelling calving front dynamics using a level-set method: Application to Jakobshavn Isbræ, West Greenland". In: *Cryosphere* 10.2, pp. 497–510. DOI: 10.5194/tc-10-497-2016.

Borstad, C. P., A. Khazendar, E. Larour, M. Morlighem, E. Rignot, M. P. Schodlok, and H. Seroussi (2012). "A damage mechanics assessment of the Larsen B ice shelf prior to collapse: Toward a physically-based calving law". In: *Geophysical Research Letters* 39.17, pp. 1–5. DOI: 10.1029/2012GL053317.

Borstad, C. P., E. Rignot, J. Mouginot, and M. P. Schodlok (2013). "Creep deformation and buttressing capacity of damaged ice shelves: Theory and application to Larsen C ice shelf". In: *Cryosphere* 7.6, pp. 1931–1947. DOI: 10.5194/tc-7-1931-2013.

Box, G. E. P. and N. R. Draper (1987). *Empirical Model-Building and Response Surfaces*. Wiley.

Brinkerhoff, D. J. and J. V. Johnson (2015). "Dynamics of thermally induced ice streams simulated with a higher-order flow model". In: *Journal of Geophysical Research F: Earth Surface* 120.9, pp. 1743–1770. DOI: 10.1002/2015JF003499.

Brinkerhoff, D., M. Truffer, and A. Aschwanden (2017). "Sediment transport drives tidewater glacier periodicity". In: *Nature Communications* 8.1, p. 90. DOI: 10.1038/s41467-017-00095-5.

Broeke, M. van den, J. Bamber, J. Ettema, E. Rignot, E. Schrama, W. J. van de Berg, E. van Meijgaard, I. Velicogna, and B. Wouters (2009). "Partitioning recent Greenland mass loss." In: *Science (New York, N.Y.)* 326.5955, pp. 984–6. DOI: 10.1126/science.1178176.

Buchardt, S. L. and D. Dahl-Jensen (2007). "Estimating the basal melt rate at North GRIP using a Monte Carlo technique". In: *Annals of Glaciology* 45, pp. 137–142. DOI: 10.3189/172756407782282435.

Bueler, E. and J. Brown (2009). "Shallow shelf approximation as a "sliding law" in a thermomechanically coupled ice sheet model". In: *Journal of Geophysical Research: Solid Earth* 114.3, pp. 1–21. DOI: 10.1029/2008JF001179. arXiv: 0810.3449.

Carr, J. R., C. R. Stokes, and A. Vieli (2013). "Recent progress in understanding marine-terminating Arctic outlet glacier response to climatic and oceanic forcing: Twenty years of rapid change". In: *Progress in Physical Geography* 37.4, pp. 436–467. DOI: 10.1177/0309133313483163.

Christensen, O. B., M Drews, J. H. Christensen, K Dethloff, K Ketelsen, I Hebestadt, and A Rinke (2007). "The HIRHAM Regional Climate Model Version 5 (beta)". In: *Technical Report 06-17;* 5, pp. 1–22.

Citterio, M. and A. P. Ahlstrøm (2013). "Brief communication "The aerophotogrammetric map of Greenland ice masses"". In: *The Cryosphere* 7.2, pp. 445–449. DOI: 10.5194/tc-7-445-2013.

Colgan, W., J. E. Box, M. L. Andersen, X. Fettweis, B. Csathó, R. S. Fausto, D. van As, and J. Wahr (2015). "Greenland high-elevation mass balance: inference and implication of reference period (1961–90) imbalance". In: *Annals of Glaciology* 56.70, pp. 105–117. DOI: 10.3189/2015AoG70A967.

Colgan, W., H. Rajaram, W. Abdalati, C. McCutchan, R. Mottram, M. S. Moussavi, and S. Grigsby (2016). "Glacier crevasses: Observations, models, and mass balance implications". In: *Reviews of Geophysics* 54, pp. 119–161. DOI: 10.1002/2015RG000504.Received. arXiv: Colgan2016.

Csatho, B. M., a. F. Schenk, G. S. Babonis, C. J. van der Veen, M. R. van den Broeke, J. H. van Angelen, S Nagarajan, S Rezvanbehbahani, and S. B. Simonsen (2014). "Laser Altimetry Reveals Complex Pattern of Greenland Ice Sheet Dynamics". In: *PNAS* 111.52. DOI: 10.1073/pnas.1411680112.

Cuffey, K. and W. S. B. Paterson (2010). *The physics of glaciers*. Fourth. Elsevier. ISBN: 9780123694614.

Dahl-Jensen, D (1985). "Determination of the flow properties at Dye 3, south Greenland by bore-hole tilting measurement and perturbation modelling". In: *J. of Glacio.* 31.108, pp. 92–98.

Dahl-Jensen, D., K. Mosegaard, N. Gundestrup, G. D. Clow, S. J. Johnsen, A. W. Hansen, and N. Balling (1998). "Past Temperatures Directly from the Greenland Ice Sheet". In: *Science* 282.5387, pp. 268–271. DOI: 10.1126/science.282.5387.268.

Dall, J., A. Kusk, U. Nielsen, and J. P. M. Boncori (2015). "Ice velocity mapping using TOPS sar data and offset tracking". In: *European Space Agency, (Special Publication) ESA SP* SP-731.March.

Damsgaard, A., D. L. Egholm, L. H. Beem, S. Tulaczyk, N. K. Larsen, J. A. Piotrowski, and M. R. Siegfried (2016). "Ice flow dynamics forced by water pressure variations in subglacial granular beds". In: *Geophysical Research Letters* 43.23, pp. 12,165–12,173. DOI: 10.1002/2016GL071579.

Das, S. B., I. R. Joughin, M. D. Behn, I. M. Howat, M. A. King, D. Lizarralde, and M. P. Bhatia (2008). "Fracture Propagation to the Base of the Greenland Ice Sheet During Supraglacial Lake Drainage". In: *Science* 320.May, pp. 778–782.

Dee, D. P. et al. (2011). "The ERA-Interim reanalysis: Configuration and performance of the data assimilation system". In: *Quarterly Journal of the Royal Meteorological Society* 137.656, pp. 553–597. DOI: 10.1002/qj.828.

ESA CCI (2015). *The European Space Agency Climate Change Initiative - Ice Sheets, program for Greenland*.

Echelmeyer, K. A., W. Harrison, C. Larsen, and J. E. Mitchell (1994). "The role of the margins in the dynamics of an active ice stream". In: *Journal of glciology* 40.136, pp. 527–538.

Enderlin, E. M., I. M. Howat, and A. Vieli (2013). "High sensitivity of tidewater outlet glacier dynamics to shape". In: *The Cryosphere* 7.3, pp. 1007–1015. DOI: 10.5194/tc-7-1007-2013.

Enderlin, E. M., I. Howat, S. Jeong, M.-J. Noh, J. van Angelen, and M. van den Broecke (2014). "An improved mass budget for the Greenland ice sheet". In: *Geophysical Research Letters* 41, pp. 866–872. DOI: 10.1002/2013GL059010.Received.

Ewert, H., A. Groh, and R. Dietrich (2012). "Volume and mass changes of the Greenland ice sheet inferred from ICESat and GRACE". In: *Journal of Geodynamics* 59-60, pp. 111–123. DOI: 10.1016/j.jog.2011.06.003.

Fahnestock, M. (2001). "High Geothermal Heat Flow, Basal Melt, and the Origin of Rapid Ice Flow in Central Greenland". In: *Science* 294.5550, pp. 2338–2342. DOI: 10.1126/science.1065370.

Fettweis, X., B. Franco, M. Tedesco, J. H. van Angelen, J. T. M. Lenaerts, M. R. van den Broeke, and H. Gallée (2013). "Estimating the Greenland ice sheet surface mass balance contribution to future sea level rise using the regional atmospheric climate model MAR". In: *The Cryosphere* 7.2, pp. 469–489. DOI: 10.5194/tc-7-469-2013.

Fleurian, B. de, O. Gagliardini, T. Zwinger, G. Durand, E. Le Meur, D. Mair, and P. Råback (2014). "A double continuum hydrological model for glacier applications". In: *The Cryosphere* 8.1, pp. 137–153. DOI: 10.5194/tc-8-137-2014.

Funk, M., K. Echelmeyer, and A. Iken (1994). "Mechanisms of fast flow in Jakobshavns Isbrae, West Greenland: part II. Modeling of englacial temperatures". In: *Journal of Glaciology* 40.136, pp. 569–585.

Gillet-Chaulet, F., G. Durand, O. Gagliardini, C. Mosbeux, J. Mouginot, F. Rémy, and C. Ritz (2016). "Assimilation of surface velocities between 1996 and 2010 to constrain the form of the basal friction law under Pine Island Glacier". In: *Geophysical Research Letters* 20.1, pp. 311–321. DOI: 10.1002/2016GL069937.

Glen, J. W. (1955). "The creep of polycrystalline ice". In: *Proceedings of the Royal Society of London. Series A. Mathematical and Physical Sciences* 228.1175, 519 LP –538.

Gogineni, S. P. (2012). *No CReSIS Radar Depth Sounder L2 Data, Lawrence, Kansas, USA. Digital Media.*

Gogineni, S., D. Tammana, D. Braaten, C. Leuschen, T. Akins, J. Legarsky, P. Kanagaratnam, J. Stiles, C. Allen, and K. Jezek (2001). "Coherent radar ice thickness measurements over the Greenland ice sheet". In: *Journal of Geophysical Research* 106.D24, pp. 33,761–33,772. DOI: 10.1029/2001JD900183.

Goldstein, R. M., H. Engelhardt, B. Kamb, and R. M. Frolich (1993). "Satellite Radar Interferometry for Monitoring Ice Sheet Motion: Application to an Antarctic Ice Stream". In: *Science* 262.5139, pp. 1525–1530. DOI: 10.1126/science.262.5139.1525.

Gong, Y., T. Zwinger, S. L. Cornford, R. Gladstone, M. Schäfer, and J. C. Moore (2016). "Importance of basal boundary conditions in transient simulations: case study of a surging marine-terminating glacier on Austfonna, Svalbard". In: *Journal of Glaciology* 63, pp. 1–12. DOI: 10.1017/jog.2016.121.

Harrington, J. A., N. F. Humphrey, and J. T. Harper (2015). "Temperature distribution and thermal anomalies along a flowline of the Greenland ice sheet". In: *Annals of Glaciology* 56.70, pp. 98–104. DOI: 10.3189/2015AoG70A945.

Helm, V., A. Humbert, and H. Miller (2014). "Elevation and elevation change of Greenland and Antarctica derived from CryoSat-2". In: *Cryosphere* 8.4, pp. 1539–1559. DOI: 10.5194/tc-8-1539-2014.

Holland, D. M., R. H. Thomas, B. de Young, M. H. Ribergaard, and B. Lyberth (2008). "Acceleration of Jakobshavn Isbræ triggered by warm subsurface ocean waters". In: *Nature Geoscience* 1.10, pp. 659–664. DOI: 10.1038/ngeo316.

Howat, I. M., a. Negrete, and B. E. Smith (2014). "The Greenland Ice Mapping Project (GIMP) land classification and surface elevation data sets". In: *The Cryosphere* 8.4, pp. 1509–1518. DOI: 10.5194/tc-8-1509-2014.

Howat, I. M., I. Joughin, M. Fahnestock, B. E. Smith, and T. A. Scambos (2008). "Synchronous retreat and acceleration of southeast Greenland outlet glaciers 2000-06: Ice dynamics and coupling to climate". In: *Journal of Glaciology* 54.187, pp. 646–660. DOI: 10.3189/002214308786570908.

Iken, A, K Echelmeyer, W Harrison, and M Funk (1993). "Mechanisms of fast flow in Jakobshavns Isbræ, West Greenland: Part I.

Measurements of temperature and water level in deep boreholes". In: *Journal of Glaciology* 39.131, pp. 15–25. DOI: 10.1017/S0022143000015689.

Jenkins, A. (2011). "Convection-Driven Melting near the Grounding Lines of Ice Shelves and Tidewater Glaciers". In: *Journal of Physical Oceanography* 41.12, pp. 2279–2294. DOI: 10.1175/JPO-D-11-03.1.

Joseph, C. A. and D. J. Lampkin (2017). "Spatial and temporal variability of water-filled crevasse hydrologic states along the shear margins of Jakobshavn Isbrae, Greenland". In: *The Cryosphere Discussions* May, pp. 1–21. DOI: 10.5194/tc-2017-86.

Joughin, I. R. and R. B. Alley (2011). "Stability of the West Antarctic ice sheet in a warming world". In: *Nature Geoscience* 4.8, pp. 506–513. DOI: 10.1038/ngeo1194.

Joughin, I. R., B. E. Smith, and W. Abdalati (2010). "Glaciological advances made with interferometric synthetic aperture radar". In: *Journal of Glaciology* 56.200, pp. 1026–1042. DOI: 10.3189/002214311796406158.

Joughin, I. R., B. E. Smith, I. M. Howat, T. Scambos, and T. Moon (2010). "Greenland flow variability from ice-sheet-wide velocity mapping". In: *Journal of Glaciology* 56.197, pp. 415–430. DOI: 10.3189/002214310792447734.

Joughin, I. R., B. E. Smith, I. M. Howat, D. Floricioiu, R. B. Alley, M. Truffer, and M. Fahnestock (2012). "Seasonal to decadal scale variations in the surface velocity of Jakobshavn Isbrae, Greenland: Observation and model-based analysis". In: *Journal of Geophysical Research* 117.F2, F02030. DOI: 10.1029/2011JF002110.

Khan, S. a. et al. (2014a). "Glacier dynamics at Helheim and Kangerdlugssuaq glaciers, southeast Greenland, since the Little Ice Age". In: *The Cryosphere* 8.4, pp. 1497–1507. DOI: 10.5194/tc-8-1497-2014.

Khan, S. A. et al. (2014b). "Sustained mass loss of the northeast Greenland ice sheet triggered by regional warming". In: *Nature climate change* 4.March, pp. 292–299. DOI: 10.1038/NCLIMATE2161.

Khan, S. A. et al. (2013). "Recurring dynamically induced thinning during 1985 to 2010 on Upernavik Isstrøm, West Greenland". In: *Journal of Geophysical Research: Earth Surface* 118, n/a–n/a. DOI: 10.1029/2012JF002481.

Khan, S. A., A. Aschwanden, A. A. Bjørk, J. Wahr, K. K. Kjeldsen, and K. H. Kjær (2015). "Greenland ice sheet mass balance". In: *Reports on Progress in Physics*, p. 4. DOI: 10.1088/0034-4885/78/4/046801.

Kjeldsen, K. K., S. A. Khan, J. Wahr, N. J. Korsgaard, K. H. Kjær, A. a. Bjørk, R. Hurkmans, M. R. Van Den Broeke, J. L. Bamber, and J. H. Van Angelen (2013). "Improved ice loss estimate of the northwestern Greenland ice sheet". In: *Journal of Geophysical Research: Solid Earth* 118.2, pp. 698–708. DOI: 10.1029/2012JB009684.

Korona, J., E. Berthier, M. Bernard, F. Rémy, and E. Thouvenot (2009). "SPIRIT. SPOT 5 stereoscopic survey of Polar Ice: Reference Images and Topographies during the fourth International Polar Year (2007-2009)". In: *ISPRS Journal of Photogrammetry and Remote Sensing* 64.2, pp. 204–212. DOI: 10.1016/j.isprsjprs.2008.10.005.

Krabill, W. (2013). *IceBridge ATM L2 Icessn Elevation, Slope, and Roughness, [1993-2012]. Boulder, Colorado USA: NASA Distributed Active Archive Center at the National Snow and Ice Data Center. Digital media.*

Kulessa, B. et al. (2017). "Seismic evidence for complex sedimentary control of Greenland Ice Sheet flow". In: *Science Advances* 3.8, e1603071. DOI: 10.1126/sciadv.1603071.

Langen, P. L., R. S. Fausto, B. Vandecrux, R. H. Mottram, and J. E. Box (2017). "Liquid Water Flow and Retention on the Greenland Ice Sheet in the Regional Climate Model HIRHAM5: Local and Large-Scale Impacts". In: *Frontiers in Earth Science* 4.January, pp. 1–18. DOI: 10.3389/feart.2016.00110.

Larour, E., H. Seroussi, M. Morlighem, and E. Rignot (2012a). "Continental scale, high order, high spatial resolution, ice sheet modeling using the Ice Sheet System Model (ISSM)". In: *Journal of Geophysical Research* 117.F1, F01022. DOI: 10.1029/2011JF002140.

Larour, E., M. Morlighem, H. Seroussi, J. Schiermeier, and E. Rignot (2012b). "Ice flow sensitivity to geothermal heat flux of Pine Island Glacier, Antarctica". In: *Journal of Geophysical Research* 117.F4, F04023. DOI: 10.1029/2012JF002371.

Larour, E., J. Utke, B. Csatho, A. Schenk, H. Seroussi, M. Morlighem, E. Rignot, N. Schlegel, and A. Khazendar (2014a). "Inferred basal friction and surface mass balance of the Northeast Greenland Ice Stream using data assimilation of ICESat (Ice Cloud and land Elevation Satellite) surface altimetry and ISSM (Ice Sheet System Model)". In: *The Cryosphere* 8.6, pp. 2335–2351. DOI: 10.5194/tc-8-2335-2014.

Larour, E., A. Khazendar, C. Borstad, H. Seroussi, M. Morlighem, and E. Rignot (2014b). "Representation of sharp rifts and faults mechanics in modeling ice-shelf flow dynamics: Application to Brunt/Stancomb-Wills Ice Shelf, Antarctica". In: *Journal of Geophysical Research: Earth Surface* 119, pp. 1918–1935. DOI: 10.1002/2014JF003157.

Larsen, S. H., S. A. Khan, A. P. Ahlstrøm, C. S. Hvidberg, M. J. Willis, and S. B. Andersen (2016). "Increased mass loss and asynchronous behavior of marine-terminating outlet glaciers at Upernavik Isstrøm, NW Greenland". In: *Journal of Geophysical Research F: Earth Surface* 121.2, pp. 241–256. DOI: 10.1002/2015JF003507.

Lea, J. M., D. W. F. Mair, and B. R. Rea (2014). "Instruments and Methods :Evaluation of existing and new methods of tracking

glacier terminus change". In: *Journal of Glaciology* 60.220, pp. 323–332. DOI: 10.3189/2014JoG13J061.

Lea, J. M., D. W. F. Mair, F. M. Nick, B. R. Rea, A. Weidick, K. H. Kjær, M. Morlighem, D. van As, and J. E. Schofield (2014). "Terminus-driven retreat of a major southwest Greenland tidewater glacier during the early 19th century: Insights from glacier reconstructions and numerical modelling". In: *Journal of Glaciology* 60.220, pp. 333–344. DOI: 10.3189/2014JoG13J163.

Lucas-Picher, P., M. Wulff-Nielsen, J. H. Christensen, G. Aðalgeirsdóttir, R. Mottram, and S. B. Simonsen (2012). "Very high resolution regional climate model simulations over Greenland: Identifying added value". In: *Journal of Geophysical Research: Atmospheres* 117.D2, n/a–n/a. DOI: 10.1029/2011JD016267.

Lüthi, M. P., C. Ryser, L. C. Andrews, G. a. Catania, M. Funk, R. L. Hawley, M. J. Hoffman, and T. a. Neumann (2015). "Heat sources within the Greenland Ice Sheet: dissipation, temperate paleo-firn and cryo-hydrologic warming". In: *The Cryosphere* 9.1, pp. 245–253. DOI: 10.5194/tc-9-245-2015.

McFadden, E. M., I. M. Howat, I. R. Joughin, B. E. Smith, and Y. Ahn (2011). "Changes in the dynamics of marine terminating outlet glaciers in west Greenland (2000–2009)". In: *Journal of Geophysical Research* 116.F2, F02022. DOI: 10.1029/2010JF001757.

Meier, M. F. and A. Post (1987). "Fast Tidewater Glaciers". In: *Journal of Geophysical Research* 92.Figure 2, pp. 9051–9058.

Meierbachtol, T. W., J. T. Harper, J. V. Johnson, N. F. Humphrey, and D. J. Brinkerhoff (2015). "Thermal boundary conditions on western Greenland: Observational constraints and impacts on the modeled thermomechanical state". In: *Journal of Geophysical Research: Earth Surface* 120, pp. 623–636. DOI: 10.1002/2014JF003375.

Moon, T, I. R. Joughin, B Smith, and I Howat (2012). "21st-century evolution of Greenland outlet glacier velocities." In: *Science (New York, N.Y.)* 336.6081, pp. 576–8. DOI: 10.1126/science.1219985.

Moon, T. and I. R. Joughin (2008). "Changes in ice front position on Greenland's outlet glaciers from 1992 to 2007". In: *Journal of Geophysical Research* 113.F2, F02022. DOI: 10.1029/2007JF000927.

Moon, T., I. R. Joughin, B. Smith, M. R. van den Broeke, W. J. Berg, B. Noël, and M. Usher (2014). "Distinct patterns of seasonal Greenland glacier velocity". In: *Geophysical Research Letters* 41, pp. 7209–7216. DOI: 10.1002/2014GL061836.Received.

Morlighem, M., E. Rignot, H. Seroussi, E. Larour, H. Ben Dhia, and D. Aubry (2010). "Spatial patterns of basal drag inferred using control methods from a full-Stokes and simpler models for Pine Island Glacier, West Antarctica". In: *Geophysical Research Letters* 37.14, n/a–n/a. DOI: 10.1029/2010GL043853.

Morlighem, M., E. Rignot, H. Seroussi, E. Larour, H. Ben Dhia, and D. Aubry (2011). "A mass conservation approach for mapping glacier ice thickness". In: *Geophysical Research Letters* 38.19, n/a–n/a. DOI: 10.1029/2011GL048659.

Morlighem, M., E. Rignot, J. Mouginot, X. Wu, H. Seroussi, E. Larour, and J. Paden (2013). "High-resolution bed topography mapping of Russell Glacier, Greenland, inferred from Operation IceBridge data". In: *Journal of Glaciology* 59.218, pp. 1015–1023. DOI: 10.3189/2013JoG12J235.

Morlighem, M, E Rignot, J Mouginot, H Seroussi, and E Larour (2014). "Deeply incised submarine glacial valleys beneath the Greenland ice sheet". In: *Nature Geoscience* May, pp. 18–22. DOI: 10.1038/NGEO2167.

Morlighem, M., J. Bondzio, H. Seroussi, E. Rignot, E. Larour, A. Humbert, and S. Rebuffi (2016). "Modeling of Store Gletscher's calving dynamics, West Greenland, in response to ocean thermal forcing". In: *Geophysical Research Letters*. DOI: 10.1002/2016GL067695.

Morlighem, M et al. (2017). "BedMachine v3: Complete bed topography and ocean bathymetry mapping of Greenland from multibeam echo sounding combined with mass conservation". In: DOI: 10.1002/2017GL074954.

Murray, T. et al. (2015). "Extensive Retreat of Greenland Tidewater Glaciers, 2000–2010". In: *Arctic, Antarctic, and Alpine Research* 47.3, pp. 427–447. DOI: 10.1657/AAAR0014-049.

Nagler, T., H. Rott, M. Hetzenecker, J. Wuite, and P. Potin (2015). "The Sentinel-1 Mission: New Opportunities for Ice Sheet Observations". In: *Remote Sensing* 7.7, pp. 9371–9389. DOI: 10.3390/rs70709371.

Nick, F. M., A. Vieli, I. M. Howat, and I. R. Joughin (2009). "Large-scale changes in Greenland outlet glacier dynamics triggered at the terminus". In: *Nature Geoscience* 2.2, pp. 110–114. DOI: 10.1038/ngeo394.

Nielsen, K., S. A. Khan, N. J. Korsgaard, K. H. Kjær, J. Wahr, M. Bevis, L. a. Stearns, and L. H. Timm (2012). "Crustal uplift due to ice mass variability on Upernavik Isstrøm, west Greenland". In: *Earth and Planetary Science Letters* 353-354.July 2007, pp. 182–189. DOI: 10.1016/j.epsl.2012.08.024.

Noël, B., W. J. Van De Berg, E. Van Meijgaard, P. Kuipers Munneke, R. S. W. Van De Wal, and M. R. Van Den Broeke (2015). "Evaluation of the updated regional climate model RACMO2.3: Summer snowfall impact on the Greenland Ice Sheet". In: *Cryosphere* 9.5, pp. 1831–1844. DOI: 10.5194/tc-9-1831-2015.

Noh, M.-J. and I. M. Howat (2015). "Automated stereo-photogrammetric DEM generation at high latitudes: Surface Extraction with TIN-based Search-space Minimization (SETSM) validation and demon-

stration over glaciated regions". In: *GIScience & Remote Sensing* 52.2, pp. 198–217. DOI: 10.1080/15481603.2015.1008621.

Pfeffer, W. T. (2007). "A simple mechanism for irreversible tidewater glacier retreat". In: *Journal of Geophysical Research* 112.F3, F03S25. DOI: 10.1029/2006JF000590.

Phillips, T., H. Rajaram, and K. Steffen (2010). "Cryo-hydrologic warming: A potential mechanism for rapid thermal response of ice sheets". In: *Geophysical Research Letters* 37.20, n/a–n/a. DOI: 10.1029/2010GL044397.

Phillips, T., H. Rajaram, W. Colgan, K. Steffen, and W. Abdalati (2013). "Evaluation of cryo-hydrologic warming as an explanation for increased ice velocities in the wet snow zone, Sermeq Avannarleq, West Greenland". In: *Journal of Geophysical Research: Earth Surface* 118.3, pp. 1241–1256. DOI: 10.1002/jgrf.20079.

Pollack, H. N., S. J. Hurter, and J. R. Johnson (1993). "Heat flow from the Earth's interior: Analysis of the global data set". In: *Reviews of Geophysics* 31.3, pp. 267–280. DOI: 10.1029/93RG01249.

Rignot, E. and J. Mouginot (2012). "Ice flow in Greenland for the International Polar Year 2008-2009". In: *Geophysical Research Letters* 39.11, n/a–n/a. DOI: 10.1029/2012GL051634.

Rignot, E. and P Kanagaratnam (2006). "Changes in the velocity structure of the Greenland Ice Sheet". In: *Science* 311.February, pp. 986–990.

Schlegel, N.-J., E. Larour, H. Seroussi, M. Morlighem, and J. E. Box (2013). "Decadal-scale sensitivity of Northeast Greenland ice flow to errors in surface mass balance using ISSM". In: *Journal of Geophysical Research: Earth Surface* 118.2, pp. 667–680. DOI: 10.1002/jgrf.20062.

Schlegel, N.-J., E Larour, H Seroussi, M Morlighem, and J. E. Box (2014). "Ice discharge uncertainties in Northeast Greenland from boundary conditions and climate forcing of an ice flow model". In: *J. Geophys. Res. - Earth Surface* 120, pp. 1–21. DOI: 10.1002/2014JF003359.

Schoof, C. (2007). "Ice sheet grounding line dynamics: Steady states, stability, and hysteresis". In: *Journal of Geophysical Research* 112.F3, F03S28. DOI: 10.1029/2006JF000664.

Schoof, C. and I. Hewitt (2013). "Ice-Sheet Dynamics". In: *Annual Review of Fluid Mechanics* 45.1, pp. 217–239. DOI: 10.1146/annurev-fluid-011212-140632.

Schoof, C. and R. C. A. Hindmarsh (2010). "Thin-film flows with wall slip: An asymptotic analysis of higher order glacier flow models". In: *Quarterly Journal of Mechanics and Applied Mathematics* 63.1, pp. 73–114. DOI: 10.1093/qjmam/hbp025.

Sciascia, R., F. Straneo, C. Cenedese, and P. Heimbach (2013). "Seasonal variability of submarine melt rate and circulation in an East

Greenland fjord". In: *Journal of Geophysical Research: Oceans* 118.5, pp. 2492–2506. DOI: 10.1002/jgrc.20142.

Seroussi, H., M. Morlighem, E. Rignot, A. Khazendar, E. Larour, and J. Mouginot (2013). "Dependence of century-scale projections of the Greenland ice sheet on its thermal regime". In: *Journal of Glaciology* 59.218, pp. 1024–1034. DOI: 10.3189/2013JoG13J054.

Seroussi, H., H. Ben Dhia, M. Morlighem, E. Larour, E. Rignot, and D. Aubry (2012). "Coupling ice flow models of varying orders of complexity with the Tiling method". In: *Journal of Glaciology* 58.210, pp. 776–786. DOI: 10.3189/2012JoG11J195.

Shapiro, N. M. and M. H. Ritzwoller (2004). "Inferring surface heat flux distributions guided by a global seismic model: Particular application to Antarctica". In: *Earth and Planetary Science Letters* 223.1-2, pp. 213–224. DOI: 10.1016/j.epsl.2004.04.011.

Slater, D., P. Nienow, A. Sole, T. Cowton, R. Mottram, P. Langen, and D. Mair (2017). "Spatially distributed runoff at the grounding line of a large Greenlandic tidewater glacier inferred from plume modelling". In: *Journal of Glaciology* 63.238, pp. 309–323. DOI: 10.1017/jog.2016.139.

Smith, B. E., H. A. Fricker, I. R. Joughin, and T. Slawek (2009). "An inventory of active subglacial lakes in Antarctica detected by ICESat (2003-2008". In: *Journal of Glaciology* 55.192, pp. 573–595. DOI: 10.3189/002214309789470879.

Sole, A., P. Nienow, I. Bartholomew, D. Mair, T. Cowton, A. Tedstone, and M. a. King (2013). "Winter motion mediates dynamic response of the Greenland Ice Sheet to warmer summers". In: *Geophysical Research Letters* 40, n/a–n/a. DOI: 10.1002/grl.50764.

Sole, a. J., D. W. F. Mair, P. W. Nienow, I. D. Bartholomew, M. a. King, M. J. Burke, and I. R. Joughin (2011). "Seasonal speedup of a Greenland marine-terminating outlet glacier forced by surface melt–induced changes in subglacial hydrology". In: *Journal of Geophysical Research* 116.F3, F03014. DOI: 10.1029/2010JF001948.

Straneo, F. and P. Heimbach (2013). "North Atlantic warming and the retreat of Greenland's outlet glaciers." In: *Nature* 504.7478, pp. 36–43. DOI: 10.1038/nature12854.

Straneo, F. et al. (2013). "Challenges to Understanding the Dynamic Response of Greenland's Marine Terminating Glaciers to Oceanic and Atmospheric Forcing". In: *Bulletin of the American Meteorological Society* 94.8, pp. 1131–1144. DOI: 10.1175/BAMS-D-12-00100.1.

Sundal, A. V., A. Shepherd, P. Nienow, E. Hanna, S. Palmer, and P. Huybrechts (2011). "Melt-induced speed-up of Greenland ice sheet offset by efficient subglacial drainage". In: *Nature* 469.7331, pp. 521–524. DOI: 10.1038/nature09740.

Van Den Broeke, M. R., E. M. Enderlin, I. M. Howat, P. Kuipers Munneke, B. P. Y. No??l, W. Jan Van De Berg, E. Van Meijgaard, and B. Wouters (2016). "On the recent contribution of the Green-

land ice sheet to sea level change". In: *Cryosphere* 10.5, pp. 1933–1946. DOI: 10.5194/tc-10-1933-2016.

Van Der Veen, C. J. (1999). "Evaluating the performance of cryospheric models". In: *Polar Geography* 23.2, pp. 83–96. DOI: 10.1080/10889379909377667.

Van Der Veen, C. J., J. C. Plummer, and L. A. Stearns (2011). "Controls on the recent speed-up of Jakobshavn Isbræ, West Greenland". In: *Journal of Glaciology* 57.204, pp. 770–782. DOI: 10.3189/002214311797409776.

Vinther, B. M. et al. (2009). "Holocene thinning of the Greenland ice sheet." In: *Nature* 461.7262, pp. 385–8. DOI: 10.1038/nature08355.

Weidick, A. (1958). "Frontal Variations at Upernaviks Isstrøm in the Last 100 Years". In: *Meddelelser fra dansk geologisk forening* 14.

Werder, M. A., I. J. Hewitt, C. G. Schoof, and G. E. Flowers (2013). "Modeling channelized and distributed subglacial drainage in two dimensions". In: *Journal of Geophysical Research: Earth Surface* 118.4, pp. 2140–2158. DOI: 10.1002/jgrf.20146.

Zwally, H. J., W. Abdalati, T. Herring, K. Larson, J. Saba, and K. Steffen (2002). "Surface melt-induced acceleration of Greenland ice-sheet flow." In: *Science (New York, N.Y.)* 297.5579, pp. 218–22. DOI: 10.1126/science.1072708.

Zwally, H. J. et al. (2011). "Greenland ice sheet mass balance: distribution of increased mass loss with climate warming; 2003–07 versus 1992–2002". In: *Journal of Glaciology* 57.201, pp. 88–102. DOI: 10.3189/002214311795306682.

COLOPHON

This document was typeset using the typographical look-and-feel `classicthesis` developed by André Miede. The style was inspired by Robert Bringhurst's seminal book on typography "*The Elements of Typographic Style*". `classicthesis` is available for both LaTeX and LyX:

https://bitbucket.org/amiede/classicthesis/

Final Version as of November 2, 2017 (`classicthesis` version 1.0).